[redacted]

CENTRAL RESEARCH LIBRARY
DOCUMENT COLLECTION

AEC RESEARCH AND DEVELOPMENT REPORT

ORNL-2046
Progress
cy. 5

MARTIN MARIETTA ENERGY SYSTEMS LIBRARIES
3 4456 0350089 7

CHEMISTRY DIVISION

SEMIANNUAL PROGRESS REPORT

FOR PERIOD ENDING DECEMBER 20, 1955

CENTRAL RESEARCH LIBRARY
DOCUMENT COLLECTION

LIBRARY LOAN COPY

DO NOT TRANSFER TO ANOTHER PERSON

If you wish someone else to see this document, send in name with document and the library will arrange a loan.

OAK RIDGE NATIONAL LABORATORY
OPERATED BY
UNION CARBIDE NUCLEAR COMPANY
A Division of Union Carbide and Carbon Corporation
UCC
POST OFFICE BOX P · OAK RIDGE, TENNESSEE

[redacted]

[redacted]

[redacted]

ORNL-2046

COPY NO. 5

Contract No. W-7405-eng-26

CHEMISTRY DIVISION

SEMIANNUAL PROGRESS REPORT

for Period Ending December 20, 1955

E. H. Taylor, Director
M. A. Bredig, Associate Director

DATE ISSUED

MAR 1 0 1956

DECLASSIFIED

CLASSIFICATION CHANGED TO: _____

BY AUTHORITY OF: TID-1148

BY: R. Morrison 7/25/57

OAK RIDGE NATIONAL LABORATORY
Operated by
UNION CARBIDE NUCLEAR COMPANY
A Division of Union Carbide and Carbon Corporation
Post Office Box P
Oak Ridge, Tennessee

[redacted]

[redacted]

INTERNAL DISTRIBUTION

[redacted]
C. E. Center
Biology Library
Health Physics Library
4-6. Central Research Library
7-12. Laboratory Records Department
13. Laboratory Records, ORNL R. C.
14. Reactor Experimental Engineering Library
15. A. M. Weinberg
16. L. B. Emlet (K-25)
17. J. P. Murray (Y-12)
18. J. A. Swartout
19. E. H. Taylor
20. E. J. Murphy
21. E. D. Shipley
22. S. C. Lind
23. F. C. VonderLage
24. W. H. Jordan
25. R. R. Dickison
26. F. L. Culler
27. A. H. Snell
28. A. Hollaender
29. M. T. Kelley
30. G. H. Clewett
31. K. Z. Morgan
32. T. A. Lincoln
33. A. S. Householder
34. C. S. Harrill
35. C. E. Winters
36. D. W. Cardwell
37. E. M. King
38. J. A. Lane
39. G. E. Boyd
40. M. A. Bredig
41. R. W. Stoughton
42. R. B. Briggs
43. G. W. Parker
44. C. J. Borkowski
45. G. H. Jenks
46. K. A. Kraus
47. H. A. Levy
48. R. S. Livingston
49. T. E. Willmarth
50. C. H. Secoy
51. C. J. Hochanadel
52. W. H. Baldwin
53. A. R. Brosi
54. R. N. Lyon
55. S. A. Reynolds
56. P. F. Thomason
57. E. G. Bohlmann
58. C. P. Keim
59. C. D. Susano
60. D. D. Cowen
61. P. M. Reyling
62. R. Livingston
63. G. H. Cartledge
64. E. R. Van Artsdalen
65. G. C. Williams
66. R. W. Johnson
67. S. D. Schiffman (K-25)
68. E. P. Wigner (consultant)
69. S. J. Cromer
70. M. J. Skinner
71. D. S. Billington
72. R. A. Charpie
73. H. G. MacPherson (consultant)
74. J. L. Gabbard
75. R. W. Dodson (consultant)
76. H. Eyring (consultant)
77. Schomaker (consultant)
78. J. W. Kennedy (consultant)
79. G. T. Seaborg (consultant)
80. J. R. McNally, Jr.

EXTERNAL DISTRIBUTION

81-88. Argonne National Laboratory
89-96. Atomic Energy Commission, Washington
97-100. Brookhaven National Laboratory
101-104. duPont Company, Wilmington
105-106. Knolls Atomic Power Laboratory

[redacted]

[redacted]

10[redacted]2. General Electric Company, Richland
[redacted] Phillips Petroleum Company (NRTS)
114-[redacted]os Alamos Scientific Laboratory
11[redacted]nd Laboratory
119-121. [redacted]York Operations Office
122. P[redacted]Branch, Washington
123. Sava[redacted]River Operations Office, Aiken
124-127. Univers[redacted] California Radiation Laboratory, Berkeley
128-129. Bettis Pl[redacted]APD)
130. Iowa State [redacted]
131. Division of Re[redacted] and Development, AEC, ORO
132. North American A[redacted]n, Inc.
133. Boeing Airplane Co[redacted]
134-248. Technical Information [redacted]on, AEC, ORO

MARTIN MARIETTA ENERGY SYSTEMS LIBRARIES

3 4456 0350089 7

[redacted]

[redacted]

Chemistry Division progress reports previously issued in this series are as follows:

ORNL-65	March, April, May, 1948
ORNL-176	June, July, August, 1948
ORNL-229	September, October, November, 1948
ORNL-336	December, 1948, January and February, 1949
ORNL-286	Period Ending June 30, 1949
ORNL-499	Period Ending September 30, 1949
ORNL-607	Period Ending December 31, 1949
ORNL-685	Period Ending March 31, 1950
ORNL-795	Period Ending June 30, 1950
ORNL-870	Period Ending September 30, 1950
ORNL-1036	Period Ending December 31, 1950
ORNL-1053	Period Ending March 31, 1951
ORNL-1116	Period Ending June 30, 1951
ORNL-1153	Period Ending September 30, 1951
ORNL-1260	Period Ending December 31, 1951
ORNL-1285	Period Ending March 31, 1952
ORNL-1344	Period Ending June 30, 1952
ORNL-1432	Period Ending September 30, 1952
ORNL-1482	Period Ending December 31, 1952
ORNL-1587	Period Ending June 20, 1953
ORNL-1674	Period Ending December 20, 1953
ORNL-1755	Period Ending June 20, 1954
ORNL-1832	Period Ending December 20, 1954
ORNL-1940	Period Ending June 20, 1955

[redacted]

[redacted]

CONTENTS

CHEMISTRY DIVISION PUBLICATIONS FROM JUNE 20 TO DECEMBER 20, 1955 ix

SUMMARY 1

INORGANIC AND PHYSICAL CHEMISTRY 5
- Adsorption on Inorganic Materials 5
- Ultracentrifugation of Inorganic Systems 5
- Anion Exchange Studies 5
  - Adsorption of Negatively Charged Complexes by Anion Exchangers 5
  - Adsorption of Negatively Charged Complexes by Cation Exchangers 6
  - Adsorption of a Number of Metals from HCl-HF Mixtures 6
  - Anion Exchange Studies in Nitrate Solutions 7
- Solubility of Silver Sulfate as a Function of Sulfuric Acid Concentration and Temperature 8
- Chemistry of Corrosion 10
  - Mechanism of Inhibition 10
  - Effect of Cupric Ions on the Potentials of Stainless Steel Electrodes in Dilute Sulfuric Acid 13
- Heat Capacity of Rhenium Heptoxide from 15 to 300° K. Entropy and Free Energy 17
  - Rhenium Heptoxide Sample 17
  - Calorimeter 18
  - Heat-Capacity Data 18
  - Thermodynamic Functions of Rhenium Heptoxide 19
  - Thermochemical Calculations 19
- Chemistry of Fused Salts 21
  - Electrical Conductance and Density 21
  - Self-Diffusion in Molten Salts 23
  - Cryoscopy 26
  - High-Temperature Calorimetry 27
  - Exchange Reactions in Fused Salts 27
  - Hydrogen Fluoride–Fluoromethane Reactions 27
  - Fluorine Exchange Between Salts and Gases 27
- High-Temperature and Structural Chemistry. Liquid Metal–Salt Solutions 28
  - Phase Equilibria in the Potassium Metal–Potassium Chloride System 28
  - Electrical Conductivity in Molten Salt–Metal Solutions 29

NUCLEAR CHEMISTRY 30
- Decay of the Ce^{139} Isomers 30
- Identification of La^{137} and Further Characterization of Ce^{137} 30
- Short-lived Fission Products 31
  - The Decay of Rb^{89} 31
  - The Decay Chain Ca^{49}-Sc^{49}-Ti^{49} 31
  - The Decay of Tc^{101} 32

ORGANIC CHEMISTRY 34
- Mechanism of the Pinacol Rearrangement 34
  - General Conclusions 42
- Rearrangement of 1,1,2-Triphenylethylene Glycol and Its Deuterated Derivative. An Attempted Kinetic Study 42

[redacted]

[redacted]

Preliminary Background Work 42
Results of Ultraviolet Spectroscopic Work 43
Titrimetric Results 43
Radiochemical Results 44
Conclusions 44
Investigation of the Cleavage and Rearrangement of Triaryl Ketols 44
Study of Abnormal Products in the Reactions of Benzyl-Type Grignard Reagents 46
Results 47
Conclusions 48

CHEMICAL PHYSICS 49
Radio-Frequency Spectroscopy 49
Quadrupole Spectroscopy 49
Paramagnetic Resonance 49
Neutron Diffraction Study of $Ca(OH)_2$ at – 140°C 51
Partial Vapor Pressures over Mixtures of Salts 52

CHEMISTRY OF SEPARATION PROCESSES 53
Fundamental Studies on Ion Exchange Resins 53
Thermodynamic Calculation of Cation Exchange Selectivities 53
Zinc-Sodium Ion Exchange Equilibrium in Sulfonated Polystyrene Resins 53
Osmotic Coefficients of 0.5% DVB Polymethacrylate Resin Salts 53
Water Sorption Studies with the Tetraalkyl Ammonium Salts of Polystryene Sulfonic Acid Resins 56
Extraction of Monovalent Electrolytes by Tributyl Phosphate 57
Pyrolysis of Butyl Phosphate Esters 59
Preparation of Diphosphine Dioxides 59
Complexing of Cations with Organophosphorus Acids 60
Neptunium Recovery from Purex Process Plutonium Wastes 62
Partitioning of Neptunium in the Plutonium Stream 62
Adsorption and Elution of Np(IV) 62
Yield of Neptunium from the Plutonium Ion Exchange Waste 63
Isolation of Np^{237} by Ion Exchange and TTA Extraction 63
Possibilities of Neptunium Recovery from Production Plant Purex Wastes 64

RADIATION CHEMISTRY 66
Effect of Ionizing Radiation on Heterogeneous Catalysts 66
Gas-Phase Irradiation 66
Alpha-Ray Irradiation of a Mixture of Acetylene and Benzene 66
Radiation-induced Chemical Reactions 67
Ceric Ion–Thallous Ion Reaction 67
$K_2Cr_2O_7$–Thallous Ion Reaction 69
$K_2Cr_2O_7$–Bromide Ion Reaction 69
Radiation Studies on Nitrate Solutions 70
Recombination Studies 70
Thermal Expansion of Thorium Nitrate Solutions 70
Radiolysis of Tri-*n*-butyl Phosphate 71
Procedure and Equipment 71
Results and Discussion 74
Warming Curves for the Condensed Product of Dissociated Water Vapor and for Hydrogen Peroxide Glass 75

[redacted]

[redacted]

REACTOR CHEMISTRY 78
Effect of Batch vs Continuous Processing on Fluidized Reactors 78
Alkali Oxide–Uranium Trioxide–Carbon Dioxide Aqueous Systems at High Temperature 78

[redacted]

[redacted]

[redacted]

[redacted]

CHEMISTRY DIVISION PUBLICATIONS FROM JUNE 20 TO DECEMBER 20, 1955

UNCLASSIFIED PUBLICATIONS

Inorganic and Physical Chemistry

J. E. Boggs, E. R. Van Artsdalen, and A. R. Brosi, "Non-exchange of F^{18} Between HF and Fluorinated Methanes," *J. Am. Chem. Soc.* **77**, 6505 (1955).

K. A. Kraus and F. Nelson, "Hydrolytic Behavior of Metal Ions. IV. The Acid Constant of Uranium(IV) as a Function of Temperature," *J. Am. Chem. Soc.* **77**, 3721 (1955).

K. A. Kraus, F. Nelson, and G. E. Moore, "Anion-exchange Studies. XVII. Molybdenum(VI), Tungsten(VI) and Uranium(VI) in HCl and HCl–HF Solutions," *J. Am. Chem. Soc.* **77**, 3972 (1955).

F. Nelson and K. A. Kraus, "Anion-exchange Studies. XVIII. Germanium and Arsenic in HCl Solutions," *J. Am. Chem. Soc.* **77**, 4508 (1955).

K. A. Kraus and F. Nelson, "Anion Exchange Studies of the Fission Products," Paper No. 837, International Conference on the Peaceful Uses of Atomic Energy, August 8–20, 1955, Geneva, Switzerland.

K. A. Kraus, "Hydrolytic Behavior of the Heavy Elements," Paper No. 731, International Conference on the Peaceful Uses of Atomic Energy, August 8–20, 1955, Geneva, Switzerland.

G. H. Cartledge, "The Pertechnetate Ion as an Inhibitor of the Corrosion of Iron and Steel," *Corrosion* **11**, 335t (1955).

G. H. Cartledge, "The Mechanism of the Inhibition of Corrosion by the Pertechnetate Ion. I. The Origin and Nature of Reaction Products," *J. Phys. Chem.* **59**, 979 (1955).

G. H. Cartledge and Wm. T. Smith, Jr., "Revision of the Electrode-Potential Diagram for Technetium," *J. Phys. Chem.* **59**, 1111 (1955).

C. E. Higgins and W. H. Baldwin, "Dehydration of Orthophosphoric Acid," *Anal. Chem.* **27**, 1780 (1955).

G. E. Boyd, *Science* **122**, 381 (1955); review of book by B. M. W. Trapnell, entitled "Chemisorption," Academic Press, New York, 1955.

Nuclear Chemistry

G. E. Boyd, J. R. Sites, Q. V. Larson, and C. R. Baldock, "Production and Identification of Long-Lived Technetium Isotopes at Masses 97, 98, and 99," *Phys. Rev.* **99**, 1030 (1955).

A. R. Brosi and B. H. Ketelle, "Radioactivity of the Cerium-137 Isomers," *Phys. Rev.* **100**, 169 (1955).

S. E. Dismuke, M. J. Feldman, G. W. Parker, and F. Ring, Jr., "Hot Laboratory Facilities and Techniques for Handling Radioactive Materials," Paper No. 723, International Conference on the Peaceful Uses of Atomic Energy, August 8–20, 1955, Geneva, Switzerland.

G. W. Parker, W. J. Martin, G. E. Creek, and P. M. Lantz, "Preparation of Kilocurie Quantities of Xenon-135," Paper No. 313, International Conference on the Peaceful Uses of Atomic Energy, August 8–20, 1955, Geneva, Switzerland.

G. W. Parker, W. J. Martin, G. E. Creek, and P. M. Lantz, "Hot Laboratory Preparations at Kilocurie Level," American Institute of Chemical Engineers for Nuclear Engineering and Science Congress, December 12–16, 1955, Preprint 226.

G. W. Parker and P. M. Lantz, *Notes on Conference at Savannah River Concerning Neptunium-237*, ORNL CF-55-12-62 (Dec. 13, 1955).

[redacted]

[redacted]

Organic Chemistry

C. J. Collins, "Molecular Rearrangements. V. The Relative Phenyl/Hydrogen Migration Abilities in the Pinacol Rearrangement of Triphenylethylene Glycol," *J. Am. Chem. Soc.* **77**, 5517 (1955).

C. J. Collins and G. A. Ropp, "A Study of the Accuracy Obtained in Van Slyke Combustion and Radioassay of Carbon-14 Compounds," *J. Am. Chem. Soc.* **77**, 4160 (1955).

Chemical Physics

E. H. Taylor and S. Datz, "Study of Chemical Reaction Mechanisms with Molecular Beams. The Reaction of K with HBr," *J. Chem. Phys.* **23**, 1711 (1955).

Radiation Chemistry

T. J. Sworski, "Direct Action of Cobalt Gamma Radiation on Nitrate Ion in Aqueous Solution," *J. Am. Chem. Soc.* **77**, 4689 (1955).

J. A. Ghormley and C. J. Hochanadel, "The Effect of Hydrogen Peroxide and Other Solutes on the Yield of Hydrogen in the Decomposition of Water by γ-Rays," *Radiation Research* **3**, No. 2, 227 (1955).

C. J. Hochanadel, "The Photolysis of Dilute Hydrogen Peroxide in the Presence of Dissolved Hydrogen and Hydrogen Plus Oxygen," *Radiation Research* **3**, No. 2, 234 (1955).

M. Burton, J. A. Ghormley, and C. J. Hochanadel, "Design of an Inexpensive High-Intensity Gamma Source," *Nucleonics* **13**, No. 10, 74 (1955).

Reactor Chemistry

W. L. Marshall, "Simplified High Temperature Sampling and Use of pH for Solubility Determinations System Uranium Trioxide–Sulfuric Acid–Water," *Anal. Chem.* **27**, 1923 (1955).

F. J. Loprest, W. L. Marshall, and C. H. Secoy, "The System UO_2CrO_4–H_2O," *J. Am. Chem. Soc.* **77**, 4705 (1955).

D. M. Richardson, A. O. Allen, and J. W. Boyle, "Dosimetry of Reactor Radiations by Calorimetric Measurement," Paper No. 154, International Conference on the Peaceful Uses of Atomic Energy, August 8–20, 1955, Geneva, Switzerland.

C. H. Secoy, "Survey of Homogeneous Reactor Chemical Problems," Paper No. 821, International Conference on the Peaceful Uses of Atomic Energy, August 8–20, 1955, Geneva, Switzerland.

[redacted]

[redacted]

CHEMISTRY DIVISION SEMIANNUAL PROGRESS REPORT

SUMMARY

INORGANIC AND PHYSICAL CHEMISTRY

In a study of adsorption of ions on inorganic materials, anion and cation exchange properties were demonstrated for a number of solids. Of these, zirconium oxide, zirconium phosphate, and zirconium tungstate were studied in some detail.

Anion exchange studies of metal complexes with organic strong-base exchangers continued. Results for elements of the fourth, fifth, and sixth groups in HCl-HF mixtures are discussed. A number of elements were studied in nitrate solutions. Of particular interest is the observation that Th(IV) can be strongly adsorbed from nitrate solutions and hence can readily be separated from many elements, including Fe(III) and the rare earths.

Work continued on the earlier observation that adsorption of many complexes by the anion exchanger, Dowex 1, is very much better from concentrated LiCl than from concentrated HCl solutions. This "abnormally" high adsorption occurs in many chlorides (e.g., $MgCl_2$, $CaCl_2$, $AlCl_3$) and presumably is typical for low-acid media. It now appears that the reason for the difference in adsorbability from low- and high-acid media resides more in properties of the resin phase than in properties of the aqueous phase. It was hence anticipated that at high electrolyte concentration cation exchange resins, too, might show good adsorption for negatively charged complexes, particularly at low acidity. Such an effect was demonstrated for the negatively charged complex $AuCl_4^-$ with the cation exchanger Dowex 50.

The solubility of Ag_2SO_4 has been determined in water and in 0.1, 0.5, and 1.0 *m* H_2SO_4 up to about 250°C in order to evaluate the useful range of the Ag, Ag_2SO_4 electrode in acid solutions. The marked increase in solubility with increasing H_2SO_4 concentration and temperature limits the useful range of temperature and acid concentration.

The study of the effect of electrolytes upon the electrode potential of iron inhibited by the pertechnetate ion was extended to chromate, molybdate, and tungstate ions as inhibitors. It was shown that, at 57.5°C, only the pertechnetate ion produced a passive potential in absence of air. Specific effects of the added electrolytes were in harmony with the hypothesis previously developed, which involved the assumption of electrostatic polarization of the interface under the influence of labile adsorption of the inhibitor.

The effects of Cu(II) ions upon the electrochemical behavior of stainless steel (type 347) have been determined in greater detail. By using Cu^{64} and composite electrodes consisting of separate components of the same steel with different surface treatments, it has been possible to distinguish the effects at cathodic and anodic areas. Thus, it was shown that the deposited copper species is found chiefly on anodic areas and that it does not readily go back into solution when the ion concentration is diminished.

The heat capacity of rhenium heptoxide between 15 and 300°K was determined; through combination with other thermodynamic data the free energy of formation of the heptoxide and of perrhenic acid was computed.

Electrical conductance and density data were obtained for all fused alkali chlorides, bromides, and iodides as functions of temperature. Heats and entropies of activation for conductance were calculated and some theoretical interpretations attempted. Self-diffusion coefficients were measured of both Na^+ and NO_3^- in fused sodium nitrate to about 375°C. The activation energy for migration is essentially the same for both cation and anion. The relative rates of diffusion of the two ions are roughly proportional to the inverse square roots of their masses. The Nernst-Einstein equation is not applicable to the calculation of electrical conductance from self-diffusion coefficients in this molten salt. Equilibrium constants were calculated from experimental data for association reactions of a number of heavy-metal halides dissolved in fused sodium nitrate. The applicability of the "common-ion effect" was demonstrated in a number of new systems. The TiF_6^{--} and ZrF_6^{--} ions are moderately stable in dilute fused sodium nitrate solutions, although they appear to dissociate somewhat at exceedingly high dilution and to associate at higher concentrations. Some preliminary studies of exchange reactions were made in molten salts. Fluoromethane does not exchange fluorine with HF

[redacted]

at temperatures up to 400°C. Preliminary experiments were started for studying the exchange of fluorine between fluoride salts and various gaseous fluorine compounds.

Phase equilibria in the system KCl-K were found to be quite similar to those in the system KF K. With a small temperature range of only 40°C for immiscibility in liquid phase, the system is intermediate between the NaCl-Na system, where the range is 200°C, and the CsCl-Cs system, where no miscibility gap exists. With improved cells made of magnesia or alumina single crystals, electrical conductance measurements in solutions of up to 3 mole % potassium metal in fused potassium chloride showed conductance by electrons of the metal to be a very minor process.

NUCLEAR CHEMISTRY

Studies of the decay of 14.9-min Rb^{89} were completed. Gamma-gamma coincidence spectroscopy and summing of gamma rays in a $4\frac{3}{4}$-in.-dia NaI(Tl) crystal were used to establish a decay scheme with levels in Sr^{89} at 1.05, 2.31, 2.59, 2.75, 3.25, and 3.52 Mev.

The beta-ray transition from Rb^{89} to the ground state of Sr^{89} was measured as 3.92 ± 0.05 Mev and is present in about 7% of the beta-ray transitions.

The decays of Ca^{49} and its daughter, Sc^{49}, have been studied by scintillation methods. Calcium-49 was observed to decay with a half life of 8.75 ± 0.20 min, exciting gamma-ray transitions in Sc^{49} with energies of 3.10 ± 0.03, 4.05 ± 0.05, and 4.68 ± 0.05 Mev. No detectable gamma-ray cascades were seen; thus the gamma rays from Ca^{49} decay characterize the decay of excited states in Sc^{49} to the ground state. Two beta-ray groups with energies of 1.95 ± 0.05 and 0.89 ± 0.15 Mev were resolved from the Ca^{49} beta-ray spectrum, and no beta-ray transitions to the ground state of Sc^{49} were found. Scandium-49 was shown to be a pure beta emitter, having an energy of 2.05 ± 0.05 Mev and a half life of 57.2 ± 0.7 min.

Preliminary work on the decay of Tc^{101} disclosed gamma rays of energy 130 ± 5, 190 ± 8, 307 ± 3 (strong), 410 ± 15, 542 ± 5, 635 ± 15, 719 ± 8, 840 ± 15 kev. That the 840-kev gamma ray is not the crossover for a 307 + 542 cascade was demonstrated by placing a source of Tc^{101} inside a $9\frac{1}{4}$-in. NaI(Tl) crystal spectrometer, with the result that the intensity of the 542-kev gamma ray relative to that of the 307-kev gamma ray remained constant; that is, there was no loss of intensity through summing.

The discovery of a hitherto unobserved 10-kev gamma-ray transition led to a proposal of a new decay scheme for La^{137} (half life $(6 \pm 2) \times 10^4$ years). The results of a study of the decay of the 140-day ground state of Ce^{139} are summarized.

ORGANIC CHEMISTRY

Diphenyl-*p*-tolylacetaldehyde-1-C^{14}, chain- and ring-labeled 1,2-diphenyl-1-*p*-tolylethylene glycol, and 1,1-diphenyl-2-*p*-tolylethylene-2-C^{14} glycol were prepared and subjected to rearrangement in cold, concentrated sulfuric acid and in boiling formic acid. Under both sets of conditions two ketones, *p*-tolyldesoxybenzoin and benzhydryl-*p*-tolyl ketone, are produced from each reactant. By using double-labeling techniques and by generating a common intermediate ion under identical conditions from the three different sources, it was possible to relate the pinacol and aldehyde-ketone rearrangements mechanistically. For the rearrangement of the aldehyde the simple ratios of the products (4.7 in sulfuric acid and 3.5 in formic acid) would appear to indicate phenyl/*p*-tolyl migration ratios of 2.35 and 1.75, respectively, which are inverted with respect to the usual migratory abilities of the two groups. It was shown that the migration ratio of the one *p*-tolyl and the two phenyl groups is not reversed and is not given by the ratio of the ketonic products. The true *p*-tolyl/phenyl migration abilities in the rearrangement of diphenyl-*p*-tolylacetaldehyde in either sulfuric or formic acid were estimated, by the use of a kinetic expression which follows from the mechanism, to be between 2 and 4 as would normally be expected.

It was shown that secondary hydroxyl removal from 1,1-diphenyl-2-*p*-tolylethylene-2-C^{14} glycol is relatively more important, with respect to tertiary hydroxyl removal, in concentrated sulfuric acid at 0°C than in formic acid at 27.6°C. This observation is explained on the basis of a greater polarizability of aryl nuclei in the solvent of higher dielectric constant.

An analytical method was worked out for determining the rate of disappearance of 1,1,2-triphenylethylene glycol under acid catalysis.

The addition of 1 mole of *o*-tolymagnesium bromide to benzil was shown to yield *both* normal

and rearranged products. Labeled anisylmagnesium bromide produces only the normal addition product when added to anisoin. *m*-Methoxyphenylmagnesium bromide (labeled) was shown similarly to add to 3,3′-dimethoxybenzil without rearrangement. The addition of *p*-tolylmagnesium bromide to benzil takes place with 7% rearrangement.

An investigation of the abnormal products formed in the carboxylation of benzyl and 2-thenyl Grignard reagents was carried out. By using the reverse isotope-dilution technique, it was demonstrated that no *o*- or *p*-toluic acids are formed in the reaction of benzylmagnesium bromide with carbon dioxide. 2-Thenylmagnesium chloride reacts to produce 61.7% of the normal product, 2-thienylacetic acid, 30.1% of the *ortho*-abnormal product, 2-methyl-3-thenoic acid, and 3.7% of the *para*-abnormal product, 5-methyl-2-thenoic acid.

CHEMICAL PHYSICS

The effect of pressure up to 9000 psi on pure quadrupole resonance frequencies in several chlorates was found to consist in a raising of these frequencies. As the effect is similar to that of lowering the temperature, it is suggested that the volume change is the important parameter. The microwave spectrometer used in the 9000-Mc region was rebuilt with a number of refinements. Observations on free radicals and on hydrogen atoms produced in calcium hydroxide by irradiation are reported.

An O-H distance of 0.980 ± 0.002 Å was found in calcium hydroxide by neutron diffraction measurements at −140°C. This is longer than the O-H distance of 0.958 Å in water.

Preparations are being made for using the differential detection of alkali metals and their halides by a surface ionization gage for the measurement of partial vapor pressures over salt mixtures.

CHEMISTRY OF SEPARATION PROCESSES

A complete and thermodynamically rigorous computation of the selectivity coefficients of variously cross-linked sulfonated polystyrene cation exchangers has been carried out for the exchange of hydrogen, lithium, potassium, and cesium ions with sodium ion. Satisfactory agreement between computed and observed selectivity coefficients was obtained except with the most highly cross-linked exchangers. It is concluded that the highly cross-linked exchangers possess a polyfunctionality arising from the introduction of variously substituted sulfonate groups in the sulfonation process.

Equilibrium quotients have been measured for the exchange of sodium with zinc ions in variously cross-linked sulfonated polystyrene resins. The results demonstrate a very strong preference of the resins for zinc, with a marked dependence of the equilibrium upon resin loading.

Osmotic coefficients of a number of salts of a very weakly cross-linked polymethacrylic acid resin have been obtained. Those for the alkali and alkaline-earth salts parallel in general the behavior of the acetates in simple aqueous solutions. A reversal occurs in the order of osmotic coefficients of alkali salts from that existing in a weakly cross-linked sulfonate resin, while the order for the alkaline-earth salts is the same for both types of resin. These differences in behavior are explicable in terms of the tendencies toward localized hydrolysis and ion-pair formation.

Water sorption isotherms for the ammonium and several tetraalkyl ammonium salts of 8% DVB sulfonated polystyrene resin are presented and discussed in terms of the four primary factors affecting their water uptake. It is concluded that the governing factor in the repression of water uptake by the tetraalkyl forms at high water activity and in the relative order of their water sorption is their relatively large size, which expands the resin network, causing increased swelling pressure and thus exclusion of water.

A simple equation was found to be adequate for expressing the extraction of monovalent electrolytes from water by tributyl phosphate.

The butyl esters of phosphoric acid containing 1, 2, or 3 ester groups undergo pyrolytic reactions involving the redistribution as well as the loss of some butyl groups. Their stability increases in the order named.

A tetrabutyl pentamethylenediphosphine dioxide has been synthesized. This compound, which has two phosphine oxide groups in the molecule, may, even though soluble in water, be of interest for solvent-extraction purposes.

Attempts to study the solution stabilities of salts of organophosphorus acids indicate that the species existing in solution are considerably more complex than has been assumed.

The occurrence of neptunium in a nearly pure state in ORNL Purex plutonium ion-exchange-column wastes permitted isolation of at least 2 g,

while an additional two or more are in the process of being recovered. The effects of sulfate concentration on the ion exchange behavior of Np(IV) explain its elution during the uranium stripping process.

Preliminary comparative tests of the Savannah River Purex Process intended to lead to a possible production source of neptunium showed that about 70% of the neptunium appears in the calcined UO_3 shipped to K-25. Although the largest part of the neptunium is thus accounted for, a study is being made of the distribution of the remaining 30%, in the hope that it may concentrate in an easily accessible part of the plutonium separation process.

RADIATION CHEMISTRY

Preliminary results indicate that irradiation with gamma rays at −78°C increases the activity of a zinc oxide catalyst for H_2-D_2 exchange at this temperature and that this increased activity is annealed out by warming the catalyst to −22°C.

Alpha-ray radiolysis of a gaseous mixture of acetylene and benzene gave indications that energy transfer occurs as expected from the ionized acetylene to the benzene.

Radiation induces the reduction of either ceric ion or chromate by thallous ion and also the reduction of chromate ion by bromide ion. The pairs of solutes efficiently scavenge the radicals produced by decomposition of the water, thereby allowing the yields to be measured and their distribution in space to be studied.

Warming curves of the product obtained in a cold trap after passing water vapor through an electric discharge were compared with those for the glass prepared by rapidly cooling 60% hydrogen peroxide. The curves were similar from −196 to −80°C. Both showed the glass transition and crystallization regions. The product of the discharge showed rapid temperature rises at −110 and −60°C, indicating reactions of unstable species.

In the gamma-ray decomposition of di-*n*-butyl phosphate, yields for disappearance of substrate and the formation of various gases, dibutyl and monobutyl phosphates, and polymer were measured. The principal products were hydrogen gas, dibutyl phosphate, and polymer. A reaction mechanism was proposed to account for the observed stoichiometry of products.

The thermal reactions of hydrogen with oxygen and of nitrogen with hydrogen and oxygen have been studied in platinum-lined steel bombs at temperatures up to 290°C and pressures to 2000 psi. These measurements are preliminary to the study of the radiation-induced back reaction of nitrogen produced by radiation decomposition of thorium nitrate solution.

The densities of 3 and 7 *m* thorium nitrate solutions were measured at several temperatures in the range from 25 to 300°C.

REACTOR CHEMISTRY

A detailed report is given of the continued phase equilibrium study of the aqueous system lithium oxide–carbon dioxide–uranium trioxide at high temperature. It is tentatively concluded that uranium may be maintained in solution in the form of the complex anions $[UO_2(HCO_3)(CO_3)_2]^{3-}$ and $[UO_2(HCO_3)_2(CO_3)_2]^{4-}$.

An investigation, in connection with fluidized reactor operation, of the effect of batch vs continuous processing on both the production of transmutation products and on the neutron losses suffered led to a quantitative estimate of the advantage of batch processing.

INORGANIC AND PHYSICAL CHEMISTRY

ADSORPTION ON INORGANIC MATERIALS

K. A. Kraus J. S. Johnson
T. A. Carlson H. O. Phillips
D. J. Coombe

For some time work has been in progress on the adsorption of ions on inorganic materials from aqueous solutions. In particular, attempts have been made to characterize various inorganic materials from the point of view of ion exchange properties. Most of this work has so far centered on various hydroxides, principally zirconium hydroxide (anion exchangers), and salts with polyvalent anions such as zirconium phosphate and zirconium tungstate (cation exchangers). Ion exchange properties for these materials have been unambiguously established. Rates of adsorption and elution, capacities, selectivities, and stabilities in various media appear promising for application as ion exchangers. Details of this work have been reported in HRP quarterly reports.[1]

ULTRACENTRIFUGATION OF INORGANIC SYSTEMS

J. S. Johnson K. A. Kraus
R. W. Holmberg

Work on determination of degrees of polymerization of inorganic polymers is continuing. At present, work is under way on Th(IV) hydrolytic polymers which are formed on moderate firing of "thorium hydroxide," or hydrous thorium oxide. A combination of equilibrium and velocity methods is employed.

Work is also under way on evaluating the usefulness of the ultracentrifuge in determining charge and hence degree of complexing in monomeric inorganic systems by the computational methods previously published.[2]

ANION EXCHANGE STUDIES

F. Nelson K. A. Kraus
D. J. Coombe

Adsorption of Negatively Charged Complexes by Anion Exchangers

Some time ago it was found that many metal complexes can be adsorbed on organic strong-base anion exchangers (e.g., Dowex 1) much more strongly from LiCl solutions than from HCl solutions of the same molality.[3] Work has continued on elucidation of this phenomenon. As had been pointed out earlier, the reason for the difference might lie in unexpected differences of activity coefficients of the pertinent components either in the resin phase or in the solution phase. If in the latter, presumably formation of undissociated complex acids would have to be assumed for the HCl solutions.

In more recent studies it was found that "abnormally high" distribution coefficients are not only observed in LiCl solutions but also in other chloride solutions of low acidity. Typical results on the adsorbability of Zn(II) and Au(III) from a number of electrolytes (LiCl, $MgCl_2$, $CaCl_2$, $AlCl_3$, and HCl) are shown in Figs. 1 and 2.

In spite of the fact that a large amount of evidence tends to support the hypothesis that undissociated complex acid formation occurs, the writers at present believe that more probably the activity coefficients of the complex salts differ substantially in the resin phase if it is immersed in LiCl or in HCl solutions. Probably the most conclusive support for this belief is the recent observation that the solubility of $CsAuCl_4$ is approximately the same in LiCl and HCl solutions, or at least is by no means as different in these two media as would have been expected from the differences in the ion exchange behavior.

In view of the fact that enormously larger adsorbabilities occur from concentrated chloride solutions of low acidity, many separations which were previously only marginal can now be improved by operation at low acidity, and purification of many concentrated salt solutions from many heavy metals becomes feasible.

---

[1] T. A. Carlson *et al.*, *HRP Quar. Prog. Rep. Jan. 31, 1955*, ORNL-1853, p 203; K. A. Kraus *et al.*, *HRP Quar. Prog. Rep. April 30, 1955*, ORNL-1895, p 197–200; *HRP Quar. Prog. Rep. July 31, 1955*, ORNL-1943, p 246–251; *HRP Quar. Prog. Rep. Oct. 31, 1955*, ORNL-2004, p 208–212.

[2] J. S. Johnson, K. A. Kraus, and G. Scatchard, *J. Phys. Chem.* 58, 1034 (1954).

[3] K. A. Kraus *et al.*, *J. Am. Chem. Soc.* 77, 1391 (1955); F. Nelson, K. A. Kraus, and D. J. Coombe, *Chem. Semiann. Prog. Rep. June 20, 1955*, ORNL-1940, p 5.

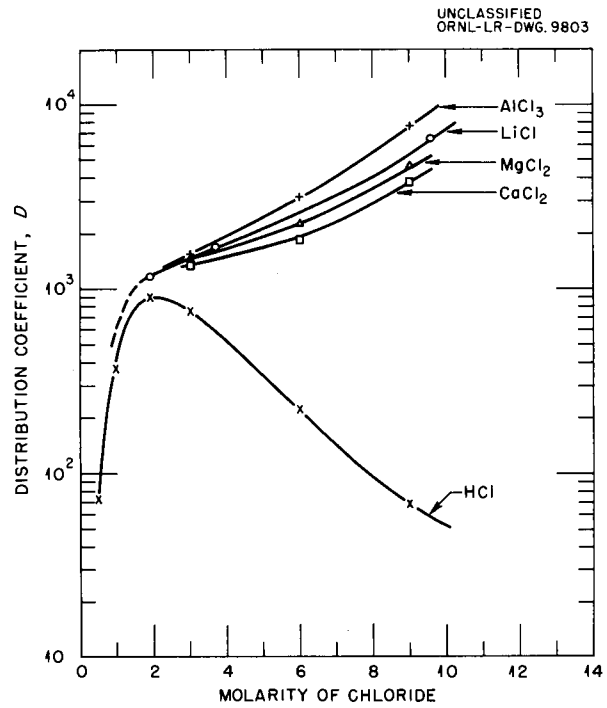

Fig. 1. Adsorption of Zn(II) from Chloride Solutions (~10% Loading of Resin).

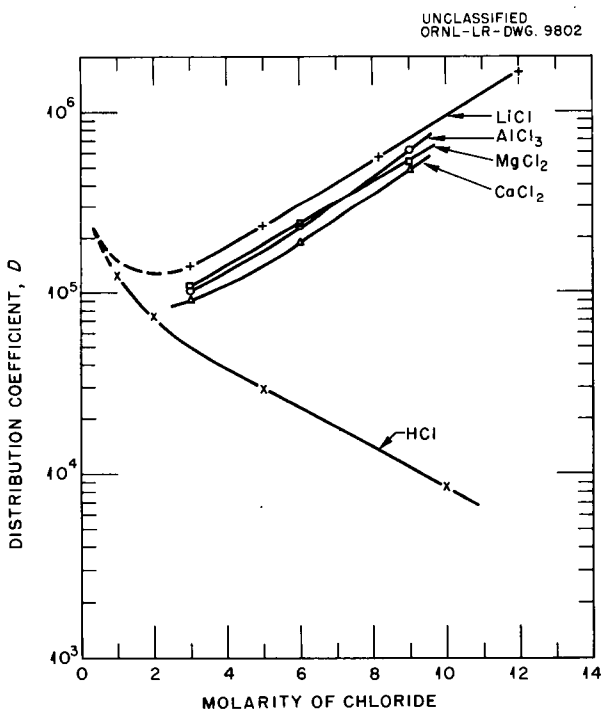

Fig. 2. Adsorption of Au(III) from Chloride Solutions (25% Loading of Resin).

Adsorption of Negatively Charged Complexes by Cation Exchangers

If one assumes that the differences in the adsorbabilities of metal complexes from HCl and from low-acid salt solutions reside in properties of the organic network of the exchangers, one might expect adsorption of negatively charged complexes by *cation* exchange resins containing similar organic networks. Further, if such adsorption occurs it is expected to be stronger from LiCl solutions than from HCl solutions. In view of these considerations, experiments were carried out on the adsorbability of Au(III) ($AuCl_4^-$) from HCl and LiCl solutions with the cation exchange resin, Dowex 50, which has the same organic network as the anion exchanger, Dowex 1, but has different functional groups (sulfonate vs quarternary amine). Surprisingly good adsorption of the chloro complex of Au(III) was found at high electrolyte concentrations. Thus D (amount per kilogram of absorber/amount per liter of solution) for Au(III) was about 35 in 12 M HCl. The values of D rise with LiCl concentration in mixtures of HCl and LiCl of constant total molarity 12 M. In shaking experiments (four days) D was about 500 in 2.4 M HCl–9.6 M LiCl. The value of D observed in 12 M LiCl with Dowex 50 was somewhat lower than this (380), presumably because equilibrium had not been reached in these experiments. Elution of Au(III) from Dowex 50 may be achieved at lower electrolyte concentrations; for example, in the range 0.1 to 1 M HCl or LiCl. There seems to be little doubt that this surprising adsorption of negatively charged complexes by the organic cation exchangers is real and reproducible. This leads to the anomalous situation that at high HCl or LiCl concentrations positively charged ions such as Na^+ or Cs^+ are not adsorbed by the cation exchanger Dowex 50, while a negatively charged complex such as $AuCl_4^-$ is strongly adsorbed.

Adsorption of a Number of Metals from HCl-HF Mixtures[4]

The adsorbability of the following elements of the third, fourth, and fifth groups from HCl-HF mixtures has been investigated with the strong-base anion exchanger Dowex 1: Ga(III), In(III), Tl(III), Ge(IV), Sn(IV), Pb(II), As(V), Sb(V), and

[4] In conjunction with R. M. Rush, summer participant, 1955. Present address: Department of Chemistry, Haverford College, Haverford, Pennsylvania.

Bi(III). Most of the experiments were carried out in 1 *M* HF as a function of HCl concentration in the range 0.1 to 12 *M* HCl. The results are summarized in Fig. 3 as plots of log *D* vs *M* HCl. For comparison, previously published[5] distribution functions of the same elements in HCl solutions alone (in absence of HF) are also given. The difference in adsorbability from HCl and HCl-HF solutions is surprisingly small, or essentially nonexistent for In(III), Tl(III), Pb(II), and As(V). In the case of Bi(III) the HCl and HCl-HF data parallel each other closely, although apparently at the lowest HCl concentration investigated (0.1 *M* HCl) adsorption from HF solutions is considerably less than from HCl alone. The adsorption functions for Ga(III) are similar in HCl and HCl–1 *M* HF, with the values of *D* generally lower in the fluoride-containing media. There was no increase in adsorbability of Ga(III) in 1 *M* HF at low HCl concentrations as is often found[6] for such systems [e.g., Mo(VI), W(VI), U(VI)]. On the other hand, the lowering of the values of *D* for Sn(IV) in the presence of HF is similar to the behavior of the elements of the sixth group [Mo(VI), etc.] as are the occurrence of an adsorption minimum and the rise of *D* with decreasing *M* HCl at low *M* HCl. Germanium(IV) is most drastically affected by the presence of HF in this group of nine elements. While adsorption at high HCl concentrations is strong in the absence of HF, it vanishes essentially in the presence of 1 *M* HF and instead adsorption occurs at low HCl concentrations in the presence of HF where adsorption was negligible in its absence. Some data for Sb(V) have been included in Fig. 3. However, they are strictly tentative and may have to be revised, since considerable difficulties were encountered in reaching equilibrium, and the data tended to scatter widely.

[5]K. A. Kraus and F. Nelson, "Anion Exchange Studies of the Fission Products," Paper No. 837, International Conference on the Peaceful Uses of Atomic Energy, August 8–20, 1955, Geneva, Switzerland.

[6]K. A. Kraus, F. Nelson, and G. E. Moore, *J. Am. Chem. Soc.* 77, 3972 (1955).

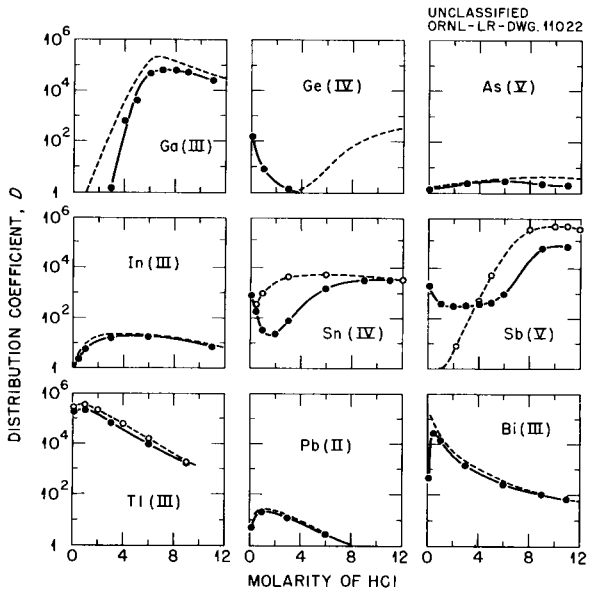

Fig. 3. Adsorbability of Some Elements of Groups III, IV, and V in HCl and HCl-HF Solutions: – – – and – – o – – HCl; —·— HCl–1 *M* HF.

Anion Exchange Studies in Nitrate Solutions

The adsorbability of a number of elements from nitrate solutions by the anion exchanger Dowex 1 has been reinvestigated. Principal emphasis centered around Th(IV) for which distribution coefficients *D* were determined by equilibration experiments (radiometric analysis, Th^{234}, $T_{1/2}$ = 24.1 days) in the range 0.1 to 8 *M* HNO_3. Similar studies were also carried out in NH_4NO_3 solutions which contained 0.02 *M* HNO_3 to avoid hydrolysis of Th(IV). No experiments were carried out above 8 *M* HNO_3, since earlier work had indicated decomposition of the resin under these conditions. The adsorbability of Th(IV) from HNO_3 and NH_4NO_3 solutions was very similar. In the region 0.1 to 1 *M* NO_3^-, adsorbability was negligible; it rose rapidly from $D \approx 1$ near 1.5 *M* NO_3^- to $D \approx 500$ near 8 *M* NO_3^-. Adsorbability of Th(IV) in strong nitric acid is considerably greater than that of U(VI) ($D_{U(VI)} \approx 15$ in 8 *M* NHO_3).[7] Adsorbability of U(VI) from NH_4NO_3 solutions is considerably greater than from HNO_3 solutions ($D_{U(VI)} \approx 150$ in 8 *M* NH_4NO_3). Adsorbability of Th(IV) and U(VI) on anion exchangers may be contrasted with extractability of these elements into diethyl ether. Thus, U(VI) generally extracts better from nitric acid than Th(IV), while Th(IV) adsorbs very much better than U(VI). Further, extractability of Th(IV) into diethyl ether is very much less from NH_4NO_3

[7]F. Nelson and K. A. Kraus, *Chem. Semiann. Prog. Rep. Dec. 20, 1953*, ORNL-1674, p 5.

solutions than from HNO_3 solutions,[8] while that of U(VI) is greater from NH_4NO_3 solutions.

The excellent adsorption of Th(IV) and of U(VI) from nitrate solutions permits easy separation of these elements from many others. In particular, the rare earths and, surprisingly, Fe(III) show negligible adsorption from nitrate solutions and their separation from Th(IV) and U(VI) can be achieved without difficulty. These separations are illustrated in Fig. 4. Part A of this figure shows separation of Fe(III) from Th(IV) and part B shows separation of Eu(III) from U(VI). Similar separations, of course, could be achieved with Eu(III) and Th(IV), or Fe(III) and U(VI). The separations were carried out with 0.25 $cm^2 \times 4.0$ cm columns of nitrate-form resin (Dowex 1, 10% DVB) which had been pretreated with 8 *M* HNO_3. Small aliquots of appropriate mixtures of the elements to be separated were added to the columns and elution was continued with 8 *M* HNO_3. As shown in the figure, the nonadsorbable elements Fe(III) (Fe^{59}) and Eu(III) (Eu^{155}) appear within the first column volume of effluent. The Th(IV) and U(VI) were retained and their elution was accomplished, with some tailing, with 0.2 *M* HNO_3.

The tailing shown in these separations unfortunately appears characteristic for anion exchange in nitrate solutions with the 10% DVB resin used here and the flow rates employed (~ 1 cm/min). Presumably better performance would be obtained at slower flow rates or at higher temperature. Changing these variables is sometimes inconvenient, however. Considerable decrease in tailing can also be achieved by the use of resins of lower cross-linking. Although in general adsorbability with such resins is less than with the highly cross-linked resins, this does not necessarily introduce severe difficulties if the adsorbability at high cross-linking is large. A typical separation [Eu(III), U(VI), Th(IV)] involving a low cross-linked resin (Dowex 1, 2% DVB) where little tailing occurs at 1 cm/min flow rate is illustrated in Fig. 5.

[8] R. Bock and E. Bock, *Z. anorg. u. allgem. Chem.* **263**, 146 (1950).

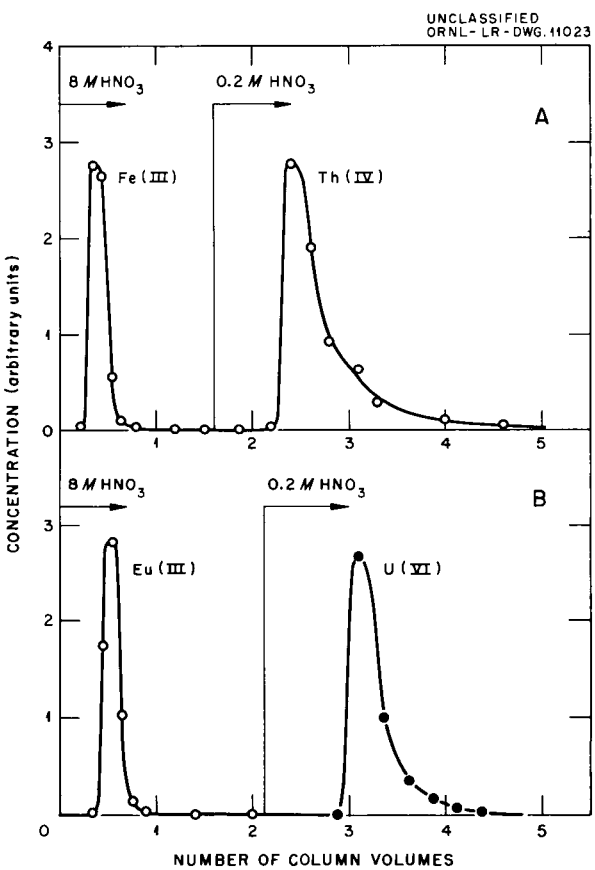

Fig. 4. Separations Involving Th(IV) and U(VI) in HNO_3.

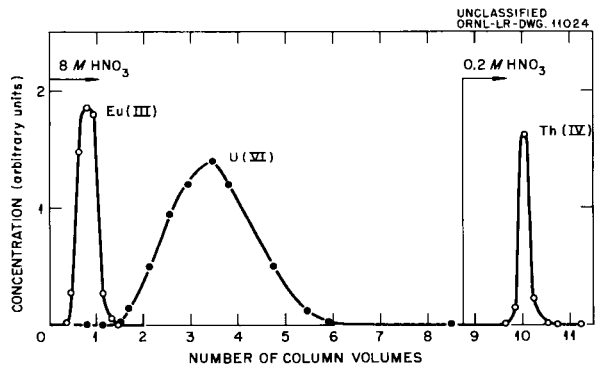

Fig. 5. Separation of Eu(III), U(VI), and Th(IV) in HNO_3.

SOLUBILITY OF SILVER SULFATE AS A FUNCTION OF SULFURIC ACID CONCENTRATION AND TEMPERATURE

H. M. Lietzke R. W. Stoughton

A limit on the useful temperature range of the silver, silver sulfate electrode in acid media might result from the decreasing tendency of HSO_4^- to

dissociate with increasing temperature. Because of the weakness of sulfuric acid at elevated temperatures, the solubility of silver sulfate should increase markedly with increasing acidity. Under these conditions, for electrode combinations requiring that silver ion be kept out of the electrode compartment, liquid-junction potentials could no longer be neglected. In order to define roughly the range in which quantitatively interpretable data can be obtained with the silver sulfate electrode in sulfuric acid solutions, the solubility of silver sulfate was determined as a function of sulfuric acid concentration and temperature.

The solubility measurements were made in an electrically heated oven fitted with a slowly turning brass block. The solubility measurements were of the synthetic type in which silver sulfate crystals and sulfuric acid solution were weighed into fused silica tubes (6-mm ID), which were then sealed and mounted in the brass block. The temperature at which the last crystal went into solution was observed in order to determine the solubility of silver sulfate at that temperature. The solubility measurements could be made only on a heating cycle, since the solution supersaturated upon cooling. After the tubes were heated, they were opened and the contents analyzed to determine the exact concentration of silver sulfate.

The solubility measurements could be reproduced with a precision of about ±1°C, although the accuracy of the measurements probably had wider limits. Figure 6 shows the solubilities in pure water and in 0.1, 0.5, and 1.0 m H_2SO_4. The values in pure water up to 100°C were obtained from the work of Barre,[9] while the two points above 100°C were determined in the course of the present work.

Rough calculations were made on the expected solubilities of Ag_2SO_4 in H_2SO_4 solutions at various temperatures based on the solubilities in pure water and a curve for the HSO_4^- acid constant vs temperature obtained from Young:[10]

$$T \log K = -775.3835 + 6.947210T - 0.021247_2T^2 .$$

The values of the activity acid constant were obtained from Young's equation, and corresponding

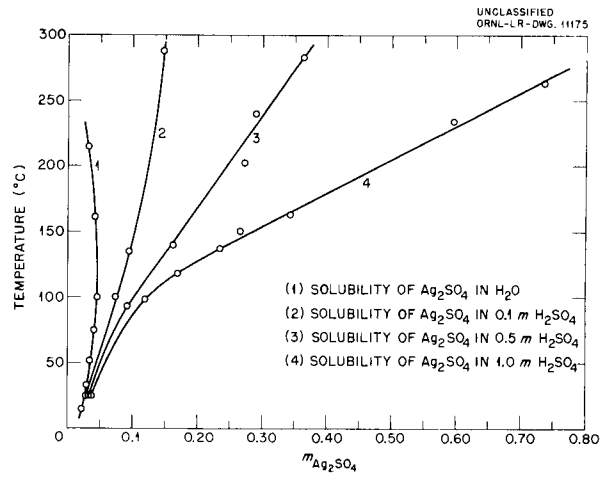

Fig. 6. Solubility of Ag_2SO_4 in H_2O and in H_2SO_4 Solutions.

concentration quotients were calculated at the required ionic strengths on the assumption that the activity coefficient of any ion γ_i is given by the expression

$$\log \gamma_i = \frac{-AZ_i^2\mu^{1/2}}{1 + 1.5\mu^{1/2}} .$$

In this equation μ is the ionic strength, Z_i is the charge of the ion, and A is the Debye-Huckel coefficient, which varies with the dielectric constant of the solvent and the temperature. It was assumed that Ag_2SO_4 dissolved in pure water according to the reaction

$$Ag_2SO_4 = 2Ag^+ + SO_4^{--}$$

The solubility product on a molality basis was calculated at the pertinent ionic strength, that is, a value equal to three times the molal solubility. Values of the molality solubility product were calculated at the desired ionic strengths by using the above equation for the variation of ionic activity coefficients with μ. Since the values of μ that were used were not stoichiometric but depended on the calculated concentrations of ions, they had to be obtained (at least in principle) by successive approximations, as did the ionic concentrations themselves. The calculations involved the further assumption that only the species Ag^+, H^+, SO_4^{--}, and HSO_4^- needed to be considered. Table 1 compares the calculated and observed solubilities

[9] M. Barre, *Ann. chim. et phys.* **24**, Series 8, 211 (1911).

[10] T. F. Young, private communication.

TABLE 1. MEASURED AND CALCULATED MOLAL SOLUBILITY OF SILVER SULFATE IN 0.1 AND 1.0 *m* SULFURIC ACID

Temperature (°C)	0.1 *m* H_2SO_4		1.0 *m* H_2SO_4	
	Calc	Obs	Calc	Obs
100	0.082	0.074	0.180	0.123
150	0.100	0.100	0.344	0.285
200	0.103	0.118	0.535	0.481

at H_2SO_4 molalities of 0.1 and 1.0 at 100, 150, and 200°C.

The calculated values show that the solubility of silver sulfate behaves roughly as expected with increasing temperature and sulfuric acid concentration. It would appear that the Ag, Ag_2SO_4 electrode may not be useful for thermodynamic measurements above about 100°C, although it may be quite useful as a reference electrode for corrosion work or approximate determinations of concentrations at much higher temperatures. The work will be described in detail in a paper to be submitted to the *Journal of the American Chemical Society.*

CHEMISTRY OF CORROSION

Mechanism of Inhibition

G. H. Cartledge R. F. Sympson[11]

In the last report[12] it was shown that inhibition of corrosion by the pertechnetate ion is destroyed and that the electrode potential of the iron specimen is debased by addition of a sufficient concentration of a foreign electrolyte. These studies have now been extended to include the chromate, molybdate, and tungstate ions as inhibitors, in addition to the pertechnetate ion. The foreign electrolytes included sodium sulfate, sodium chloride, potassium thiocyanate, and potassium perrhenate. In order to obtain reliable electrode potentials in the minimum time, the measurements were made at 57.5°C.

The metallic specimens were electrolytic iron. The electrodes were abraded with 2/0 emery, degreased, and then coated with an insulating lacquer except for a section 1 to 2 cm long at the end. The experimental half-cell was contained in a constant-temperature oil bath and connected to a saturated calomel electrode outside the bath by a bridge containing 0.1 *N* potassium chloride. Potential measurements were made with either a vibrating-reed electrometer or a modified Leeds & Northrup line-operated pH meter, the output of which was connected to a Brown recorder. The solution was stirred by passage of a stream of either air or nitrogen which had been freed from oxygen by passage over copper turnings heated to 450°C. Both gas streams were saturated with water vapor at 57.5°C. Further details of the experiments will appear in a paper to be published in *The Journal of Physical Chemistry.*

In each experiment, two iron electrodes were immersed in the inhibitor and left for 4 to 16 hr, at which time a stable potential had been established. Successive portions of foreign electrolyte were then added, and the potential was allowed to become stabilized after each addition. When a certain concentration was reached, the potential, which had previously been very stable, first became unsteady in that there were rapid oscillations over a range of 5 to 20 mv or more. Subsequently, the potential began a steady debasing, and corrosion was ultimately observed. In certain experiments the mixed electrolyte was removed after the potential had fallen by a few hundred millivolts and was replaced by fresh inhibitor solution alone. In these cases the potential began immediately to return to more noble values, thus indicating the reversibility of the process by which the debasing was induced.

Table 2 summarizes the values of the stable potentials attained before addition of foreign electrolytes. The table gives the average electrode potential and the average deviation from the mean value for the total number of electrodes shown in parentheses.

In agreement with Pryor and Cohen,[13] it was found that noble potentials were produced by molybdate and tungstate ions only in the presence of air. Even the chromate-ion mixture induced only moderate (and very erratic) ennobling in the absence of air, whereas the pertechnetate ion showed the least dependence upon oxygen. Flade[14]

[11] Summer research participant, Ohio University.

[12] G. H. Cartledge, *Chem. Semiann. Prog. Rep. June 20, 1955*, ORNL-1940, p 6.

[13] M. J. Pryor and M. Cohen, *J. Electrochem. Soc.* 100, 203 (1953).

[14] F. Flade, *Z. physik. Chem.* 76, 513 (1911).

TABLE 2. STABLE INITIAL ELECTRODE POTENTIALS, 57.5°C

Inhibitor	Formality	pH	Initial Potential (mv) (S.C.E.)	
			Aerated	Deaerated
MoO_4^{--}	1×10^{-3}	6.52	+86 ± 10 (10)	−713 ± 1 (2)
	1×10^{-4}	6.52	+109 ± 23 (4)	
WO_4^{--}	1×10^{-2}	7.18	+64 ± 9 (10)	−754 ± 3 (3)[a]
	1×10^{-3}	6.67	+87 ± 22 (8)	
CrO_4^{--}[b]	1×10^{-3}	6.54	+162 ± 22 (4)	<−164 (variable)
TcO_4^{-}	1×10^{-3}	6.68	+144 ± 23 (7)	
	4.7×10^{-4}	6.4	+157 ± 17 (12)	+88 ± 1 (2)

[a]Omitting one electrode which was entirely at variance with three other closely agreeing electrodes.
[b]Mixture of K_2CrO_4 and $K_2Cr_2O_7$ 1×10^{-3} *f* in Cr.

found that anodically passivated iron rapidly becomes active in sulfuric acid at potentials that are reasonably definite for specified concentrations and temperatures. The pH dependence of this so-called Flade potential has been shown[15,16] to be given by the relation $e_H = 0.58 - 0.058$ pH on the hydrogen scale at 20°C. Although Flade was unable to determine the value above room temperature, he observed an ennobling of approximately 50 mv on going from 0 to 15°C. If it is assumed that there is a similar rate of increase up to 60°C and if the pH values appropriate to the present experiments are applied, the activating potential becomes approximately −10 mv (S.C.E.) for 10^{-2} *f* WO_4^{--} and approximately 45 mv for the other solutions. It is evident that all the initial potentials shown in Table 2 were in the passive region under aeration, whereas only the pertechnetate ion gave such a potential in the absence of air. The blue and brassy film colorations seen in the tests in deaerated molybdate and tungstate solutions, coupled with the sharp rise in anodic polarization observed by Pryor and Cohen[13] when the polarization curves were determined repeatedly in the absence of air, suggest that in these cases an insoluble ferrous salt may have been forming gradually at the anodes. The difference of 41 mv between the base potentials in deaerated molybdate and tungstate solutions compares with 43 mv, as calculated from the difference in pH and the known pH dependence of the iron potential.[17]

The data showed that all four inhibitors were sensitive to added electrolytes, although there were significant differences both in degree and in the order of response to the chloride and sulfate ions. Typical potential-time curves are shown in Figs. 7 and 8. The comparative sensitivities to electrolytes in aerated solutions are shown in Table 3.

It will be noted, first, that the molybdate ion showed the highest sensitivity and the tungstate ion the lowest. It is also apparent that the pertechnetate ion was definitely most sensitive to the sulfate ion, of the three ions added, and that the relative effectiveness of the sulfate ion decreased in the chromate and molybdate measurements; in the tungstate solutions, Cl^- was more effective than SO_4^{--}. Use of two concentrations of molybdate and tungstate ions showed, especially for the tungstates, the greater susceptibility at the lower inhibitor concentration.

The high sensitivity of the inhibitors to ions, the decreasing order of sensitivity to sulfate, chloride, and perrhenate ions, and the prompt reversals of potential observed when the added

[15]U. F. Franck, *Z. Naturforsch.* **4a**, 383 (1949).
[16]K. J. Vetter, *Z. physik. Chem.* **202**, 1 (1954).
[17]K. F. Bonhoeffer, *Z. Elektrochem.* **55**, 151 (1951).

TABLE 3. CONCENTRATIONS OF ADDED IONS THAT INDUCED DEBASING

Inhibitor	Concentration ($/ \times 10^4$)			
	Cl^-	SO_4^{--}	ReO_4^-	SCN^-
1×10^{-3} / TcO_4^-	24 to 32			22 to 42
4.7×10^{-4} / TcO_4^-	17 to 25	4.2 to 6.2	Stable at 100	
1.0×10^{-3} / CrO_4^{--}	25 to 38	12 to 31		
1×10^{-3} / MoO_4^{--}	6.2 to 9.4	6.2		<9.4
1×10^{-4} / MoO_4^{--}	<6.2	<1.6		
1×10^{-2} / WO_4^{--}	200 to 300	400 to 2000		
1×10^{-3} / WO_4^{--}	25 to 50	50 to 75		

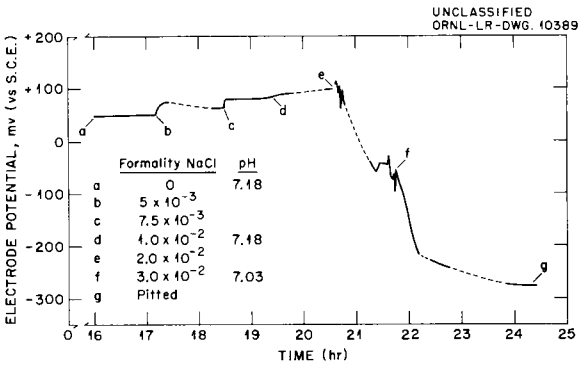

Fig. 7. Electrode Potentials of Iron in Aerated 1×10^{-3} / Na_2WO_4 with Addition of NaCl. Experiment 8, electrode No. 1.

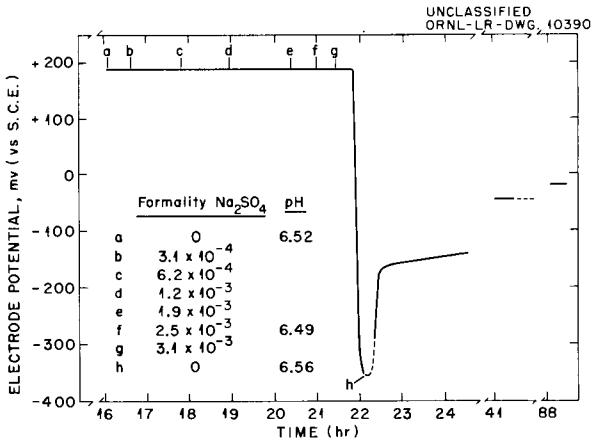

Fig. 8. Electrode Potentials of Iron in Aerated 1×10^{-3} / Chromate Solution with Addition and Removal of Na_2SO_4. Experiment 16, electrode No. 1.

ion is removed are all in harmony with the hypothesis of labile, competitive adsorption discussed in another paper.[18]

In Fig. 7 it may be noted that each addition of chloride ions, up to the point of instability, produced a definite ennobling of the potential. This was observed in *every* addition to all four inhibitors, the effect being least with the chromate solutions. In one experiment, thiocyanate ion was added in stages to a 1×10^{-3} / molybdate solution. Additions to make the thiocyanate ion concentration 6.2×10^{-5}, 3.1×10^{-4}, and 9.4×10^{-4} / produced rapid elevations of 17, 30, and 29 mv, respectively, in the potential. In *no* case did additions of sulfate ions lead to such a conspicuous result (see Fig. 8). Even when the chloride ion concentration reached a value that later led to debasing, the final addition frequently caused a slight and brief ennobling before debasing began. The results clearly demonstrate two mechanisms by which the chloride and thiocyanate ions affect the electrode processes, one of which is lacking in the action of the sulfate ion.

It was previously suggested[19] that, according to the hypothesis of electrostatic polarization of the

[18] G. H. Cartledge, *J. Phys. Chem.* **60**, 28 (1956).

[19] *Op. cit.*, p 32.

interface by adsorbed ions, adsorption of chloride ions should lead to a decrease in the corrosion activation energies, especially of the cathodic process, and hence that the stimulation of corrosion would be accounted for without special hypotheses. Gerischer[20] has shown that, in the electrode reaction $(Pt)Fe^{++} \rightleftharpoons Fe^{+++}$, the exchange current increases essentially in accordance with an adsorption isotherm when chloride ions are added in the concentration range 0 to 10^{-3} *f*. This increase was attributed to strong adsorption of the chloride ions, whereby the activation energy for the transfer of electrons between Fe^{++} and Fe^{+++} ions was diminished. The same author showed also that the transfer coefficient, α, in the kinetic expression for the exchange current was altered upon addition of chloride ions to the Fe^{++}-Fe^{+++} solution. In the case of iron passivated by nitric acid, Vetter[21] showed that the corrosion-equivalent current was increased approximately linearly by addition of chloride ions in concentrations of $(1 \text{ to } 5) \times 10^{-3}$ *f*.

Now, if the noble potentials of inhibited specimens arise in reality from steady states in the effective oxidation-reduction system polarized by the residual corrosion, stimulation of corrosion by addition of chloride ions should debase the potential further below the reversible value, if the primary effect were on the anodic process. The fact that the initial additions uniformly raised the potential must therefore mean that the stimulation affected chiefly the cathodic process, in accordance with the hypothesis proposed.

The significance of the results of this study for the theory of inhibitor action will be discussed in greater detail in a paper to be published.

Effect of Cupric Ions on the Potentials of Stainless Steel Electrodes in Dilute Sulfuric Acid

G. H. Cartledge F. A. Posey

Previous work[22,23] concerned with the factors which influence the potentials of stainless steel electrodes stabilized in dilute sulfuric acid solutions indicated that additions of certain ions exert a marked effect even at low concentrations ($< 10^{-4}$ *f*). These ions are, in general, species which participate in well-known redox reactions in solution. The experiments reported here represent an extension of the results obtained previously on the effect of additions of cupric ions. The steel used was type 347, and the procedures were the same as in the earlier work.

The exploratory experiments cited above,[22,23] conducted under standardized conditions of temperature, volume, pH, geometry of solution, stirring rate, oxygen pressure, electrode area, and pretreatment, indicated that steel potentials varied linearly with the logarithm of the concentration of the additive.

The linearity of the electrode potential-log $[Cu^{++}]$ plots resembles that of thermodynamically reversible systems and poses the question of whether or not the potential changes observed may be related to ion concentrations by thermodynamic theory, regardless of the fact that thermodynamically irreversible processes slowly occur on the electrodes. It has been established,[23] by using radioactive Cu^{64} as a tracer, that copper in some valency state is "irreversibly" retained by these steel electrodes. If the deposited copper species is in electrochemical equilibrium with divalent copper in solution and if the steel electrode potential is modified only by changes in the ratio (activity of cupric ions in solution)/(activity of copper species retained by surface of electrode), the complete Nernst expression, Eq. 1, should describe the observations correctly:

$$(1) \qquad E = \text{const} + \frac{RT}{nF} \ln \frac{a_{ox.}}{a_{red.}} \quad .$$

The experiments using tagged atoms proved that $a_{red.}$ is less than unity even at the highest $a_{ox.}$ employed – that is, the amount of copper retained by the electrodes is substantially less than that necessary to form a monolayer on the metal surface. Differentiation of Eq. 1 leads to the following expression for the variation of electrode potential with $a_{ox.}$:

$$(2) \qquad \frac{dE}{d \ln a_{ox.}} = \frac{RT}{nF} \left(1 - \frac{d \ln a_{red.}}{d \ln a_{ox.}} \right) \quad .$$

Reference to the values of $dE/d \log [Cu^{++}]$ previously reported shows that these quantities are

[20] H. Gerischer, *Z. Elektrochem.* **54**, 366 (1950).

[21] K. J. Vetter, *Z. Elektrochem.* **55**, 274 (1951).

[22] G. H. Cartledge, *Chem. Semiann. Prog. Rep. June 20, 1953*, ORNL-1587, p 13.

[23] G. H. Cartledge and R. P. Yaffe, *Chem. Semiann. Prog. Rep. Dec. 20, 1953*, ORNL-1674, p 11.

always less than 0.071, the value of 2.303 RT/nF for a one-electron change at the experimental temperature, 85°C, in agreement with the prediction of Eq. 2. Experiments with tagged cupric ions[23] also proved the existence of a linear relation between the logarithm of the amount of copper retained by the electrodes and the logarithm of the cupric ion concentration in solution; that is, the relation had the form of a Freundlich isotherm. This relationship can be determined experimentally by simple tracer techniques [since $a_{red.}$ = (const) · (cpm on electrode)] and is represented by Eq. 3:

$$\frac{d \ln a_{red.}}{d \ln a_{ox.}} = \rho \ . \tag{3}$$

By substituting Eq. 3 in Eq. 2, a relation, Eq. 4,

$$\frac{dE}{d \ln a_{ox.}} = \frac{dE}{d \ln [Cu^{++}]} = \frac{RT}{nF} (1 - \rho) \ , \tag{4}$$

is obtained in which all quantities are known or can be determined except the value of n. This n, by analogy with thermodynamically reversible systems, should then correspond to the number of electrons in the electrode process for each cupric ion involved. Knowledge of this quantity, if the above picture is correct, should thus reveal the identity of the valence state of the copper species retained by the stainless steel electodes.

In this treatment it is tacitly assumed that the activity of a fractional monolayer of the reduced species is proportional to its quantity, as was assumed by Herzfeld[24] in his original derivation of the equation for the potential of a partially covered inert electrode.

If, however, more than one oxidation-reduction process is involved in the establishment of the potential, this simple theory will require modification. Specifically, it will be necessary to consider the polarization characteristics of the electrode for the different half-reactions and the alterations in these characteristics produced by addition of the foreign ions.

Accordingly, experiments during the past few months have been directed along the following lines, with concentration upon copper(II) sulfate as the additive:

1. to obtain as precise information as possible concerning the reproducibility of results for electrodes from the same steel with similar surface preparation,
2. to measure more accurately the relation between the deposition of Cu^{64} upon the electrodes and the concentration of cupric ions in solution, making use of both abraded and electropolished electrodes,
3. to determine the degree of reversibility of both the electrode potential and the radioactivity of the electrode when the concentration of cupric ions is progressively diminished,
4. to determine the polarization curves for abraded and electropolished electrodes and the effect of cupric ions upon these curves,
5. to study the anodic and cathodic processes separately by making "composite electrodes" consisting of an electropolished electrode joined through a suitable resistance to an abraded electrode of the same steel; these studies have included measurements of the pickup of Cu^{64} from solution, the interelectrode current, the mixed and separate potentials, and the effect of cupric ions on these quantities.

The studies are incomplete, but certain of the results are shown to indicate the complexity of the problem. Thus, Table 4 summarizes a number of experiments in which the electrochemical slope, $dE/d \log [Cu^{++}]$, and the deposition of Cu^{64} were determined for separate electropolished and abraded electrodes.

It will be noted that, for each surface preparation, closely agreeing results were obtained, although the electropolished specimens had an apparent n value of 2 instead of 1, as found for the abraded specimens. Figures 9 and 10 show the type of data upon which the calculation of the n values depends. It is significant that, although different electrodes have different electrochemical slopes, the ρ values also vary in such a way as to give the same value of n.

In Figs. 11 and 12 the effect of progressive removal of the cupric ions is shown. Whereas the electrode potential falls with essentially the same slope that was observed during the addition of cupric ions, this change is accompanied by hardly any loss of the Cu^{64} activity of the electrode. (More drastic treatment can remove much of this deposited species, probably by oxidation.)

Figure 13 illustrates the polarization curves of the components of a composite electrode. It will be noted that the cathodic polarization is dominant,

[24] K. F. Herzfeld, *Physik. Z.* 14, 29 (1913).

TABLE 4. SUMMARY OF TRACER EXPERIMENTS ON THE EFFECT OF CUPRIC IONS ON THE ELECTRODE POTENTIAL OF STAINLESS STEEL

Experiment No.	Type of Electrode	Electrochemical Slope, $dE/d \log [Cu^{++}]$	ρ	n (Calculated from Eq. 4)
1	Abraded (type 305)	0.057	0.16	1.0_5
2	Abraded (type 305)	0.053	0.25	1.0_1
3	Abraded (type 307)	0.057	0.20	0.9_9
4	Electropolished (type 307)	0.023	0.35	1.9_2
5	Electropolished (type 307)	0.027	0.24	2.0_0
6	Abraded (type 307)	0.045	0.36	1.0_1

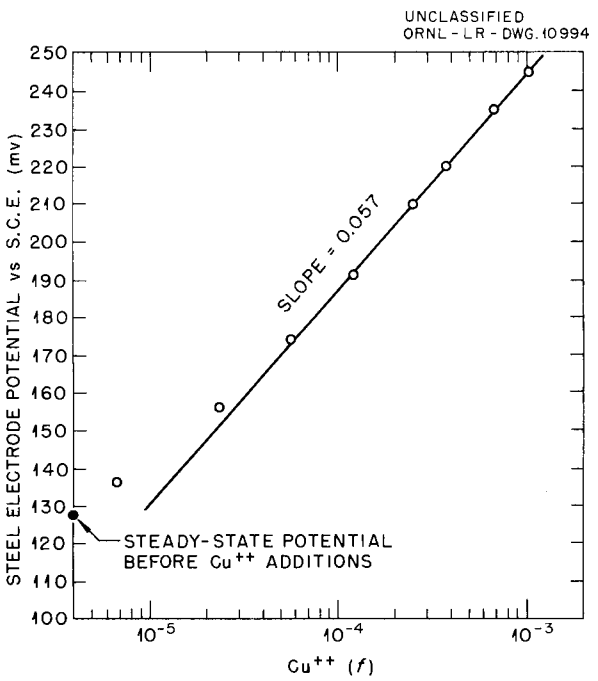

Fig. 9. Addition of $(Cu^{64})^{++}$ to Type 347 Stainless Steel Electrodes Stabilized in Aerated 0.1 N H_2SO_4 at 85°C. $RT/\mathfrak{F}$ at 85°C = 0.071.

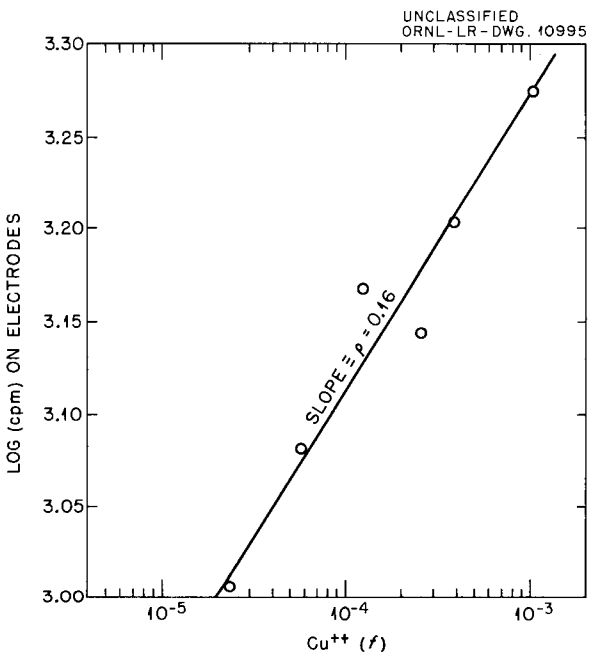

Fig. 10. Addition of $(Cu^{64})^{++}$ to Type 347 Stainless Steel Electrodes Stabilized in Aerated 0.1 N H_2SO_4 at 85°C.

so that the mixed potential, as measured, is close to the separate anodic potential. Figure 14 shows the rate of change of potential when a constant polarizing current was applied and then removed.

The polarization curves for the components of a composite electrode in sulfuric acid and in the solution when sufficient cupric sulfate has been added to make the concentration 2.56×10^{-3} f are shown in Fig. 15. The ennobling of the potential caused by the cupric ions is seen to arise chiefly by elevation of the open-circuit potential of the anode and, to a smaller extent, by both the ennobling of the cathode and the decrease in its polarization resistance (dE/di). Curves C and D show that when electrodes that had gone through a copper

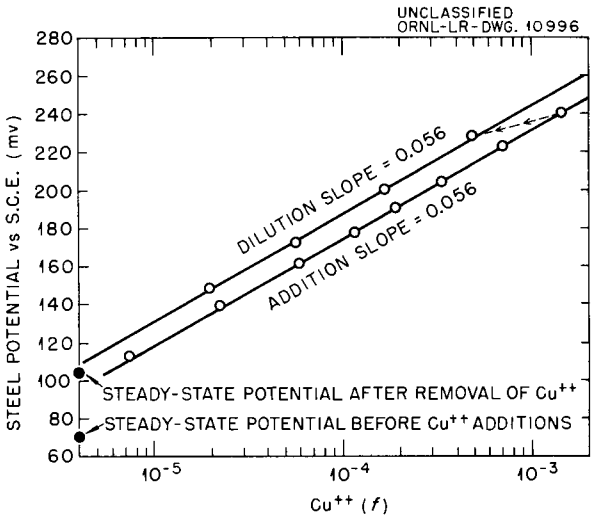

Fig. 11. Addition of $(Cu^{64})^{++}$ to Type 347 Stainless Steel Electrodes Stabilized in Aerated 0.1 N H_2SO_4 at 85°C; Dilution from 1.4×10^{-3} f Cu^{++} to Pure 0.1 N H_2SO_4. $RT/\mathfrak{F}$ at 85°C = 0.071.

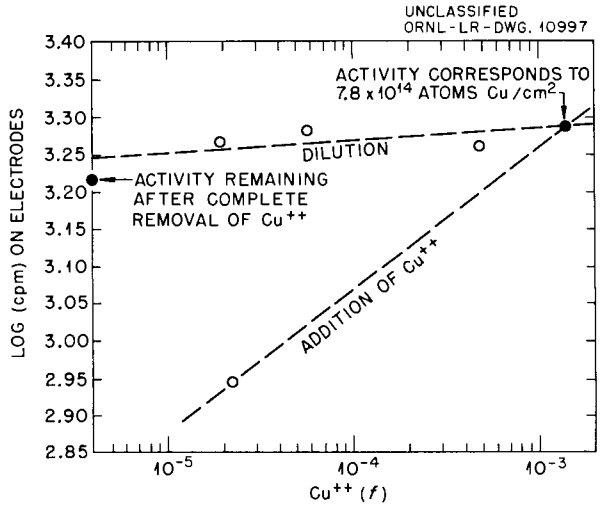

Fig. 12. Addition and Removal of $(Cu^{64})^{++}$; Type 347 Stainless Steel Electrodes Stabilized in Aerated 0.1 N H_2SO_4 at 85°C. Variation of activity of Cu^{64} on electrodes with Cu^{++} concentration in solution.

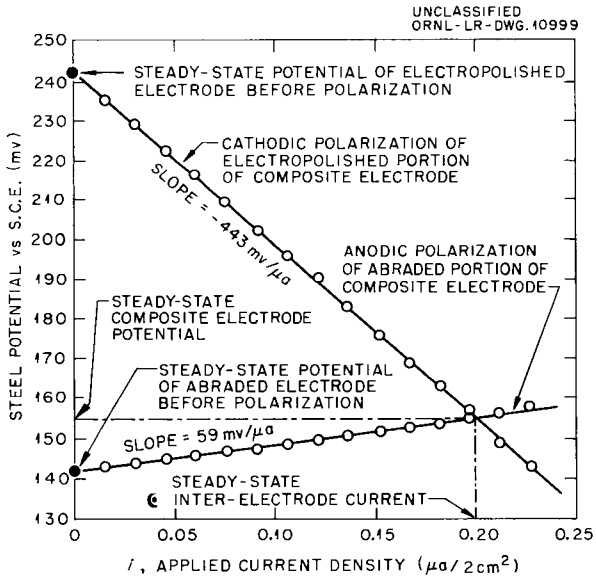

Fig. 13. Polarization Curves for Composite Electrode (Abraded and Electropolished) Stabilized in Aerated 0.1 N H_2SO_4 at 85°C.

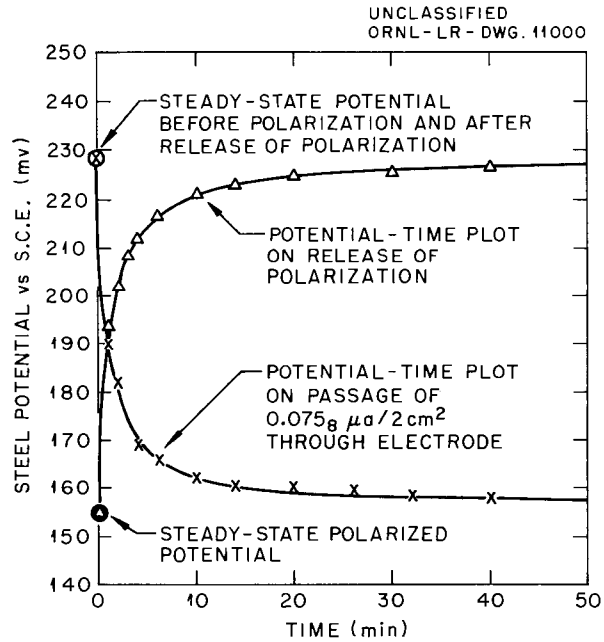

Fig. 14. Potential-Time Behavior of Electropolished Type 347 Stainless Steel Electrode in 0.1 N H_2SO_4 at 85°C with Constant Applied Polarization Current.

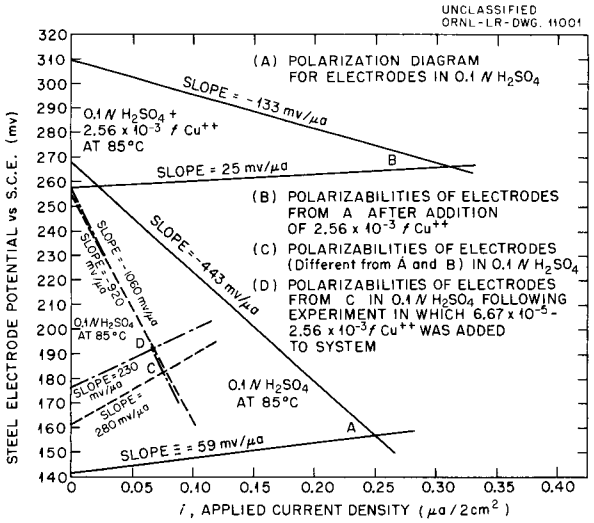

Fig. 15. Effect of Cu^{++} on Polarization Characteristics of Abraded and Electropolished Portions of Composite Type 347 Stainless Steel Electrodes.

sulfate experiment were measured afterward in sulfuric acid alone, the cathodic potential and polarization were essentially unchanged, whereas both the potential and the polarization characteristics of the anode were somewhat altered. The current flowing between the two halves of a composite electrode was found to increase upon addition of cupric ions, although the potentials of the electrodes came closer together as the cupric ion concentration increased.

Equipment has been assembled (by W. E. Clark) for extending the work to include the effect of radiation upon the electrochemical behavior of stainless steel.

HEAT CAPACITY OF RHENIUM HEPTOXIDE FROM 15 TO 300°K. ENTROPY AND FREE ENERGY

R. H. Busey

The low-temperature heat capacity of rhenium heptoxide has been measured over the temperature range 15 to 300°K. The measurements were made in an adiabatic manner by use of the apparatus described previously.[25] The entropy of rhenium heptoxide obtained from these data by application of the third law of thermodynamics, when combined with other thermochemical and equilibrium data, makes possible the computation of more reliable values for the free energy of formation of the heptoxide and perrhenic acid than heretofore possible. No previous heat-capacity data are available for this or for any other heptoxide.

Rhenium Heptoxide Sample

The sample of rhenium heptoxide used was obtained on loan from the University of Tennessee rhenium project. The heptoxide was made from rhenium metal produced by reduction of purified $KReO_4$. The rhenium metal made in this manner usually contains a trace of potassium and only spectroscopic amounts of other elements. The rhenium heptoxide made by burning this metal in oxygen is resublimed at a lower temperature. This method of preparation should yield a product of high purity (>99.9%); consequently, the yellow, crystalline heptoxide was used without further purification. All handling of the sample was done in a vacuum-type dry box. After the sample was placed in the calorimeter and the cap sealed on, the sample was held in a vacuum (through the small hole in the cap of the calorimeter) for 22 hr at room temperature to remove any trace of water. The vapor pressure of water over perrhenic acid is 0.45 mm at room temperature, and the vapor pressure of Re_2O_7 is calculated to be 2×10^{-10} mm at the same temperature.[26] A preliminary sample weight was obtained when the calorimeter was filled, and a final check weight was obtained when the sample was removed from the calorimeter. The sample weight was 168.787 g (*in vacuo*), which represents 0.34829 mole of Re_2O_7. One atmosphere pressure of helium was added to ensure rapid thermal equilibrium.

Noddack and Noddack[27] state that the yellow color of Re_2O_7 fades at -80°C, but they give no details of the observation. This is of interest because such a phenomenon may have an associated energy effect. To check this observation a 30-g sample of Re_2O_7 contained in a weighing bottle was exposed to a high vacuum. A pressure of 0.16 mm of nitrogen was then introduced and an

[25] R. H. Busey, *A Combination Isothermal-Adiabatic Low-Temperature Calorimeter*, ORNL-1828 (Jan. 26, 1955).

[26] Wm. T. Smith, Jr., L. E. Line, Jr., and W. A. Bell, *J. Am. Chem. Soc.* 74, 4964 (1952).

[27] I. Noddack and W. Noddack, *Z. anorg. u. allgem. Chem.* 181, 1 (1929).

unsilvered Dewar of liquid nitrogen placed around the sample. No change in color was observed in cooling to nitrogen temperatures. A high vacuum (10^{-6} mm) was again established and the sample allowed to warm slowly to room temperature (2 hr required) and again to cool slowly (2 hr required) to nitrogen temperatures. In neither case was a color change observed.

Calorimeter

A gold calorimeter was used to hold the sample of rhenium heptoxide. It was made from 20-mil gold sheet, using Heliarc-welded joints. The calorimeter weighs 133 g, is 3.2 cm in diameter and 7.3 cm in height, and has an internal volume of 50.7 ml. Ten radial vanes of 5-mil gold sheet 2.2 cm wide and 6.4 cm long were forge-welded their full length to the inside cylindrical wall of the calorimeter to facilitate heat transfer. The calorimeter is provided with a gold, Wood's-metal-filled, thermocouple well on the bottom and three eyelets on the top for suspending the calorimeter with nylon thread from the top of the adiabatic shield. The filling port is similar to that employed by Adams, Johnston, and Kerr.[28] In order to make replacement possible, the sealing groove or trough circumscribing the filling port is Heliarc-welded to the top of a 6.5-mm-OD filling port. The cap provided with the usual gas evacuation hole is soldered to the calorimeter by use of Wood's metal in the trough. After the calorimeter is evacuated and filled with helium to a pressure of 1 atm, the small hole in the cap is closed with Wood's metal. This type of cap eliminates the possibility of solder dropping into the calorimeter and should prove satisfactory for measurements on low-vapor-pressure corrosive compounds to be measured in this laboratory in the future.

A combination resistance thermometer-heater was wound on the calorimeter as follows. The cylindrical portion of the calorimeter wall was coated with a solution of G-E adhesive 7031 and lens paper and allowed to air-dry. The resistance thermometer-heater made from B & S No. 40 (gold + 0.15% silver added) enameled wire was then wound on the calorimeter, covering the whole cylindrical side. A total of 710 turns was used, which gave the thermometer a resistance of 378 ohms at room temperature and an average dR/dT of 1.23 ohms/deg from 50 to 300°K. Several coats of G-E adhesive 7031 solution were applied to hold the wire securely to the calorimeter, which was finally dried in an oven at 125°C for 1 hr.

The differential thermocouple well was constructed as follows. A 2-mil copper sheath was sealed with G-E adhesive 7031 around the calorimeter, completely covering the resistance thermometer, and lens paper was interposed between the sheath and the resistance thermometer. The overlapping edges were tinned, making it possible to solder the sheath firmly over the resistance thermometer. In the middle of one of these edges, a 7-mm-wide ribbon was provided when the sheath was cut. The ribbon was tinned and rolled up to form a well for the differential thermocouple. The copper sheath was then covered with gold foil to reduce heat leak by radiation. After the calorimeter was dried in air overnight, it was again placed in an oven at 125°C for 1 hr.

Only two heater leads of B & S No. 40 enameled copper wire are provided at the calorimeter. The current and potential leads are connected to these lead wires via two 3-cm lengths of B & S No. 18 enameled copper wire, which are thermally anchored to the bottom of the adiabatic shield. The copper lead wire between the calorimeter and the shield is calibrated; hence an appropriate correction for the heat generated in the leads is made.

Heat-Capacity Data

The heat-capacity observations on rhenium heptoxide determined by the adiabatic method are given in Table 5. Temperature increments of the individual determinations can be inferred from the adjacent mean temperatures. No correction for curvature has been made. The measurements were continuous in that the calorimeter was never cooled overnight by more than 1 to 2 deg. The energy to the shields is readily adjusted to keep the calorimeter at almost constant temperature overnight. The results are expressed in terms of the defined thermochemical calorie equal to 4.1840 absolute joules. The ice point was taken to be 273.16°K, and the molecular weight of rhenium heptoxide was taken as 484.62. The measurements of series 1 were made before the sample was cooled, and those of series 3 were made because of temporary difficulty in cooling the sample to the lowest temperatures in series 2.

[28] G. B. Adams, Jr., H. L. Johnston, and E. C. Kerr, *J. Am. Chem. Soc.* **74**, 4784 (1952).

TABLE 5. HEAT CAPACITY OF Re_2O_7

T_{av} (°K)	C_p (cal·deg^{-1}·mole^{-1})	T_{av} (°K)	C_p (cal·deg^{-1}·mole^{-1})
Series 1		Series 2	
300.93	39.88	178.41	30.55
307.49	40.28	185.90	31.30
		193.54	32.01
Series 2		201.37	32.72
19.53	2.811	209.24	33.39
22.83	3.695	217.22	34.06
26.37	4.614	225.67	34.73
29.43	5.363	234.23	35.41
32.23	6.050	242.82	36.04
35.23	6.787	251.45	36.63
38.62	7.591	260.10	37.25
42.49	8.470	268.75	37.85
46.91	9.466	277.42	38.42
51.65	10.45	286.09	39.00
56.42	11.49	294.76	39.50
61.56	12.57	303.75	40.06
67.13	13.72		
72.89	14.83	Series 3	
78.25	15.88	15.36	1.631
84.01	16.99	17.74	2.337
89.92	18.13	20.56	3.135
95.94	19.22	23.58	3.888
102.04	20.29	26.55	4.646
108.55	21.40	30.08	5.521
115.52	22.49	33.47	6.348
122.23	23.52	36.46	7.080
128.79	24.51	39.84	7.884
135.64	25.48	43.52	8.714
142.83	26.45	47.74	9.636
149.95	27.35	52.08	10.54
156.97	28.19	56.27	11.44
164.21	29.02	60.67	12.38
171.30	29.80		

Thermodynamic Functions of Rhenium Heptoxide

Smoothed values of the thermodynamic properties obtained from large-scale graphs are given in Table 6. The entropy below 15°K was estimated by utilizing the Debye T^3 law. The smoothed heat capacities listed are believed to be accurate to 5% at 15°K, to 1% at 25°K, and to 0.1% above 40°K. The entropy of the heptoxide given at 298.16°K should be accurate to 0.1%, that is, 49.54 ± 0.05 cal·deg^{-1}·mole^{-1}.

Thermochemical Calculations

The vapor-pressure measurements of Smith, Line, and Bell[26] on rhenium heptoxide and perrhenic

TABLE 6. SMOOTHED VALUES OF THERMODYNAMIC PROPERTIES OF Re_2O_7

T (°K)	C_p^0	S^0	$\frac{H^0 - H_0^0}{T}$	$-\frac{F^0 - H_0^0}{T}$
	(cal·deg^{-1}·mole^{-1})			
15	1.533	0.525	0.390	0.135
20	2.956	1.164	0.857	0.307
25	4.254	1.963	1.406	0.557
30	5.502	2.849	1.985	0.864
35	6.725	3.789	2.575	1.214
40	7.902	4.765	3.168	1.597
45	9.032	5.761	3.757	2.004
50	10.12	6.769	4.339	2.430
60	12.24	8.802	5.480	3.322
70	14.28	10.844	6.593	4.251
80	16.25	12.880	7.678	5.202
90	18.14	14.904	8.736	6.168
100	19.93	16.908	9.766	7.142
110	21.62	18.888	10.768	8.120
120	23.20	20.838	11.739	9.099
130	24.69	22.754	12.678	10.076
140	26.08	24.635	13.586	11.049
150	27.36	26.479	14.462	12.017
160	28.54	28.283	15.306	12.977
170	29.66	30.047	16.118	13.929
180	30.71	31.773	16.900	14.873
190	31.69	33.460	17.653	15.807
200	32.60	35.109	18.378	16.731
210	33.45	36.720	19.075	17.645
220	34.27	38.296	19.748	18.548
230	35.06	39.837	20.396	19.441
240	35.82	41.345	21.023	20.322
250	36.55	42.822	21.630	21.192
260	37.26	44.269	22.217	22.052
270	37.94	45.687	22.786	22.901
273.16	38.15	46.129	22.963	23.166
280	38.60	47.079	23.340	23.739
290	39.24	48.445	23.877	24.568
298.16	39.73	49.540	24.304	25.236
300	39.85	49.785	24.399	25.386

acid make possible the calculation of the following entropy changes at 298.16°K:

(1) $Re_2O_7(cryst) = Re_2O_7(g)$,

$\Delta S^\circ = 55.5 \pm 0.2$ cal·deg^{-1}·mole^{-1} ;

(2) $2HReO_4(cryst) = Re_2O_7(cryst) + H_2O(g)$,

$\Delta S^\circ = 22.0 \pm 0.1$ cal·deg^{-1}·mole^{-1} .

These data, combined with the above value for the entropy of rhenium heptoxide (49.54 cal·deg^{-1}·

mole^{-1}) and the entropy[29] of $H_2O(g)$ (45.13 cal·deg^{-1}·mole^{-1}), give:

$$S^{\circ}_{298.16}\,[Re_2O_7(g), \text{ ideal gas at 1 atm}] = 105.0 \pm 0.3 \text{ cal·deg}^{-1}\text{·mole}^{-1},$$

$$S^{\circ}_{298.16}\,[HReO_4(cryst)] = 36.4 \pm 0.2 \text{ cal·deg}^{-1}\text{·mole}^{-1}.$$

Two separate determinations of the heat of formation of rhenium heptoxide have been made; Roth and Becker[30] obtained –297.5 ± 2.0 kcal·mole^{-1} and Boyd *et al.*[31] obtained –295.9 ± 2.0 kcal·mole^{-1}. The average of the two values, –296.7 ± 2.0 kcal·mole^{-1}, combined with the entropy of formation,[32] –139.78 cal·deg^{-1}·mole^{-1}, gives –255.0 ± 2.0 kcal·mole^{-1} for the free energy of formation of rhenium heptoxide. The free energy of formation of crystalline perrhenic acid, –157.0 ± 1.0 kcal·mole^{-1}, may be obtained from the free energies of formation of $H_2O(g)$, –54.64 kcal·mole^{-1} (ref. 33), and $Re_2O_7(cryst)$, –255.0 kcal·mole^{-1}, combined with the standard free energy change of reaction 2, 4.5 kcal·mole^{-1}, computed from the vapor-pressure equation of Smith *et al.*[26]

CHEMISTRY OF FUSED SALTS

E. R. Van Artsdalen

Electrical Conductance and Density

I. S. Yaffe

The density and specific electrical conductance have been measured for all molten alkali chlorides, bromides, and iodides up to about 200°C above the melting points, and the corresponding equivalent volume and equivalent conductance have been calculated at various temperatures from the data. The data not reported heretofore[34] are presented in Table 7 expressed in terms of the type of equations described previously. It is expedient to make comparisons among different substances at some corresponding temperature. The melting points can be considered as corresponding temperatures and the physical properties compared at the same fraction above the melting point. On this basis a corresponding temperature, θ, is defined as $\theta = T/T_m$, where T is the temperature (°K), and T_m is the melting point (°K). Figure 16 shows the equivalent volume of the liquid alkali chlorides, bromides, and iodides as a function of the equivalent volume of the solid at the melting point. Equivalent-conductance data for all these salts as a function of θ are presented in Fig. 17. It can be seen that there are trends among the various salts. The activation energy, $\Delta H^{\ddagger}$, discussed previously,[34] is temperature dependent and is plotted in Fig. 18. The entropy of activation, $\Delta S^{\ddagger}$, is shown in Table 7. The data reported here serve to complete the series.

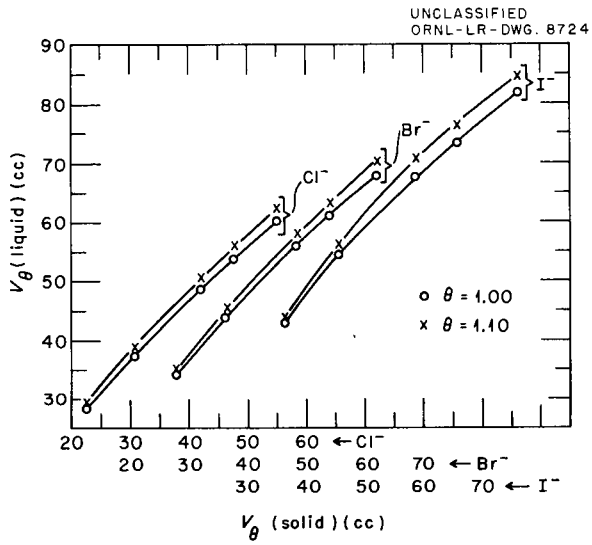

Fig. 16. Equivalent Volume of Fused Halides.

Present knowledge of the fused-salt state is so incomplete that it has not been possible to arrive at a detailed theoretical interpretation of electrical conductance. In general it may be said that

[29] K. K. Kelley, *Contributions to the Data on Theoretical Metallurgy. Part XI. Entropies of Inorganic Substances*, Bureau of Mines Bulletin 477, 1950.

[30] W. A. Roth and G. Becker, *Z. physik. Chem.* A159, 27 (1932). Data have been recalculated and summarized in *Selected Values of Chemical Thermodynamic Properties*, by F. D. Rossini *et al.*, NBS-500, U.S. Government Printing Office, Washington, 1952.

[31] G. E. Boyd, J. W. Cobble, and Wm. T. Smith, Jr., *J. Am. Chem. Soc.* 75, 5783 (1953).

[32] S^0_{Re} = 8.89 cal·deg^{-1}·mole^{-1} [see Wm. T. Smith, Jr., G. D. Oliver, and J. W. Cobble, *J. Am. Chem. Soc.* 75, 5785 (1953)]; $S^0_{O_2}$ = 49.01 cal·deg^{-1}·mole^{-1} (see ref. 29).

[33] F. D. Rossini *et al.*, *Selected Values of Chemical Thermodynamic Properties*, NBS-500, U.S. Government Printing Office, Washington, 1952.

[34] I. S. Yaffe and E. R. Van Artsdalen, *Chem. Semiann. Prog. Rep. June 20, 1955*, ORNL-1940, p 12.

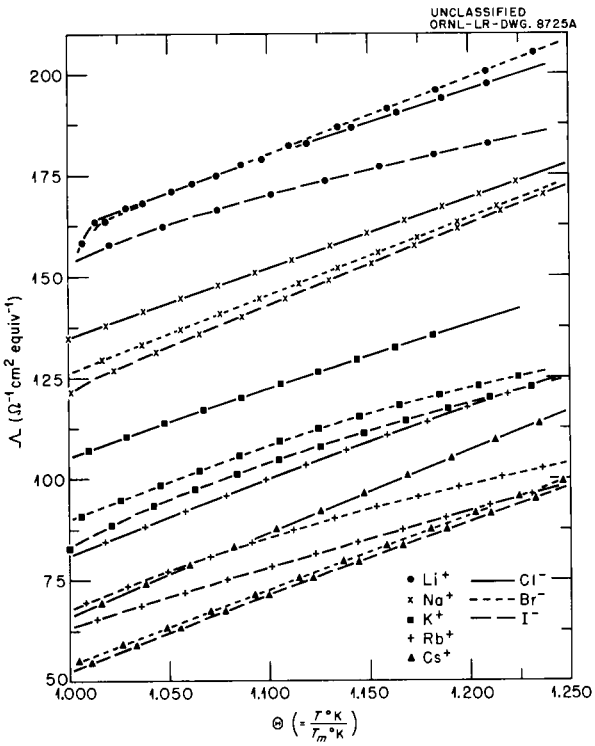

Fig. 17. Equivalent Conductance of Alkali Halides.

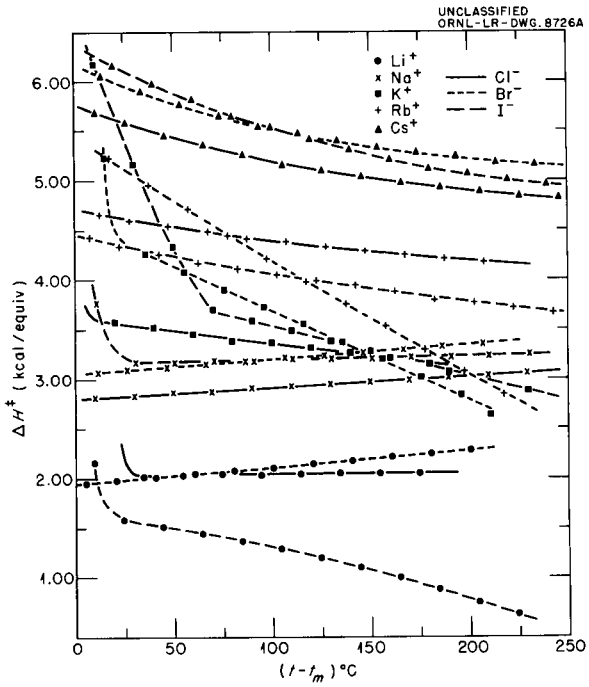

Fig. 18. Energy of Activation for Conductance.

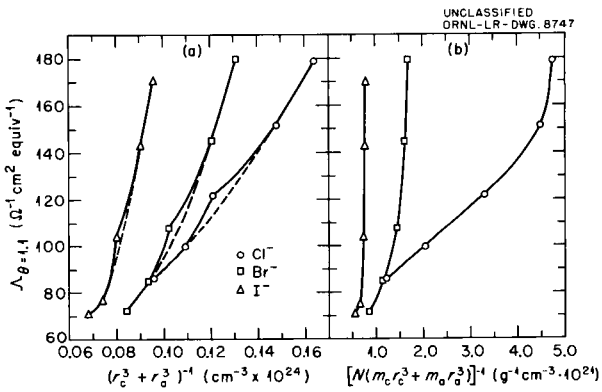

Fig. 19. Equivalent Conductance vs Functions of Volume and Mass.

conductance would be expected to depend upon the size and mass of the conducting ions. Figure 19 shows that a plot of equivalent conductance, Λ, against the reciprocal volume does not represent a smooth function. However, a more or less smooth plot is obtained when Λ is plotted against the reciprocal of the product of mass and volume of the conducting ions. Data for the alkali chlorides, bromides, and iodides were summarized in a paper presented at a Symposium on Nonaqueous Electrochemistry before the American Chemical Society Meeting in September and will be published as a part of this Symposium.

Preliminary measurements of conductance and density have been made on pure molten lanthanum chloride, lanthanum bromide, and gadolinium chloride.[35] The anhydrous salts were obtained by vacuum dehydration of purified hydrated salts, followed by sublimation at 1000°C. First determinations were not so precise as desired, and the work will be repeated with a slight modification of experimental technique, which it is hoped will lead to better and more reliable data.

Development work on a "matched transformer bridge" has been successfully completed. This bridge has been designed and built with the close cooperation of members of the Instrumentation and Controls Division, particularly E. Fairstein. It

[35]Obtained through the courtesy of B. Weaver and C. P. Keim of the Stable Isotopes Research and Production Division.

TABLE 7. DENSITY AND CONDUCTANCE OF ALKALI HALIDES

Salt	Measured Range (°C)	Density, $\rho = a - b \times 10^{-3}t$ (g/cc)		Standard Deviation (g/cc)	Specific Conductance, $\kappa = a + b \times 10^{-3}t - c \times 10^{-6}t^2$ (mhos·cm^{-1})			Standard Deviation (mhos·cm^{-1})	$-\Delta S^{\ddagger}$ at 850°C (cal·deg^{-1}·mole^{-1})
		a	b		a	b	c		
LiBr	552–740	2.8878	0.6520	0.0004	$+1.009_5$	0.7834	2.057	0.002	6.2
LiI	475–670	3.539_7	0.9176	0.003	−0.578	1.348	9.695	0.006	8.2
CsBr	637–860	3.9109	1.2234	0.0003	-1.413_7	0.4255	1.228	0.002	6.3

has been possible to determine the a-c resistance of standard 0.8- and 1-ohm d-c resistors with an accuracy of better than 0.05%. Preliminary experimentation, in which molten sodium nitrate was the unknown, was satisfactory when a new type of cuplike concentric arrangement of platinum electrodes was used. A platinum-rhodium alloy electrode assembly has been ordered. It is planned to use this bridge and the electrodes to measure the electrical conductance of highly corrosive fused salts, particularly fluorides, which cannot be used with "fused" quartz capillary cells.

Self-Diffusion in Molten Salts

A. S. Dworkin D. Brown[36]

The self-diffusion coefficients of both Na^+ and NO_3^- ions have been determined in molten sodium nitrate in the temperature range 315 to 375°C. The data for Na^+ have been reported previously[37] but are included here for reference and discussion purposes. The technique for measuring self-diffusion in aqueous solutions has been described in detail by Wang and Kennedy[38] and tested also by numerous investigators. In the experiments with molten sodium nitrate the rate of diffusion is measured similarly by allowing a tracer ion to diffuse from a capillary, one end of which is closed, into a large, stirred bath of "dead" sodium nitrate.

Ten different quartz capillaries were used in the measurements. They had a bore of 0.6 to 0.7 mm, lengths between 3.3 and 4.7 cm, and contained from 22 to 34 mg of $NaNO_3$. The duration of experiments was 50 to 99 hr for Na^+ ion diffusion and 93 to 177 hr for NO_3^- ion. From 57 to 77% of the initial concentration of tracer was permitted to diffuse out of the capillaries during the measurement; in about half the cases the amount lay between 65 and 70%. The capillaries were filled in the apparatus shown in Fig. 20 by the following method. Molten $NaNO_3$ from the reservoir G was sucked into the filling tube E by means of a screw syringe. The filling tube was then maneuvered into the quartz capillary D. The salt was forced into the capillary, filling it from the bottom as the filling tube was raised, thereby preventing the trapping of air bubbles.

When the capillaries were filled they were transferred to the furnace in which the measurements were made. The salt was not allowed to freeze until completion of the experiment; otherwise, air bubbles would have formed in the capillary. The diffusion coefficient, D, was calculated from the equation

$$(1)\quad D = 0.93337 \left(\frac{l^2}{t}\right) \log \left[0.81057 \left(\frac{c_0}{c}\right) \right],$$

where l is the length of the capillary, c_0 is the initial concentration of tracer, and c is its concentration after time t. The initial Na^{22} tracer concentration was determined by filling a capillary with active $NaNO_3$; dipping it into a dead $NaNO_3$ bath (maintained at the desired temperature) to equilibrate it thermally and to wash active material from the outside of the capillary; removing it from

[36] Summer employee, Arizona State College.

[37] A. S. Dworkin, D. Brown, and E. R. Van Artsdalen, *Chem. Semiann. Prog. Rep. June 20, 1955*, ORNL-1940, p 13.

[38] J. H. Wang and J. W. Kennedy, *J. Am. Chem. Soc.* 72, 2080 (1950).

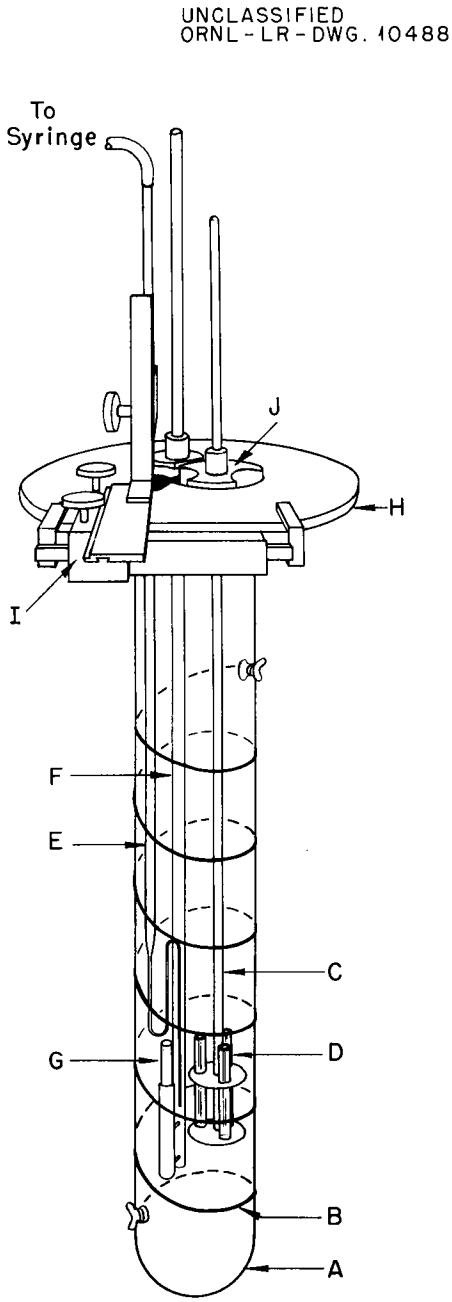

Fig. 20. Capillary Filling Device. A, pyrex tube; B, nichrome heating ribbon; C, platinum capillary holder; D, quartz capillaries; E, quartz filling tube drawn to fine capillary at end; F, pyrex tube – cup holder and thermocouple tube; G, platinum cup – salt reservoir; H, aluminum top; I, tridimensional control for filling tube; J, three-position plug for capillary holder.

the bath; cleansing, drying, and weighing; and counting in a 4π high-pressure ion chamber. The average of 14 c_0 determinations for Na^{22} was 13.8 (on a 10^{10} scale) ± 1% per milligram of $NaNO_3$; c_0 for the individual runs was computed from this value and the measured weight of salt in the capillary. The initial O^{18} concentration of the nitrate was obtained in a similar way. After the outside of the capillary was cleansed of all dead salt, the $NaNO_3^{18}$ in the capillary was washed into a small beaker by a stream of distilled water from a fine hypodermic needle and evaporated to dryness. A mass spectrographic analysis was made for the O^{18} content of the oxygen. The initial tracer material showed an O^{18} content of 0.7090%, while the dead bath had 0.2078%. The ratio c_0/c is given by

$$\frac{c_0}{c} = \frac{0.7090 - 0.2078}{x - 0.2078} ,$$

where x is the O^{18} content of the $NaNO_3$ in the capillary after diffusion. The dead salt bath contained about 800 g of cp $NaNO_3$.

The results of the measurements are plotted in Fig. 21. The self-diffusion coefficient of Na^+ in fused $NaNO_3$ is expressed by the equation

$$(2) \qquad D_+ = 1.288 \times 10^{-3}\, e^{-4970/RT} .$$

The probable error in $\Delta H^{\ddagger}$ is 80 cal (±1.6%) and the probable error in D_+ is 0.033 (± 1.2 to 1.8%). The diffusion coefficient for NO_3^- ion in fused $NaNO_3$ is likewise given by the equation

$$(3) \qquad D_- = 0.8974 \times 10^{-3}\, e^{-5083/RT} .$$

The probable error in $\Delta H^{\ddagger}$ is 80 cal (±1.6%), while the probable error in D_- is 0.013 (± 0.7 to 1.1%). The relative rates of self-diffusion of Na^+ and NO_3^- in this salt are very nearly proportional to the inverse square roots of their masses. This result is suggestive of the applicability of Graham's law of effusion as an approximation. It appears that $\Delta H^{\ddagger}$ is temperature-independent over the rather short temperature range of these investigations. It is significant that the heat of activation for self-diffusion of Na^+ is approximately equal to that for NO_3^-. This indicates that the potentials restricting the migration of these ions are essentially the same and that the migration of each ion past the other

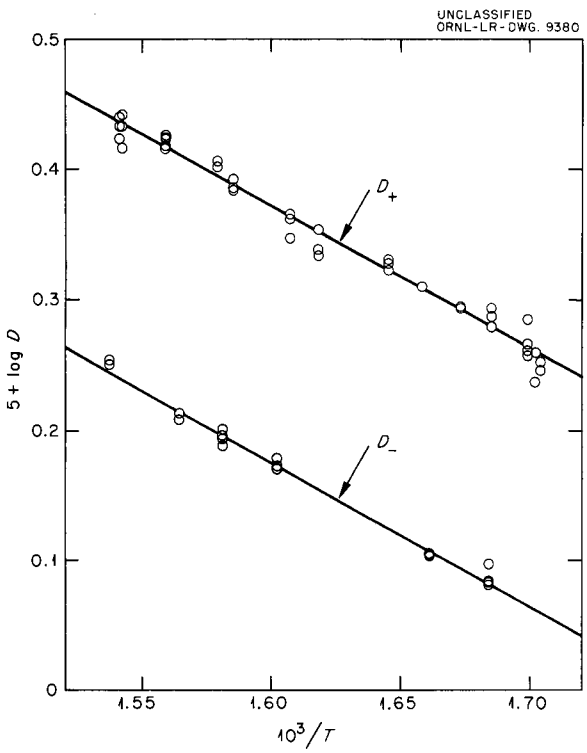

Fig. 21. Self-Diffusion Coefficients in Fused Sodium Nitrate. D_+ of Na^+ and D_- of NO_3^-.

is a complementary process. The entropy of activation for self-diffusion of the ions in $NaNO_3$ has been calculated by means of the equation

$$D = e\,\lambda^2 \frac{kT}{h} e^{\Delta S^{\ddagger}/R} e^{-\Delta H^{\ddagger}/RT} \tag{4}$$

proposed by Eyring,[39] where λ is the migration distance, k the Boltzmann constant, h is Planck's constant, and $\Delta S^{\ddagger}$ and $\Delta H^{\ddagger}$ the entropy and heat of activation, respectively. For the purpose of this calculation λ has been estimated from the known molar volume of fused sodium nitrate, and the calculation has been made at 615.4°K, the mid-point of the experimental study. The values are $\Delta S^{\ddagger}_{+} = -8.2$ e. u. and $\Delta S^{\ddagger}_{-} = -8.9$ e. u., which appear to be reasonable although no quantitative significance should be attached to them at this time. They may be compared with the calculated $\Delta S^{\ddagger}$ for electrical conductance in molten sodium nitrate, $\Delta S^{\ddagger} = -6.0$ or -8.5 e. u., depending on whether the dielectric constant is considered to be 3 or 15. These latter values were obtained by using Wetmore's data[40] for conductance by sodium nitrate and the equation given previously.[41]

The Nernst-Einstein equation

$$\Lambda_i = \frac{D_i z_i \mathcal{F}^2}{RT} \tag{5}$$

cannot be used to calculate transport numbers for the individual ions from the self-diffusion coefficient of molten sodium nitrate at 615.4°K. The measured value[40] of Λ is 51.0 mhos·cm^{-2}·equiv^{-1}. The sum of the Λ's calculated from the Nernst-Einstein equation and from the experimentally measured values of D is 65.7 mhos·cm^{-2}·equiv^{-1}. Thus this equation predicts a conductivity that is 29% too large.

A number of Na^+ diffusion runs were made with larger quartz capillaries, approximately 1-mm bore, to determine whether capillary size might be of special significance and to obtain an idea of the probable error. The results are shown in Table 8, where they are compared with the values calculated from Eq. 2. It is clear that the deviations in both precision and accuracy are greater with the larger capillaries. This can probably be ascribed to a greater influence of convection currents with larger-bore capillaries. However, it can be noted that at 343°C, where the most detailed comparison was made, there is very little difference between the results. Temperature-coefficient data are the same with capillaries of both sizes. It is important, however, that the larger capillaries give somewhat higher results.

A study of the self-diffusion of both ions in fused potassium nitrate is currently under way. This should give information about the effect of cation size. It is planned to make measurements of a series of other salts, particularly of halides with cations and anions of different sizes. Preliminary work along these lines has been initiated, but considerable difficulty has been experienced in filling capillaries at temperatures around 800°C by the method described above; so a new scheme is under study for this purpose.

[39] S. Glasstone, K. J. Laidler, and H. Eyring, *The Theory of Rate Processes*, p 524, McGraw-Hill, New York, 1941.

[40] J. Byrne, H. Fleming, and F. E. W. Wetmore, *Can. J. Chem.* 30, 922 (1952).

[41] I. S. Yaffe and E. R. Van Artsdalen, *Chem. Semiann. Prog. Rep. June 20, 1955*, ORNL-1940, p 12.

TABLE 8. SELF-DIFFUSION OF Na^+ IN $NaNO_3$ – EFFECT OF LARGE-BORE CAPILLARIES

Temperature (°C)	D_+ (Measured, 1-mm bore)	D_+ (Calculated, 0.65-mm bore)
316	1.898 ± 0.044 (3 points)	1.840
324.6	1.985 ± 0.095 (2 points)	1.955
343.0	2.229 ± 0.061 (9 points)	2.225
367.5	2.688 ± 0.064 (3 points)	2.595
369.4	2.745 ± 0.069 (3 points)	2.625

Cryoscopy

J. E. Sutherland E. R. Van Artsdalen

The measurements described in the last report[42] involving incomplete dissociation of certain halides dissolved in molten sodium nitrate have been extended. The "common-ion effect" has been shown to be applicable to a number of additional halides. The following reactions appear to be the most important:

$$MX_2 \rightleftharpoons M^{++} + 2X^- \qquad K_{20}$$

$$MX_2 + 2X^- \rightleftharpoons MX_4^{--} \qquad K_{24}$$

Indeed, no evidence has been obtained for the existence of other species under the conditions of these experiments. Equilibrium constants for these reactions have been calculated from experimental data at about 300°C for the series of salts presented in Table 9.

Many other salts have been studied in fused $NaNO_3$ by the freezing-point-depression method. Most of them behave ideally or in the pattern shown by the examples in Table 9. However, there are a few exceptions and these are under further investigation. Some suggestive information has been obtained that deviations from simple additivity may be observed when relative sizes of solute and solvent ions differ greatly. In particular, results of this nature obtained with KNO_3 as solvent must await a better determination of its cryoscopic constant before definite conclusions can be reached.

Samples of K_2TiF_6 and K_2ZrF_6 were prepared by wet chemical methods. Analyses showed them to be of high purity. Freezing-point-depression measurements were made with these salts in sodium nitrate. A small amount of chemical reaction took place between them and the sodium nitrate, yielding traces of nitrogen oxides. Beyond this, however, the freezing-point-depression measurements showed that both TiF_6^{--} and ZrF_6^{--} are moderately stable in fused $NaNO_3$ at its melting point. However, it appears that they dissociate somewhat as infinite dilution is approached, presumably to yield F^- and the corresponding MF_5^- ion. The ZrF_6^{--} is more stable than TiF_6^{--}. The degree of dissociation decreases with rising concentration, and, at concentrations above 0.05 *m*, K_2TiF_6 acts as if it is less than completely dissociated to $2K^+$ and TiF_6^{--}, while K_2ZrF_6 shows some evidence of this behavior above about 0.1 *m*. Taken at face value this would indicate partial association of TiF_6^{--} with either K^+ or other TiF_6^{--} ions. The results with these potassium salts agree with and extend previous studies[43] made with Na_2ZrF_6 prepared by dry chemical techniques.

TABLE 9. EQUILIBRIUM CONSTANTS

	K_{20}	K_{24}	K_{02}
CdF_2	0.038 ± 0.004	0.9 ± 1.0	27
$CdCl_2$	0.0031 ± 0.0004	4.4 ± 0.8	320
$CdBr_2$	0.00035 ± 0.00011		2900
$PbCl_2$	0.033 ± 0.005	(0.2)	30
$ZnCl_2$	0.0026 ± 0.0002	5.1 ± 0.2	380

[42] J. E. Sutherland and E. R. Van Artsdalen, *Chem. Semiann. Prog. Rep. June 20, 1955*, ORNL-1940, p 14.

[43] A. S. Dworkin *et al.*, *Chem. Semiann. Prog. Rep. Dec. 20, 1953*, ORNL-1674, p 21, esp. 26.

High-Temperature Calorimetry

D. J. Sasmor

The work in high-temperature calorimetry was delayed by breakdown of the amplifiers of the adiabatic calorimeter. Repairs are being made. The complete electrical system has been permanently wired and incorporated in control panels. Calibration work will continue with the use of synthetic sapphire as the standard.

Exchange Reactions in Fused Salts

J. E. Boggs[44] L. N. Devonshire[45]
E. R. Van Artsdalen

Series of exploratory experiments were performed to develop procedures for investigating kinetics and mechanisms of exchange reactions among various ionic species in fused salts. The more difficult aspects of these studies involve quantitative separation of reactants so that tracer analyses can be made on pure materials. Sometimes it is possible to make good separations by precipitation from aqueous solution, but it is necessary first to establish that no induced exchange takes place in such a step.

A major part of these studies was concerned with the exchange of oxygen between various complex anions containing constitutional oxygen. The tracer was O^{18}, which was followed mass spectrographically. A typical kind of preliminary study involved the exchange of oxygen between NO_3^- and CO_3^{--} when the sodium salts were used. Rapid exchange of oxygen was found between nitrate and carbonate in a 3 mole % solution of Na_2CO_3 in $NaNO_3$ at 350°C. However, exchange appeared to be quite slow when each of these reactants was dissolved at a concentration of 3 mole % in a silver iodide–silver chloride eutectic mixture at 350°C. Experiments to determine the specific influence of silver ion on the exchange were inconclusive. It is suggested that a possible mechanism for exchange of this type may involve the O^{--} ion as an intermediate. Much more work remains to be done, including investigation of the effect of dissolved O_2 and H_2O, before the details of kinetics and mechanisms can be understood.

[44]Summer employee, University of Texas.

[45]Summer research participant, University of Alabama.

Hydrogen Fluoride–Fluoromethane Reactions

J. E. Boggs

Previous studies[46] showed that there was no exchange of F^{18} between HF and several fluoromethanes up to temperatures of 500°C. The work has been extended to include fluoromethane itself, which was prepared by the pyrolysis of an intimate mixture of anhydrous KF and sodium methylsulfate, CH_3OSO_3Na. The fluoromethane was shown to be of high purity by the usual physical tests; it did not exchange fluorine with HF at temperatures below 400°C. The studies could not be extended above this temperature because of decomposition of CH_3F. Thus none of the series of compounds CF_4, CHF_3, CH_2F_2, CH_3F, and CF_2Cl_2 exchange fluorine with HF. Therefore, it is impossible to use this method of kinetic study for estimating differences in C-F bond dissociation energies.

Florine Exchange Between Salts and Gases

T. A. Gens[47]

Heterogeneous catalysts for the synthesis of fluorocarbons would be exceedingly useful. Presumably, a potential catalyst for such a synthesis would be capable of exchanging fluorine with fluorocarbons at a reasonable rate. It has been decided to carry out an exploratory study of exchange of fluorine between a series of typical salts and various gaseous compounds of fluorine.

It is planned to incorporate F^{18} into various fluoride salts, circulate a fluorocarbon gas over them in a furnace capable of maintaining a range of fixed temperatures, and observe how readily fluorine exchange occurs. An all-glass high-vacuum system has been built, with one portion designed to remove air and moisture and to carry out trap-to-trap distillations of fluorocarbons. A second portion of the glass vacuum system is designed for circulating and counting the gases. The gas will be circulated through a special scintillation counter so that a continuous record of exchange may be obtained. The necessary electronic counting and control equipment is on order and its assembly should be completed shortly.

[46]J. E. Boggs, *Chem. Semiann. Prog. Rep. Dec. 20, 1954*, ORNL-1832, p 20.

[47]ORINS Fellow 1955–56, University of Florida.

The only useful tracer for fluorine is F^{18}, which has a 112-min half life. Therefore, it must be produced daily for experimental purposes. A number of practice runs to prepare F^{18} have been made by the methods described by Boggs.[46] A few metal fluorides containing F^{18} were prepared by exchange with HF^{18} produced from the material irradiated in the ORNL Graphite Reactor and in the LITR.

HIGH-TEMPERATURE AND STRUCTURAL CHEMISTRY. LIQUID METAL–SALT SOLUTIONS[48]

Phase Equilibria in the Potassium Metal–Potassium Chloride System

M. A. Bredig J. W. Johnson

The study of the liquid-liquid and liquid-solid phase equilibria in the KCl-K system was all but completed.[49] Figure 22 gives a phase diagram which is believed to be subject finally to only very minor corrections, if any. Its principal features, some of them rather similar to those of the KF-K system, are the following: (1) high solubility, 27.5 ± 0.5 mole %, of the salt in the liquid metal at the monotectic temperature of 752°C, 18°C below the melting point of the pure salt; (2) a small temperature range of approximately 40°C, as compared with 200°C for the NaCl-Na and with 60°C for the KF-F systems, for the coexistence of two liquid phases; (3) a distinct deviation from a straight line near the monotectic for the plot of the logarithm of the solubility of the solid salt in the liquid metal vs $1/T$; (4) a considerable deviation, by a factor of about 2, from Raoult's law for the monotectic, relatively high in metal content (about 11 mole %). Neither feature 3 nor 4 should probably be taken to indicate any considerable solubility of potassium in solid KCl near the monotectic temperature, even though the unusual similarity of the molar volumes in the liquid state might suggest such a possibility. This solubility was found experimentally at 730°C, that is, 22°C below the monotectic temperature where it has its maximum, as 0.5 mole % of potassium, which is too low to affect significantly the position of the liquidus curve.

As expected, and as was true for the KF-K system, the KCl-K system is intermediate between the corresponding sodium system with its large area of liquid immiscibility and the cesium system with its complete miscibility (Fig. 22).

In the present two-phase equilibration experiments the scattering of the values for the solubility of metal in liquid salt was somewhat greater than it was in the other systems, and there was a tendency for the values to be excessively high. This was tentatively attributed to a lesser tendency of the two liquid phases to segregate, perhaps connected with the fact that the molar volumes of liquid KCl and potassium are more similar than those of other alkali-metal-salt pairs. For this reason, an alternate method for the determination of the liquid-liquid equilibria, namely, thermal analysis (cooling curves), was applied to the determination of the temperature, as a function of composition, at which the precipitation of a second liquid phase produces a rather small thermal effect. Thus, in two compositions, 20 and 30 mole % potassium, reproducible breaks were obtained in the cooling curves at 778 and 789°C, respectively. This technique, in which the ratio of the mass of the stainless steel container to that of the sample was held to the utmost minimum by using very thin-walled capsules, was consequently also applied to determine more accurately the liquidus curve between the melting point of the salt and the monotectic. It will be further developed to improve the determination of the

[48] In cooperation with Wm. T. Smith, Jr., consultant, University of Tennessee.

[49] For a few earlier data on this system, see M. A. Bredig *et al.*, *Chem. Semiann. Prog. Rep. June 20, 1954*, ORNL-1755, p 22.

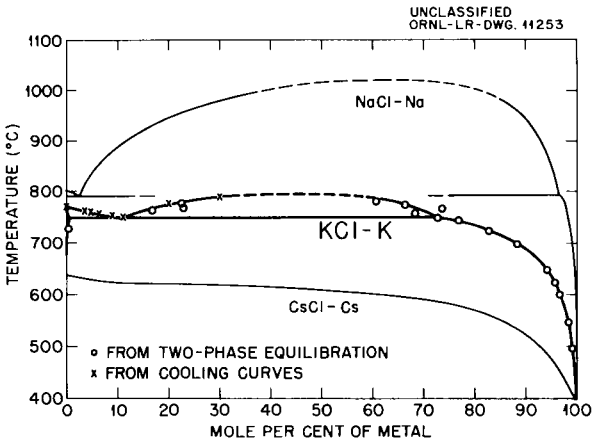

Fig. 22. The KCl-K System in Comparison with the Corresponding Na and Cs Systems.

two-liquid-phase equilibria in this and other systems.

Electrical Conductivity in Molten Salt–Metal Solutions[48]

M. A. Bredig H. R. Bronstein

The experiments on the electrical conductivity of molten KCl-K solutions reported previously[50] were continued. The beryllium oxide conductance cell turned out to be porous and had to be replaced by cells made of single crystals of magnesia and of alumina (synthetic sapphire). Difficulties are still encountered with cracking, which apparently results from thermal strains. It was further found difficult to obtain metal concentrations in the molten mixtures of more than 3 mole %. It appears that distillation of potassium metal to the cold top of the tank, even in argon gas at a pressure of 40 psia, is more rapid than anticipated and that for measurements in more highly concentrated solutions an entirely different apparatus and method may have to be developed.

However, in the range below 3 mole % metal, satisfactory results were obtained. The dotted line in Fig. 23 indicates the conductivity that would result from an additive behavior of metal and salt in the solution with respect to conductance. Such behavior is not actually expected, and the observed conductivity indicated by the smooth line indeed rises very slowly with the addition of metal. This indicates that the electronic contribution to the conductance is very minor, quite in agreement with a conclusion arrived at by Mollwo[51] on the basis of optical absorption and electrical transport measurements on *F*-center-colored alkali halides in the molten state. Apparently, the conclusion that "undissociated" alkali metal atoms rather than metal ions and "free" (metallically conducting) electrons are present in the molten salt solution apply not only to the very low metal concentrations of the *F*-center-containing alkali halides but also to moderately low concentrations such as those of the present experiments. To establish the shape of the conductivity curve as a continuous function of composition up to the highest metal concentrations, that is, the pure metal, will be an interesting experiment and is the purpose of this continued study.

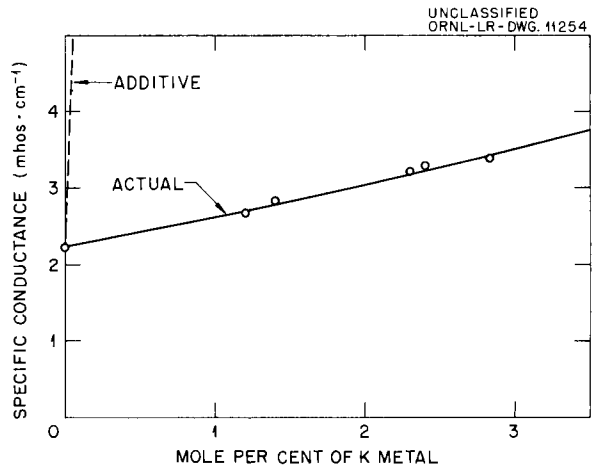

Fig. 23. Specific Conductivity of Solutions of Potassium Metal in Molten Potassium Chloride.

[50] M. A. Bredig, H. R. Bronstein, and J. W. Johnson, *Chem. Semiann. Prog. Rep. June 20, 1955*, ORNL-1940, p 17–19.

[51] E. Mollwo, *Nachr. Akad. Wiss. Göttingen, Math. physik. Kl. IIa*, New Series, 1, No. 18, 203–207 (1935).

NUCLEAR CHEMISTRY

DECAY OF THE Ce^{139} ISOMERS

B. H. Ketelle H. Thomas[1]
A. R. Brosi

The decay of the 140-day ground state of Ce^{139} has been investigated. It has been determined, by use of a 4π scintillation spectrometer, that decay directly to the ground level of La^{139} occurs in less than 1% of the transitions. The same instrument has been used to measure the L/K capture ratio to the 166-kev excited level and the conversion coefficient of the 166-kev transition. The K conversion coefficient was found to be 0.22 ± 0.01, and the L/K capture ratio was found to be 0.37 ± 0.02. The energy available for decay to the excited level is 85 ± 3 kev, as computed from the experimental L/K capture ratio. A value of 0.88 ± 0.01 was obtained for the K fluorescent yield at a Z value of 57 from beta-ray spectrometer measurements and coincidence counting. An isomeric level 740 ± 5 kev above the ground state of Ce^{139} has been found. The half life of the transition is 55 ± 3 sec, and its K conversion coefficient is 0.08 ± 0.02. Mass and element assignments have been established, and approximate cross sections have been determined for activation of each level in Ce^{139} by the (n,γ) reaction on Ce^{138} in the ORNL Graphite Reactor. These cross sections are 7 mb for activation of the isomeric state and 1 barn for activation of the ground state. A decay scheme with spin assignments based on the results reported here is shown in Fig. 24. A more complete report of this work will be published in *The Physical Review.*

[1]Summer participant in the Instrumentation and Controls Division, Mississippi State College.

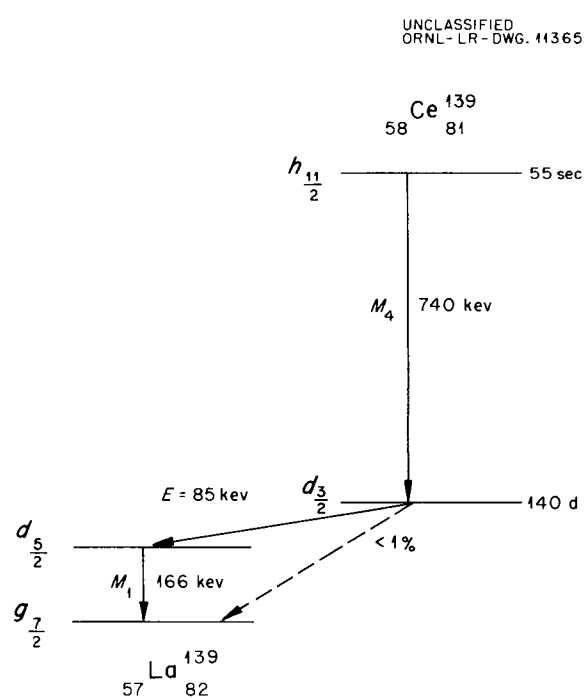

Fig. 24. Cerium-139 Decay Scheme.

IDENTIFICATION OF La^{137} AND FURTHER CHARACTERIZATION OF Ce^{137}

A. R. Brosi B. H. Ketelle

Lanthanum-137 has been produced by neutron bombardment of cerium and was found to decay by K electron capture with a half life of $(6 \pm 2) \times 10^4$ years. A further study of the Ce^{137} decay scheme has been made because this half life is much longer than expected from the spin assignments made in earlier work. The discovery of a hitherto unobserved 10-kev gamma transition has led to a proposal of the decay scheme shown in Fig. 25. This decay scheme has a different ground-state spin, which leads to the conclusion that

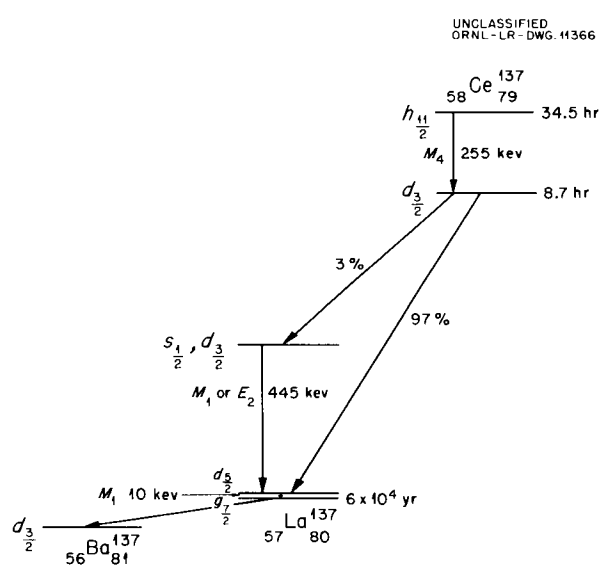

Fig. 25. Decay Schemes of Ce^{137} and La^{137}.

electron-capture decay of La^{137} would be second-forbidden. Since the disintegration energy is unknown, it can only be said at the present time that this conclusion is not inconsistent with the long half life.

SHORT-LIVED FISSION PRODUCTS

The Decay of Rb^{89}

G. D. O'Kelley Q. V. Larson
E. Eichler N. H. Lazar[2]

Studies of the Rb^{89} decay scheme were completed. The source purity was improved by using an ion exchange separation of the Rb and Cs activities formed in the decay of fission-product Kr and Xe. In general, the fission-product gas apparatus and the scintillation methods used were the same as described previously.[3]

The half life of Rb^{89}, measured on a 2π beta proportional counter, was found to be 14.9 ± 0.3 min. By using 3 × 3 in. NaI(Tl) crystal scintillation spectrometers in conjunction with a 20-channel pulse-height analyzer, a number of gamma rays were characterized and assigned to the decay of Rb^{89}. A summary of the energies and intensities of these gamma rays is given below:

Gamma-Ray Energy (Mev)	Intensity Relative to the 1.05-Mev Gamma Ray
0.663 ± 0.006	0.217 ± 0.026
1.05 ± 0.02	1.00
1.26 ± 0.01	0.717 ± 0.090
1.55 ± 0.03	0.048 ± 0.010
2.20 ± 0.02	0.190 ± 0.025
2.59 ± 0.03	0.169 ± 0.031
2.75 ± 0.05	0.037 ± 0.007
3.52 ± 0.07	0.029 ± 0.005

Gamma-gamma coincidence spectroscopy and summing of gamma rays in a $4\frac{3}{4}$-in.-dia NaI(Tl) crystal used in anticoincidence with a surrounding, solution-phosphor tank established the decay scheme for Rb^{89} shown in Fig. 26. The ground-state beta-ray transition was measured as 3.92 ± 0.05 Mev and was found to be present in about 7% of the beta-ray transitions.

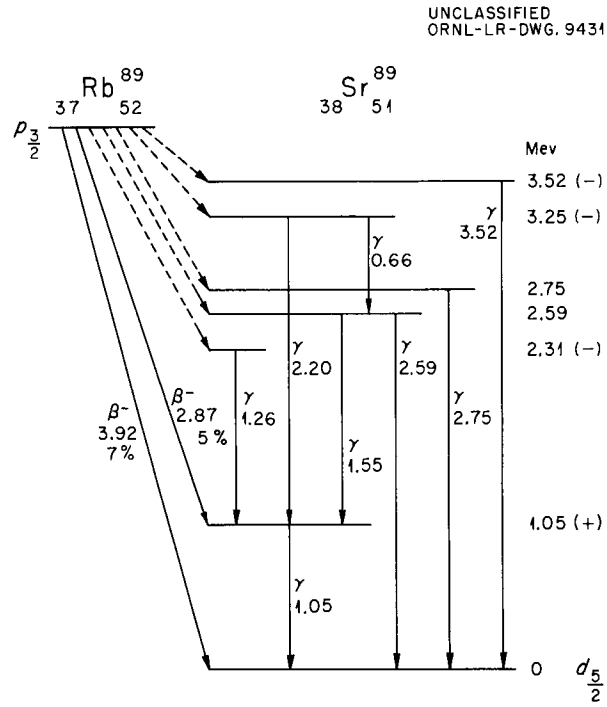

Fig. 26. Decay Scheme Proposed for Rb^{89}.

A complete description of the Rb^{89} studies has been prepared and submitted for publication.

The Decay Chain Ca^{49}-Sc^{49}-Ti^{49}

G. D. O'Kelley E. Eichler
N. H. Lazar

The decays of Ca^{49} and its daughter, Sc^{49}, have been studied by beta- and gamma-ray scintillation spectroscopy. Sources of Ca^{49} were prepared by slow-neutron irradiation of either analytical reagent grade $Ca(NO_3)_2$ or spectroscopically pure $CaCO_3$ enriched in Ca^{48} to 51.4%. In measurements of the radiations from Sc^{49}, sources chemically separated from samples of the Ca^{49} parent were used.

The half life of Ca^{49} was determined as 8.75 ± 0.20 min, using a gamma-ray scintillation spectrometer set on the 3.10-Mev peak of the Ca^{49} gamma-ray spectrum. The decay of the Sc^{49} beta particles was followed on a 2π beta proportional counter and yielded a half life of 57.2 ± 0.7 min.

Gamma-ray measurements with 3 × 3 in. NaI(Tl) scintillation spectrometers disclosed three gamma rays of energy 3.10 ± 0.03, 4.05 ± 0.05, and 4.68 ± 0.05 Mev and relative intensities of 1.0,

[2]Physics Division.

[3]G. D. O'Kelley, E. Eichler, and N. H. Lazar, *Chem. Semiann. Prog. Rep. June 20, 1955*, ORNL-1940, p 22, esp. 25–27.

0.11 ± 0.02, and 0.0038 ± 0.0010. Gamma-gamma coincidence spectrometry of Ca^{49} showed that neither the 4.05- nor the 4.68-Mev gamma rays were in coincidence with the 3.10-Mev gamma ray and that any gamma-ray transitions between the 4.05- and 3.10-Mev states were present in less than 2% of the intensity of the 3.10-Mev transition.

The bremsstrahlung spectrum from a source of Sc^{49} was used to set a limit on the number of 1.35-Mev transitions from the known first excited state[4,5] of Ti^{49}. In this way, the maximum number of 1.35-Mev gamma rays per Sc^{49} beta disintegration was estimated to be about 5×10^{-4}.

From absolute counting of the Ca^{49} beta particles and the 3.10-Mev gamma ray and from the relative intensities of the gamma rays, the number of beta particles per gamma ray was found to be 0.95 ± 0.10, where the quoted error reflects the authors' uncertainty in the sodium iodide peak efficiency for the 3.10-Mev gamma ray. Within the experimental error, all beta-ray transitions occur to excited states.

Scintillation methods were employed for studies of the beta spectra from Ca^{49} and Sc^{49}. The Ca^{49} beta-ray spectrum was analyzed into two components with energies of 1.95 ± 0.05 and 0.89 ± 0.15 Mev and with an intensity ratio of $I_{0.9}/I_{1.95}$ = 0.14. This intensity ratio may be compared with the ratio of intensities of the 4.05- and 3.10-Mev gamma rays, namely, 0.11, since all beta decays are to excited states. The Sc^{49} beta-ray energy was found to be 2.05 ± 0.05 Mev.

A summary of the beta-ray data is presented in Table 10, where abundances of the Ca^{49} beta groups and energies of the two lowest energy beta groups are inferred from the gamma-ray measurements. The experimental measurements described have been incorporated into the decay scheme shown in Fig. 27. An article on the work discussed above has been accepted for publication by *The Physical Review*.

[4] M. M. Bretscher *et al.*, *Phys. Rev.* 96, 103, 826 (1954).

[5] W. W. Pratt, *Phys. Rev.* 97, 131 (1955).

TABLE 10. SUMMARY OF BETA-DECAY DATA ON Ca^{49} AND Sc^{49}

Nuclide	Beta-Ray Energy (Mev)	Abundance	log *ft*
Ca^{49}	(0.37)*	0.0034*	4.5
Ca^{49}	(1.00)*	0.10*	4.6
Ca^{49}	1.95 ± 0.05	0.90*	4.9
Sc^{49}	2.05 ± 0.05	1.00	5.7

*Calculated from gamma-ray data.

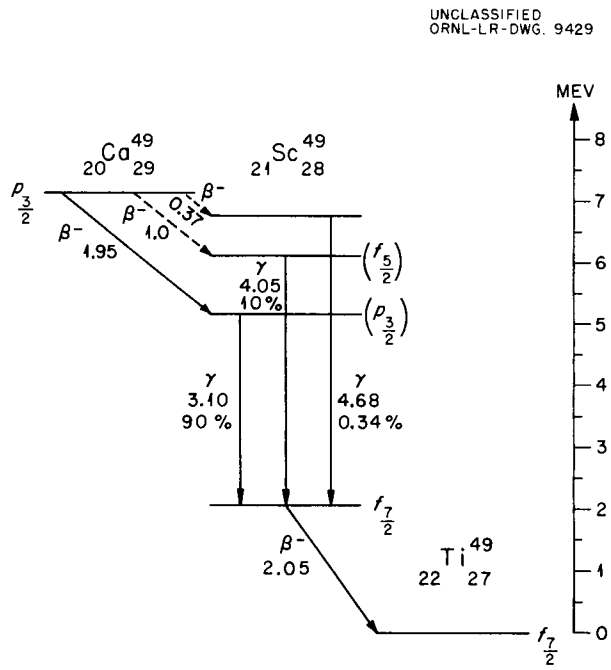

Fig. 27. Proposed Decay Scheme for the Chain Ca^{49}-Sc^{49}-Ti^{49}.

The Decay of Tc^{101}

G. D. O'Kelley Q. V. Larson
G. E. Boyd

The first investigations in the Laboratory[6] of 13.5 ± 0.2 min Tc^{101g} disclosed two gamma rays of 0.30- and 0.56-Mev energy and a 1.20 ± 0.05 Mev beta-ray group coincident with the 0.30-Mev gamma ray. Subsequently, Rutledge, Cork, and Burson,[7] in an investigation of gamma rays associated with neutron-induced activities, reported that there was no evidence either from magnetic spectrograph or from scintillation spectrometer measurements of other than a single, 306.9-kev gamma ray in Tc^{101g}.

[6] G. E. Boyd and B. H. Ketelle, *Phys. Rev.* 83, 216 (1951).

[7] W. C. Rutledge, J. M. Cork, and S. B. Burson, *Phys. Rev.* 86, 775 (1952).

More recently,[8] a significantly different half life of 14.3 ± 0.1 min has been reported. The work reported here is an extension of these previous measurements and is being continued with the hope that a detailed decay scheme can be evolved for Tc^{101}.

Sources of Tc^{101} were chemically separated from Mo^{101}, which had been prepared by slow-neutron irradiation of chemically pure MoO_3 or this same compound enriched in Mo^{100}. The technetium activity was extracted from 1 *N* NaOH into an equal volume of a 0.3 g/liter solution of cetyldimethylbenzylammonium chloride in chloroform. Careful measurements on the separation of 6-hr Tc^{99m} from Mo^{99} by this technique demonstrated that an 80% yield and a decontamination factor of 10^5 from molybdenum were possible with one extraction, washing the organic phase twice with 1 *N* NaOH.

Measurements of the Tc^{101} gamma-ray spectrum on a 3 × 3 in. NaI(Tl) scintillation spectrometer, with the source centered 9.8 cm above the top surface of the crystal, disclosed gamma rays of the following energies: 130 ± 5, 190 ± 8, 307 ± 3 (strong), 410 ± 15, 542 ± 5, 635 ± 15, 719 ± 8, 840 ± 15 kev.

That the 840-kev transition is not the crossover transition for a 307 + 542 cascade was demonstrated by inserting a source of Tc^{101} inside a 9¼-in. NaI(Tl) crystal spectrometer and examining the resulting pulse-height distribution for summing. The 542-kev gamma ray, which is only a fraction of the intensity of the 307-kev gamma ray, would have almost completely disappeared from the pulse-height spectrum due to summing if the 307- and 542-kev gamma rays were in coincidence. The gamma-ray intensity ratio, $I(307)/I(542)$, as measured with the 9¼-in. NaI(Tl) spectrometer, had the same value as that obtained on the 3 × 3 in. NaI(Tl) spectrometer, within the experimental error of about 10%. It appears, therefore, that the 840-kev transition is due to the de-excitation of a level at that energy and is not a crossover transition. It is possible that the gamma rays at 307, 542, 635, and 719 are ground-state transitions as well, but coincidence measurements will be required to fit the 130-, 190-, and 410-kev gamma rays into a consistent decay scheme.

[8] D. R. Wiles, *Phys. Rev.* 93, 181 (1954).

ORGANIC CHEMISTRY

MECHANISM OF THE PINACOL REARRANGEMENT

B. M. Benjamin C. J. Collins

Diphenyl-*p*-tolylacetaldehyde-1-C^{14} (IV), chain- and ring-labeled 1,2-diphenyl-1-*p*-tolylethylene glycol (V*a*, V*b*, and V*c*), and 1,1-diphenyl-2-*p*-tolylethylene-2-C^{14} glycol (VI*a*) have been prepared and subjected to rearrangement in cold, concentrated sulfuric acid and in boiling formic acid:

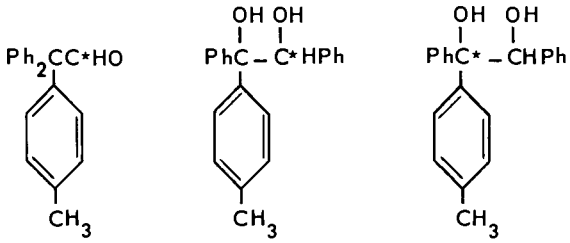

IV V*a* V*b*

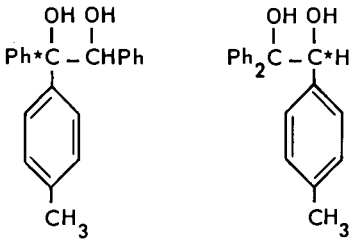

V*c* VI*a*

The yields of ketones VII and VIII were determined by the radioactivity dilution method. The results of these experiments are given in Table 11. Compounds IV, V*a*, and VI*a* were subjected to the same conditions in different experiments, and in each experiment the mixed ketones were cleaved with alkali:

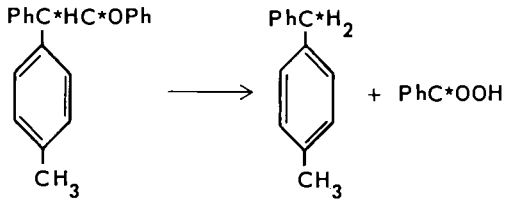

VII*ab* IX*a*

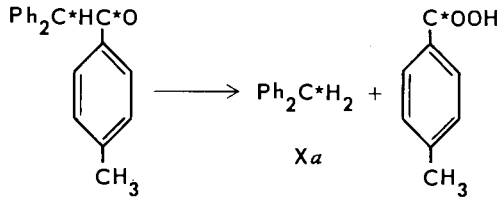

VIII*ab*

The neutral fraction, consisting of phenyl-*p*-tolylmethane (IX*a*) and diphenylmethane (X*a*), was then oxidized with chromic acid:

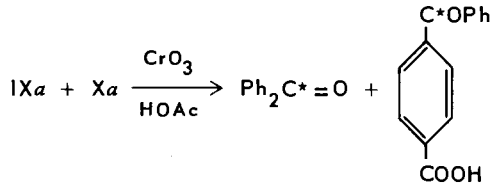

The benzophenone, separated as the neutral fraction, was assayed for its radioactivity content whenever possible as the 2,4-dinitrophenylhydrazone, whereas the *p*-benzoylbenzoic acid was carefully purified by repeated crystallizations and assayed for its radioactivity content. The results of these experiments are given in Table 12.

Glycol V*c* was next accorded the same treatment just described for the chain-labeled glycol, and the ketonic products were subjected to the identical degradative scheme:

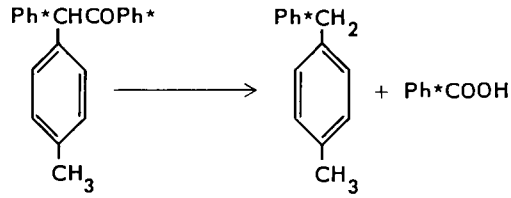

VII*cd* IX*c*

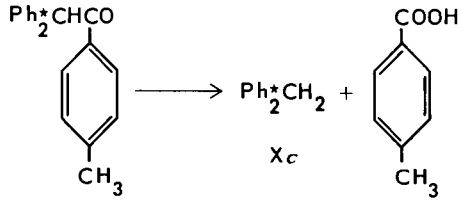

VIII*cd*

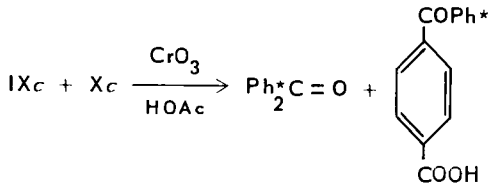

In the latter instance the neutral (benzophenone) fractions were discarded, and only the ring-labeled *p*-benzoylbenzoic acid fractions were purified and assayed. The results of these experiments are also given in Table 12. Several additional experiments were then performed upon the glycols V and VI, with 98% formic acid at 27.6 ± 0.1°C as the solvent. Under these conditions the aldehyde (IV) is a product from each glycol and is quite stable. The aldehyde (IV) produced in each experiment could be determined by conversion nearly quantitatively to its 2,4-dinitrophenylhydrazone under conditions which did not favor the formation of the derivatives of VII and VIII. The yields of VII and VIII were determined by means of the radioactivity dilution techniques. The results of these experiments are given in Table 13.

From the data of Tables 11, 12, and 13, mechanisms for the rearrangement of IV and V have been written for reaction in cold, concentrated sulfuric acid and reaction in boiling formic acid. These mechanisms are given in Charts 1 and 2, respectively. For the sulfuric acid reaction the contribuitons of paths *A* through *E* (Chart 1) have been evaluated, and the ratio of the contributions of paths *D* and *E* from glycol V have been shown to be in the same ratio as the yields of compounds VII and VIII obtained directly from the aldehyde (line 1, Table 11). It has been assumed that the very slight amount of chain-label C^{14} in the benzophenone and *p*-benzoylbenzoic acid fractions which appears to be a result of scrambling (~2%) is real and is a result of the participation of paths *A* and *B*, although these contributions could be considered to be zero without appreciably changing the calculations which follow. If *c* is assumed to be equal to the mole fraction of VII formed through

TABLE 11. YIELDS OF KETONES DETERMINED BY THE RADIOACTIVITY DILUTION METHOD

Reactant	Reagent	Yield of Ketone* (%) VII	Yield of Ketone* (%) VIII	Ratio VII/VIII
IV	96% H_2SO_4 at 0°C	82.5	17.5	4.7
	Boiling 98% formic	77.7	22.3	3.48
V*a*, β form	96% H_2SO_4 at 0°C	86	14	6.15
		83.6	16.4	5.11
V*b*, α form	96% H_2SO_4 at 0°C	85.1	14.9	5.82
		Av 84.9	Av 15.1	
V*a*, β form	Boiling 98% formic	87.7	12.3	7.13
V*b*, α form	Boiling 98% formic	88.3	11.7	7.57
		Av 88.0	Av 12.0	
VI*a*	96% H_2SO_4 at 0°C	83.0	17.0	4.9
	Boiling 98% formic	71.7	28.3	2.54
		71.0	29.0	2.45
		Av 71.4	Av 28.6	

*The values given in these two columns represent the yields of ketones in the products, and thus for each experiment the yields of VII and VIII will equal 100. In the sulfuric acid–catalyzed reactions the combined yields of products were 94 to 99%. The combined yields in the formic acid–catalyzed reactions were quantitative.

TABLE 12. FRACTION OF RADIOACTIVITY IN DEGRADATION PRODUCTS VII AND VIII

Activities of IV, V*a*, and VI taken as 1

Reactant	Acid Reagent	Activity* of Benzoylbenzoic Acid	Activity* of Benzophenone
IV	96% H_2SO_4 at 0°C	0.013	
	Boiling formic	0.115	
V*a*, β form	96% H_2SO_4 at 0°C	0.018	0.015
	Boiling formic	0.040	0.038
V*b*, α form	Boiling formic	0.955	0.960
VI*a*	96% H_2SO_4 at 0°C	0.278	
	Boiling formic	0.174	
		0.165	
		0.165	
V*c*, β form	96% H_2SO_4 at 0°C	0.563	
	Boiling formic	0.765	

*Activities of degradation products are given with respect to IV, V*a*, and VI, taken as 1.

path C, then $(0.98 - c)$ is the mole fraction of VII formed through path D, and it follows from Chart 1 that

$$c + (0.98 - c)0.5 = 0.563 \quad \text{(line 10, Table 12);}$$

therefore $c = 0.146$ and $(0.98 - c) = 0.834$. Since ketone VII, formed through paths A, C, and D, represents 84.9% of the product and since ketone VIII, formed through paths B and E, represents 15.1% of the product, it readily follows that the mole fractions of reactant converted to the products through each path may be calculated as follows:

$$m_a,\ 0.017;\quad m_b,\ 0.003;\quad m_c,\ 0.124;$$

$$m_d,\ 0.708;\quad m_e,\ 0.148.$$

The ratio m_d/m_e, calculated from the double labeling and isotope-dilution data for glycol V, is thus 4.8, in excellent agreement with the ratio VII/VIII of 4.7 obtained when the aldehyde IV itself is subject to identical conditions. (If it is assumed that $m_a = m_b = 0$, then $m_c = 0.110$, $m_d = 0.742$, $m_e = 0.151$, and $m_d/m_e = 4.9$.)

Now if x_1, x_2, and x_3 are the instantaneous, time-variable concentrations of the ions X_1, X_2, and X_3, respectively, then from Chart 1,

$$(1)\quad \frac{dx_2(t)}{dt} = k_P x_1(t) - k_\phi x_2(t) - k_H x_2(t)\ ,$$

$$(2)\quad \frac{dx_3(t)}{dt} = k_T x_1(t) - k_{Tol} x_3(t) - k'_H x_3(t)\ .$$

Since the reactions of Chart 1 were, in the experiments, allowed to go to completion, Eqs. 1 and 2 are now integrated between the limits zero and infinity. If the values $x_1(t) \int_0^\infty dt$, $x_2(t) \int_0^\infty dt$, and $x_3(t) \int_0^\infty dt$ are replaced with the "integration areas" s_1, s_2, and s_3, then, since at $t = 0$ and at $t = \infty$ the concentrations of all intermediates are zero,

$$(3)\quad \dot{x}_2 = k_P s_1 - k_\phi s_2 - k_H s_2 = 0\ ,$$

$$(4)\quad \dot{x}_3 = k_T s_1 - k_{Tol} s_3 - k'_H s_3 = 0\ .$$

Thus,

$$(5)\quad s_2 = \frac{k_P s_1}{k_\phi + k_H}\ ,$$

TABLE 13. YIELDS OF ALDEHYDE (IV) AND KETONES VII AND VIII UPON FORMIC ACID TREATMENT OF GLYCOLS V AND VI

Compound	Reagent	Yield of 2,4-DNPH Derivative of IV (%)	Corrected Yield of Aldehyde (%)	Yield (%)	
				VII	VIII
V*a*	Formic acid, 27.6°C			51.0	
		44.4			
		44.9	49[a,b]		
	Formic acid, 27.6°C for 24 hr, then boiled for 6 hr			88.3	11.7
V*b*	Formic acid, 27.6°C	44.9			
		43.6			
		Av 44.5			
VI*a*	Formic acid, 27.6°C			5.05[c]	
		83.4			
		83.7			
		84.7	87[a,d]		
		Av 83.9			

[a]Although the pure aldehyde could be converted quantitatively to its 2,4-dinitrophenylhydrazone, mixtures of IV, VII, and VIII did not give this derivative quantitatively, and the smaller the proportion of IV, the lower the yield.

[b]The yield of aldehyde has been taken as 100 − 51 = 49%.

[c]Oxidation of this sample followed by radioactivity assay of the *p*-benzoylbenzoic acid obtained demonstrated that 100% of the molar radioactivity of the ketone VII*b* was present in the 4-methylbenzhydryl portion of the molecule.

[d]The yield of 2,4-dinitrophenylhydrazone has been divided by the correction factor 0.975.

$$(6) \qquad s_3 = \frac{k_T s_1}{k_{Tol} + k'_H} \quad .$$

At complete reaction the ratio m_d/m_e is given by

$$(7) \qquad \frac{m_d}{m_e} = \frac{k_H s_2}{k'_H s_3} \quad .$$

It then readily follows[1] that

$$(8) \qquad \frac{k_T}{k_P} = \frac{k_H}{k_\phi} \cdot \frac{k_{Tol}}{k'_H} \cdot \frac{m_e}{m_d} \cdot \left(\frac{1 + k'_H/k_{Tol}}{1 + k_H/k_\phi} \right) \quad .$$

The ratio k_T/k_P is given by the following:

$$\frac{k_H}{k_\phi} = \frac{m_c}{m_d + m_e} = \frac{0.124}{0.708 + 0.148} = 0.145 \quad .$$

The ratio k_{Tol}/k'_H can be approximated by either of the following proportions (see Table 14):

$$k_{Tol}/k'_H : 9.3 = 7.33 : 1.44 \quad ,$$

$$k_{Tol}/k'_H : 9.3 = 6.9 : 1.15 \quad ,$$

from which values of 47 and 56 are obtained. Thus k_T/k_P (Eq. 8) is calculated to be either 1.3 or 1.6, corresponding to *p*-tolyl/phenyl migration ratios of 2.6 and 3.2, respectively.

For the boiling formic acid–catalyzed reaction, it appears that although paths *A* and *B* undoubtedly contribute to the over-all mechanism their total participation is probably less than 1%. Similarly, although there is definite evidence that path *G* contributes to the mechanism (since 4% of the

[1]Equation 8 was obtained by use of the "area theorem" of J. Z. Hearon. The authors are indebted to him for pointing out the utility of this theorem in chemical kinetics and for the derivation of Eq. 8.

CHART 1

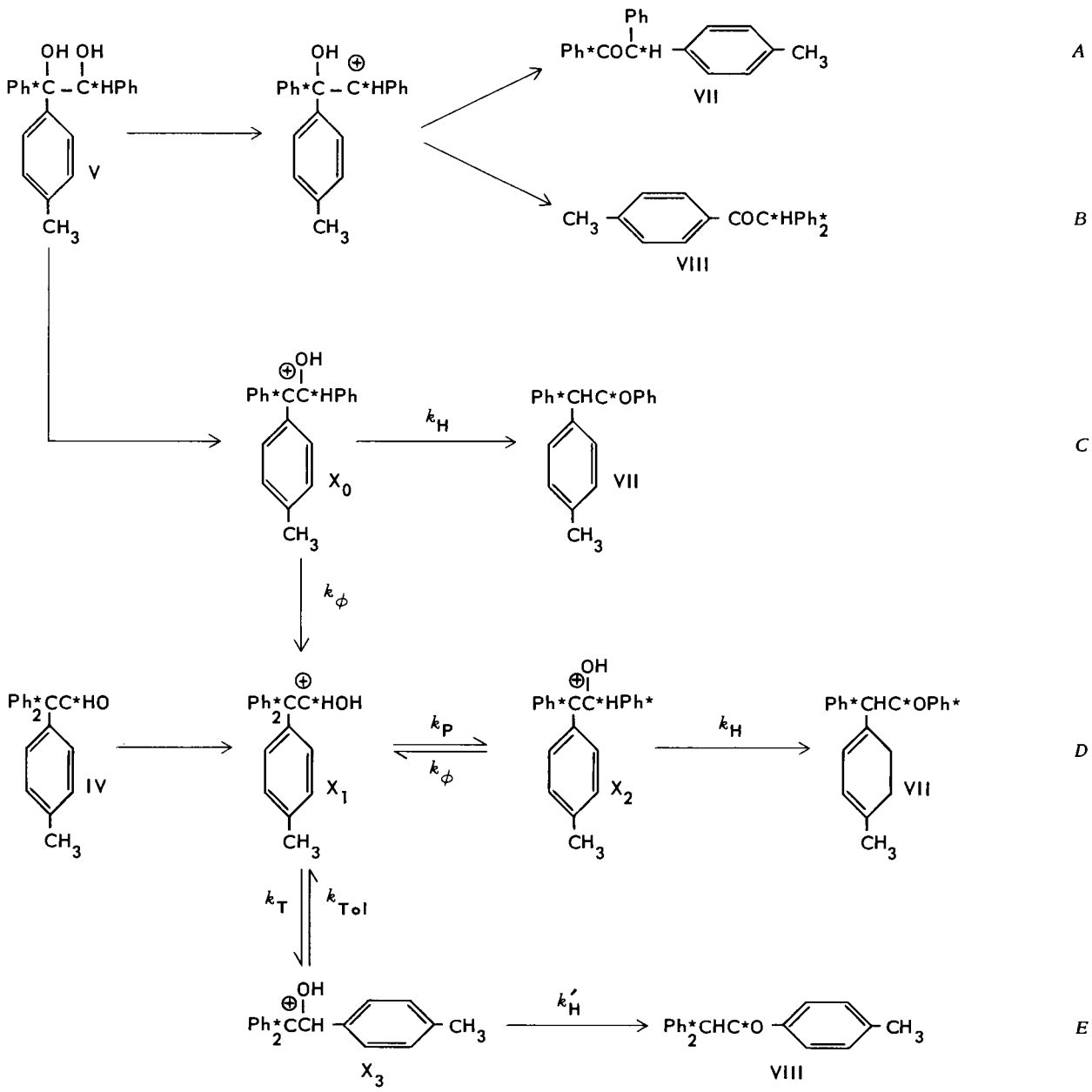

ketone VIII which is formed contains its C^{14} in the benzhydryl portion of the molecule), the extent of participation of path G must be only 0.04×0.12, or less than 0.5% of the total reaction. If it is assumed that the ratio m_b/m_g is about 3 (the normal ratio of tolyl/phenyl migratory abilities) then path H must participate to the extent of less than 1.5% of the total reaction. For these reasons, the contributions of paths A, B, G, and H are neglected in order to simplify the calculation. If c, d, and f are mole fractions, respectively, of ketone VII formed through paths C, D, and F, then

$$0.765 = c + 0.5d + 0.5f \quad \text{(line 11, Table 12)},$$

$$d + f = 1 - c \ ,$$

$$f = (1 - c)0.115 \ ,$$

$$d = (1 - c)0.885 \ ;$$

CHART 2

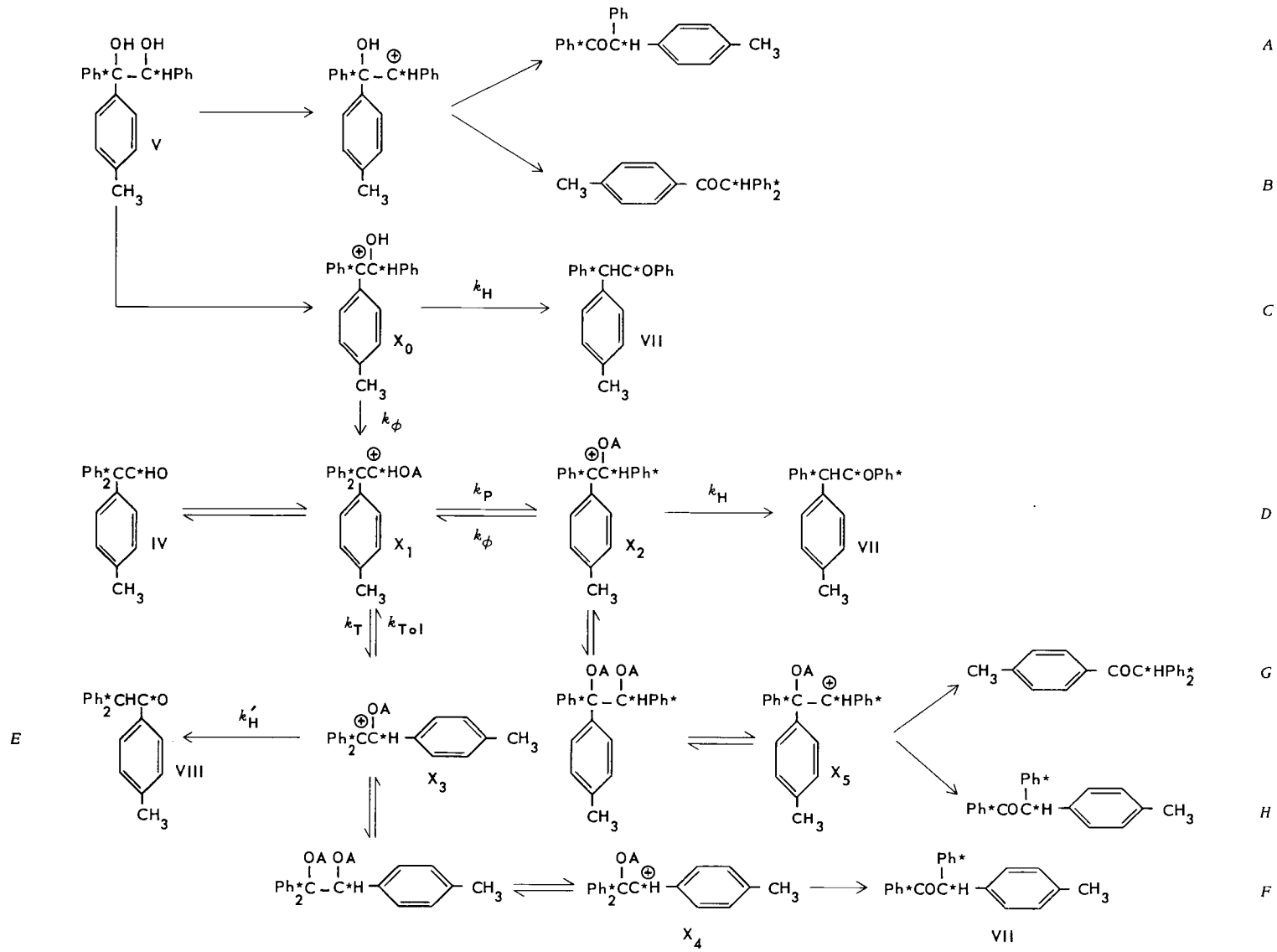
A
B
C
D
E
G
H
F
V
IV
VII
VIII
X_0
X_1
X_2
X_3
X_4
X_5
k_H
k_ϕ
k_P
k_T
k_{Tol}
k'_H
A = H– or HCO–

TABLE 14. RATIO OF SPECIFIC RATE CONSTANTS FOR ARYL AND HYDROGEN MIGRATION FOR VARIOUS CARBONIUM IONS IN H_2SO_4 AND HCOOH

Carbonium Ion	k_{Ar}/k_H in H_2SO_4	k_{Ar}/k_H in HCOOH	Reference
$Ph_2\overset{\oplus}{C}(OH)CHPh$	7.33	1.44	*
	6.9	1.15	This report
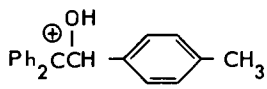	47–56 (calculated; see text)	9.3	This report

*C. J. Collins, *J. Am. Chem. Soc.* 77, 5517 (1955).

therefore $c = 0.530$, $d = 0.416$, and $f = 0.054$, and m_c, m_d, m_e, and m_f the contributions of paths C, D, E, and F, are:

$$m_c = 0.530(0.88) = 0.466 ,$$

$$m_d = 0.416(0.88) = 0.366 ,$$

$$m_e = 0.120 ,$$

$$m_f = 0.054(0.88) = 0.048 ,$$

$$\text{Total} = 1.000 .$$

The ratio

$$\frac{m_d + m_f}{m_e} = \frac{0.366 + 0.048}{0.120} = 3.45$$

is in excellent agreement with VII/VIII = 3.48, the ratio obtained when aldehyde IV itself is subjected to these same conditions. The ratio k_H/k_ϕ is given by

$$\left(\frac{k_H}{k_\phi}\right)_{100°C} = \frac{m_c}{m_d + m_e + m_f}$$

$$= \frac{0.466}{0.366 + 0.120 + 0.048} = \frac{0.466}{0.534} = 0.87 .$$

It is interesting that from Table 13, representing the formic acid–catalyzed reaction at 27.6°C, the ratio k_H/k_ϕ at that temperature may be determined as

$$\left(\frac{k_H}{k_\phi}\right)_{27.6°C} = \frac{49}{51} = 0.96 .$$

It thus appears that k_H/k_ϕ is reasonably constant between these two temperatures. It may be calculated also from Table 13 that

$$\left(\frac{k_{Tol}}{k'_H}\right)_{27.6°C} = \frac{87}{8} = 11 .$$

It is possible to determine $(k_{Tol}/k'_H)_{100°C}$ from the data relative to the rearrangement of VI*a* in Tables 11 and 12 and from the calculated values of the contributions of the paths of Chart 2. Given in Chart 3 is an over-all mechanism for the rearrangement of glycol VI, based upon the scheme of Chart 2. It has already been shown that once ion X_1 is formed, whether from the aldehyde IV or from the glycol V, it rearranges to VII and VIII in the same ratio when the conditions of the reaction are maintained constant. Now although it is not

possible by performing double-labeling experiments upon glycol VI alone to distinguish the contribution of path K to the formation of ketone VIII from that of path E (Chart 3), it is yet possible to calculate these contributions, since the ratio $(m_d + m_f)/m_e$ is known from IV or V under these same conditions. Thus if $m_{f'}$ $m_{d'}$ and m_f are the mole fractions of the total reaction product, proceeding to ketone VII through paths J, D, and F, and if m_k and m_e are the mole fractions of total reaction product,

CHART 3

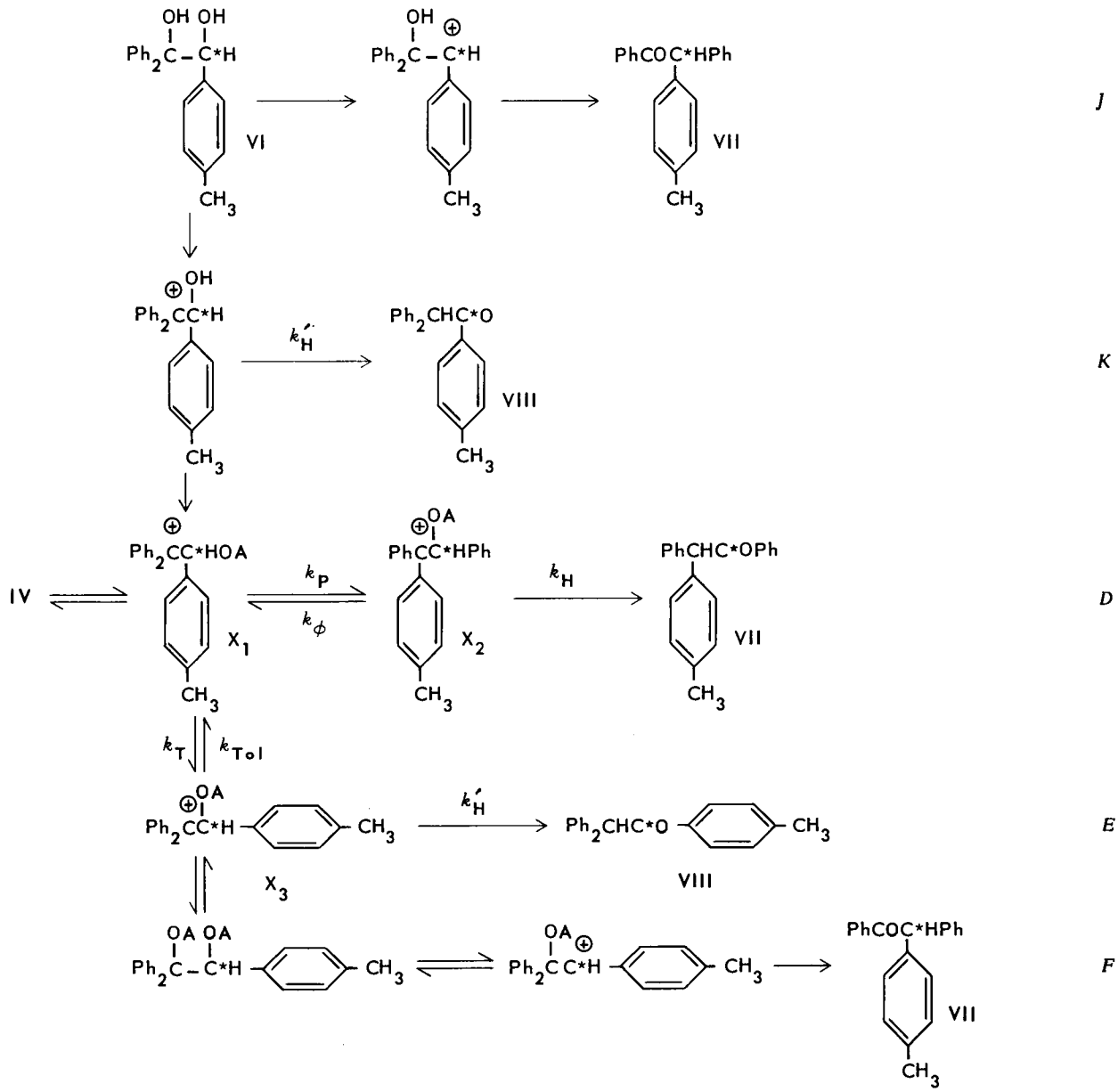

proceeding to ketone VIII through paths K and E, then

$$m_j + m_d + m_f = 0.714 ,$$

$$m_k + m_e = 0.286 ,$$

$$\frac{m_j + m_f}{m_j + m_f + m_d} = 0.165 ,$$

$$m_d + m_f = m_d\left(\frac{0.414}{0.366}\right) ,$$

$$\frac{m_d + m_f}{m_e} = 3.5 ,$$

from which

$$m_j = 0.040 ,$$

$$m_k = 0.093 ,$$

$$m_d = 0.596 ,$$

$$m_e = 0.193 ,$$

$$m_f = 0.078 ,$$

and

$$\left(\frac{k_{Tol}}{k'_H}\right)_{100°C} = \frac{m_d + m_e + m_f}{m_k} = 9.3 ,$$

in good agreement with the value

$$\left(\frac{k_{Tol}}{k'_H}\right)_{27.6°C} = 11 .$$

Equation 8, the exact solution for the mechanism of Chart 1, obviously requires modification before it can be applied to the formic acid–catalyzed reaction, the mechanism for which is given in Chart 2. This is true because path F has been recognized as an important contributor to the overall reaction. It might be anticipated that path F should affect the final ratio k_T/k_P in Eq. 8 by only 9%, the extent to which this path contributes to the reaction. Since the products from both paths E and F proceed through ion X_3, however, the error involved is much greater than 9%, because

$$\frac{m_f}{m_e + m_f} \times 100 = 29\% .$$

A further difficulty in applying Eq. 8 to the present data is that the ratio k_H/k_ϕ (Chart 2) might not be the same in ions X_0 and X_2 when A = H as it is when A = HCO. A rough estimate of k_T/k_P from Eq. 8 is 2.2, however, using $k_H/k_\phi = 0.87$, $k_{Tol}/k'_H = 9.3$, and the product ratio

$$\frac{m_e + m_f}{m_d} = 0.46 .$$

This corresponds to a p-tolyl/phenyl migration ratio of 4.4. It seems likely, despite the uncertainties involved, that the true p-tolyl/phenyl migration ratio is thus greater than 1.

General Conclusions

For the rearrangement of the aldehyde IV, the simple ratios of the products VII/VIII (4.7 in sulfuric acid and 3.5 in formic acid) would appear to indicate phenyl/p-tolyl migration ratios of 2.35 and 1.75, respectively, which are inverted with respect to the usual migratory abilities of the two groups. It has been shown that the migration ratio of the one p-tolyl group and the two phenyl groups of aldehyde IV is not reversed and is not given by the ratio of the ketonic products. The true p-tolyl/phenyl migration abilities in the rearrangement of IV in either sulfuric or formic acid have been estimated by the use of Eq. 8 to be between 2 and 4, as would normally be expected.

It has been shown that secondary hydroxyl removal from 1,1-diphenyl-2-p-tolylethylene-2-C^{14} glycol (VIa) is relatively more important, with respect to tertiary hydroxyl removal, in concentrated sulfuric acid at 0°C, than in formic acid at 27.6°C. This observation is explained on the basis of a greater polarizability of aryl nuclei in the solvent of higher dielectric constant.

REARRANGEMENT OF 1,1,2-TRIPHENYLETHYLENE GLYCOL AND ITS DEUTERATED DERIVATIVE. AN ATTEMPTED KINETIC STUDY

I. A. Kaye[2]

Preliminary Background Work

The preliminary work involved an attempt to find a homogeneous solution in which the rearrangement of 1,1,2-triphenylethylene glycol might be studied

[2]Research participant, Brooklyn College.

kinetically. The following information was obtained:

1. At room temperature no reaction was observed between equimolecular amounts of pinacol and sulfuric acid in methanol.

2. When the above solution was refluxed for 18 hr, there was obtained, from 0.290 g of pinacol, 0.180 g of phenyl benzhydryl ketone, mp = 133 to 135.5°C.

3. In 20% methanolic sulfuric acid (reaction mixture was not homogeneous) there was obtained, from 0.290 g of pinacol, 0.145 g of ketone, mp = 131 to 136°C, after 19 hr at room temperature.

4. No reaction was evidenced in a benzene solution of di-*n*-butyl hydrogen phosphate, either at room temperature or under reflux.

Listed below are the radiochemical results of run A, which was a methanolic solution containing equivalents of pinacol and sulfuric acid held at 60°C for 24 hr, and run B, which was the same as run A but in 20% methanolic sulfuric acid (radioactivity of starting ring-labeled triphenylethylene glycol = 1.182 mc/mole):

	Run A	Run B
Yield of triphenylacetaldehyde, %	9.83	3.25
Activity of DNP of benzophenone, mc/mole	1.122	1.104
Activity of benzoic acid, mc/mole		0.089
Total activity, mc/mole		1.193

By following the course of the rearrangement with an ultraviolet spectrophotometer, the reaction was found to proceed at a convenient rate in (a homogeneous) formic acid solution at room temperature.

Results of Ultraviolet Spectroscopic Work

The apparent first-order constant, k_H, for the rearrangement of 1,1,2-triphenylethylene glycol in formic acid was 0.0115 at 28.8°C and 0.0454 at 37.7°C, and for 1,1,2-triphenylethylene glycol-2-H^2 the constant, k_D, was 0.00778 at 28.8°C and 0.0278 at 37.7°C, with

$$\left(\frac{k_H}{k_D}\right)_{27.85°C} = 1.48 \ ,$$

$$\left(\frac{k_H}{k_D}\right)_{37.85°C} = 1.63 \ .$$

These are not true first-order constants, since the reaction mixture is not a simple mixture of unreacted pinacol, triphenylacetaldehyde, and phenyl benzhydryl ketone; subsequent work has shown that formic acid derivatives of the pinacol and aldehyde are also formed during the reaction. At 37.80°C the ultraviolet spectrum of a formic acid solution of triphenylacetaldehyde was followed. The strong yellow color originally present in the solution disappeared in two to three days. This was true also of the peak at 404 mμ. The absorption at 326 mμ dropped from the original 0.3925 to 0.377 in 1 hr and rose to a constant of 0.424 in over a day and remained constant at this value for more than a day. Apparently, the rate of ketone formation from the aldehyde is negligibly small, relative to its rate of formation from the glycol.

Titrimetric Results

A micro method for the estimation of the glycol, involving titration with lead tetraacetate, was developed. By use of this analytical tool, a kinetic run at 27.8°C was conducted. However, it was found that the apparent rate of disappearance of the glycol was much slower than the apparent rate of increase of the ketone, determined previously spectroscopically. This was traced to the formation of formic acid, bound in some fashion to one or more of the constituents of the reaction mixture. Subsequently, it was shown that no formate was bound by incubating phenyl benzhydryl ketone at 27.8°C for 2 hr, but, under the same conditions, about 22.5% of the aldehyde was combined with formic acid (calculated as a monoformate). This did not account for all the formate bound in the kinetic run, and so it is apparent that a formate ester of the glycol is formed in the reaction.

After 23¼ hr a solution of the glycol in formic acid at 27.8°C contained only 4.34% of free glycol. Titrimetric results indicate that there is no aldehyde-formate or formate ester of the glycol present but that there is 12 to 13% of glycol present as an *ortho*-formate. The titration values indicate that

1. the *ortho*-formate is apparently stable as a suspension in dilute aqueous sodium hydroxide at or below 35°C,
2. the *ortho*-formate probably does disappear on further reaction with formic acid,
3. the formic acid can be removed from the *ortho*-ester with lithium aluminum hydride,

4. the *ortho*-formate is converted quantitatively to a monoformate ester in a 5% aqueous solution in ethanol (2 hr at room temperature),
5. the formate bound as an ester, but not as *ortho*-ester, can be estimated by reaction with lead tetraacetate in acetic acid solution,
6. from the foregoing (5), the *ortho*-formate is stable in acetic acid and at room temperature, which might possibly serve to indicate that the *ortho*-formate is also stable at room temperature in anhydrous formic acid.

Radiochemical Results

By using ring-labeled glycol (1.182 mc/mole) in formic acid at 27.8°C for 23.25 hr, the following results were obtained. Run A differed from run B in that the formic acid was removed in run A by a slow *in vacuo* distillation. In run B, the formic acid was removed with aqueous alkali.

Titrimetric Results

	Run A	Run B
Free glycol, final %	5–8	4.34
Total glycol, final %	15.3	15.5–17.7
Radiochemical Results		
Aldehyde yield, %	52.15	45.89
Ketone yield, %	31.82	29.59
Aldehyde/ketone ratio	1.64	1.56
Activity of DNP of benzophenone, mc/mole	0.3113	
Activity of the benzoic acid, mc/mole	0.01628	
Total activity, mc/mole	0.3276	

[3]Research participant, University of Tennessee.

Conclusions

The mechanism of the rearrangement, in formic acid, of 1,1,2-triphenylethylene glycol is vastly more complicated than had been anticipated when this investigation was undertaken, since it involves the presence of at least two intermediate formate esters. The titrimetric method described in this report has been used successfully, however, for studying the rate of disappearance of the glycol in formic acid.

INVESTIGATION OF THE CLEAVAGE AND REARRANGEMENT OF TRIARYL KETOLS

J. F. Eastham[3] V. F. Raaen

A study of two reactions which was initiated in the summer of 1954 has been continued. The reactions involved are (1) the addition of arylmagnesium halides to benzils and (2) the alkaline cleavage of triaryl ketols produced by this Grignard reaction. The point of interest has been rearrangements occurring during these reactions:

(1)

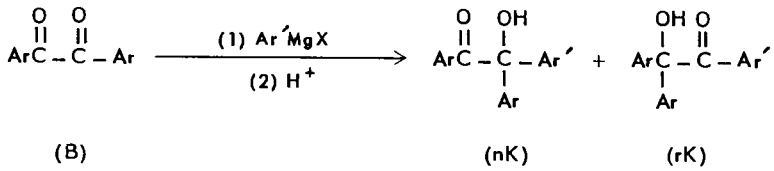

(2)

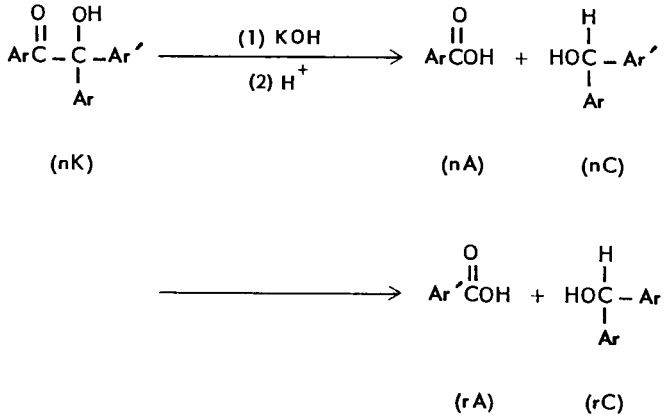

It had been shown that, in the Grignard reaction (1) with benzil (B, Ar = phenyl) when the aryl group added (Ar′) is *o*-tolyl, the only isolable crystalline product is the rearranged ketol (rK). When Ar′ is C^{14}-labeled phenyl, both the normal ketol (nK) and the rearranged ketol (rK) can be produced from benzil. In four runs made on this latter reaction, yields of rearranged ketol were 33, 10, and 5%, and none. The variable controlling the amount of rearrangement has not been determined for the addition of phenylmagnesium bromide to benzil. Repetition of the addition of *o*-tolylmagnesium bromide to benzil has always yielded the rearranged product. Apparently, the steric influence of the *o*-methyl group allows reproducible rearrangement. To determine whether some extenuating electronic influences on the aryl groups involved might also allow reproducible rearrangement, the syntheses of the tri-*p*-methoxyphenyl and tri-*m*-methoxyphenyl ketols have been carried out by the Grignard reaction (1).

Methyl-labeled *p*-bromoanisole was prepared by a reaction between *p*-bromophenol and C^{14}-dimethyl sulfate. The sulfate was prepared by the sodium methoxide catalyzed exchange between dimethyl sulfate and C^{14}-methyl alcohol. Addition of the Grignard reagent (Ar′ = labeled *p*-anisyl) to anisil (B, Ar = *p*-anisyl) occurred without rearrangement. Degradation of the product (nK) was done by chromic acid oxidation to inactive *p*-anisic acid (nA) and dimethoxybenzophenone of the same molar activity as the bromoanisole used. If any rearranged ketol (rK) had been produced, some activity would have appeared in the *p*-anisic acid (rA). In a similar reaction sequence, the *m*-methoxy derivatives were employed (B, Ar = *m*-anisyl; Ar′ = methyl-labeled *m*-anisyl). Again, addition occurred without rearrangement. Since the product (nK) was in this case an oil, it was reduced to a crystalline glycol, 1,1,2-tris-(*m*-methoxyphenyl)-ethylene glycol, before cleavage by lead tetraacetate. Cleavage yielded inactive *m*-methoxy benzaldehyde (characterized as its dinitrophenylhydrazone) and di-*m*-methoxybenzophenone (as its dinitrophenylhydrazone) of the same molar activity as the starting *m*-bromoanisole.

Addition of *p*-tolylmagnesium bromide to benzil (1) (Ar = phenyl; Ar′ = *p*-tolyl) produces an oil which can be reduced to a crystalline mixture of 1,2,1- and 1,1,2-diphenyl-*p*-tolylethylene glycol (dihydroforms of nK and rK). The normal glycol was isolated from this mixture by crystallization. The rearranged glycol was shown to be in the mixture to the extent of 7.5% by isotopic-dilution technique. The reproducibility of this rearrangement has not been checked.

In studying the alkaline cleavage rearrangement (2) of triaryl ketols (nK) it has been demonstrated that little (<4%) rearrangement occurs with phenylbenzoin when the labeled ketol (nK; Ar = phenyl; Ar′ = labeled phenyl) is used. Cleavage of anisylanisoin (nK; Ar = *p*-anisyl; Ar′ = labeled *p*-anisyl) proceeds with much more rearrangement. Under conditions that completely cleave phenylbenzoin in less than 2 hr, anisylanisoin was only 55% cleaved in 6 hr. Radioassay of the *p*-anisic acid produced by this 55% cleavage (nA and rA) showed a 43% approach to the equilibrium amount of activity expected for a statistical rearrangement of Ar and Ar′ groups, that is, one-third the activity of the starting ketol (nK). Degradation of the 45% uncleaved ketol showed that considerable rearranged ketol (rK) had been produced by the action of alkali. This oxidative degradation gave *p*-anisic acid with 66% of the equilibrium amount of activity.

The normal Grignard addition product (I) was isolated by adding *o*-tolylmagnesium bromide to benzil (see Chart 4). Eastham was successful in the isolation of the abnormal addition or rearranged product (II). Reduction of the ketol (I) with lithium aluminum hydride yields a glycol (III) which, on oxidative cleavage with chromic acid, yields benzoic acid and phenyl *o*-tolyl ketone. The glycol is presumably a diastereoisomer of the glycol formed by the addition of *o*-tolylmagnesium bromide to benzil. Neither ketol (I) nor glycol (III) has been described previously.

The ketol (I) does not rearrange appreciably in dilute alcoholic potassium hydroxide at room temperature but undergoes rearrangement and cleavage in more concentrated refluxing alcoholic potassium hydroxide solution to yield benzhydrol, *o*-toluic acid, and rearranged ketol (II). Since the acid fraction is made up largely of *o*-toluic acid (85%), it is presumed that rearrangement precedes cleavage.

Reduction of the ketol (I) with red phosphorus and hydrogen iodide did not yield a crystalline

CHART 4

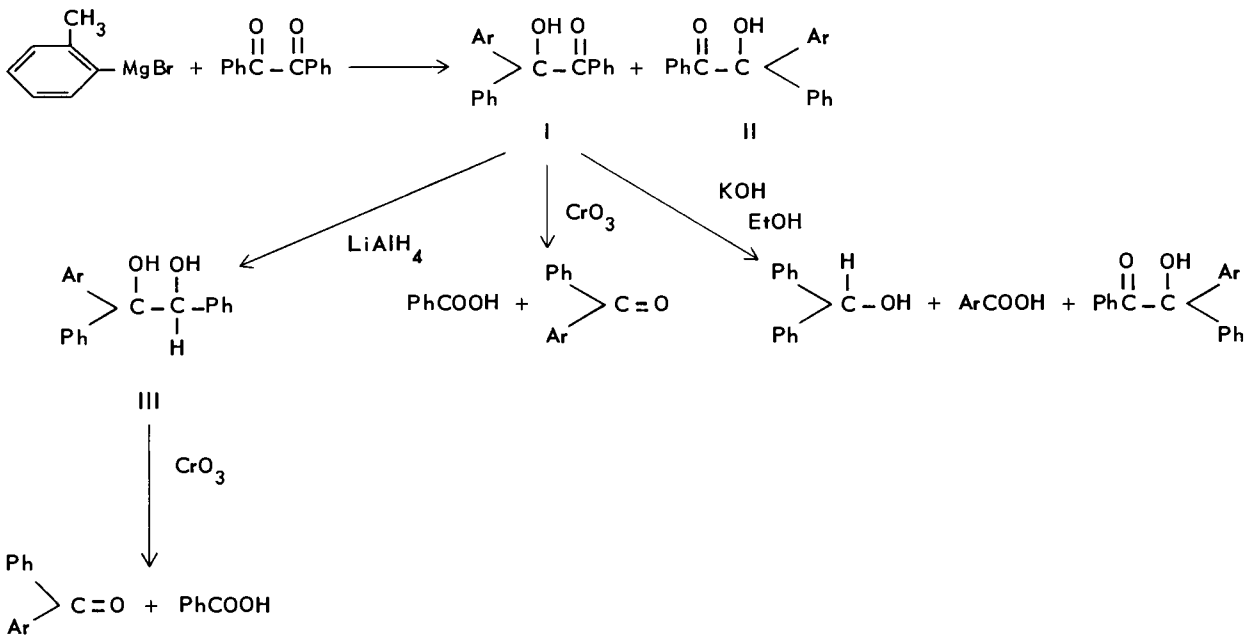

Ar = *o*-tolyl

compound as expected for the previously characterized ketone (IV):

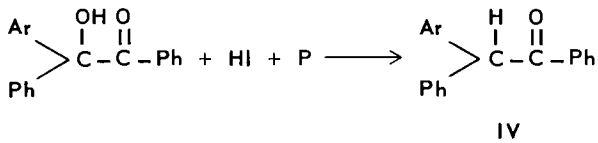

STUDY OF ABNORMAL PRODUCTS IN THE REACTIONS OF BENZYL-TYPE GRIGNARD REAGENTS

E. Campaigne[4]

The formation of abnormal products in the reaction of benzyl-type Grignard reagents has frequently been observed. For example, the reaction of benzylmagnesium chloride with formaldehyde leads to *o*-methylbenzyl alcohol as the principal product, rathen than β-phenylethanol. The abnormal product is usually *ortho*-, although in two cases[5] *para*-products have been obtained in small yield.

No abnormal products have been observed in the reaction of benzylmagnesium halides with carbon dioxide. With the heterocyclics, such as 2-thenylmagnesium chloride, carbon dioxide has been shown to give some abnormal *ortho*-products, as well as normal product. Gaertner[6] isolated 2-methyl-3-thenoic acid, 15% of theoretical, and 2-thienylacetic acid, 29% of theoretical, from the crude acids obtained on carboxylation of 2-thenylmagnesium chloride. He therefore concluded that these were the only acid products and that they were formed in a ratio of 2 parts of 2-thienylacetic acid to 1 part of 2-methyl-3-thenoic acid:

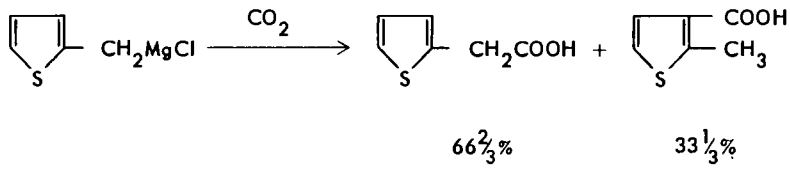

[4]Research participant, Indiana University.

[5]P. R. Austin and J. R. Johnson, *J. Am. Chem. Soc.* 54, 647 (1932); J. G. Burtle and R. L. Shriner, *J. Am. Chem. Soc.* 69, 2059 (1947).

[6]R. Gaertner, *J. Am. Chem. Soc.* 73, 3934 (1951).

The quantitative data in the above work are poor. The crude products are usually separated by fractional crystallization into pure isomers, which are weighed. Therefore, solubility differences would introduce some error, and small amounts of other products might be lost.

The isotope-dilution technique is well suited to analysis of this type, since small amounts of specific products can be obtained by this method. It was therefore proposed to investigate the reaction of benzyl Grignard with carbon dioxide, to determine whether any *ortho*- or *para*-carboxylation occurred, and also to study the 2-thenyl system in the same way.

Results

By use of the cyclic reactor, benzylmagnesium bromide was prepared in 91% yield. When 4.7 mmoles of this solution was carboxylated with $C^{14}O_2$, 285 mg of crude acids was obtained. An aliquot of this crude product was recrystallized twice from heptane and diluted with phenylacetic acid and again recrystallized. Assay of this material showed that the molar activity of the original crude acid was 21.3 mc/mole. To other small aliquots were added known weights of "dead" *o*-toluic and *p*-toluic acids, and these were then reisolated by four recrystallizations from 10% acetic acid, followed by one recrystallization from water. The molar activity of these samples corresponded approximately to 1×10^{-3}, which means less than 0.01% of *o*- or *p*-toluic acids was present.

Since these acids were isolated from mixtures known to contain radioactive phenylacetic acid, a model system, containing 128.5 mg of *o*-toluic acid and 19.5 mg of $C_6H_5CH_2C^{14}OOH$ (molar activity = 21.3), was prepared. Recrystallization of this *o*-toluic acid in the same manner as above gave a product having an apparent molar activity of 3.4×10^{-3}. Therefore, it can be safely stated that no *o*- or *p*-toluic acids are formed in the carboxylation of benzylmagnesium bromide.

2-Thenyl chloride was prepared by chloromethylation of thiophene and was converted to 2-thenylmagnesium chloride in the cyclic reactor. It was necessary to use extreme care in this preparation, since it was found that the Grignard was somewhat unstable even after preparation. The preparation was carried out at high dilution under an atmosphere of helium. An 8.1-mmole amount of the Grignard in solution was carboxylated with excess $C^{14}O_2$, and from this reaction mixture was isolated 831 mg (72.3%) of crude acids. A portion of these acids was recrystallized once from 10% acetic acid and twice more from water and then assayed by the dilution technique. The molar activity of the preparation was thus established as 30.11 mc/mole.

Aliquot samples of the above crude acid mixture were diluted with pure samples of 2-thienylacetic acid, 2-methyl-3-thenoic acid, and 5-methyl-2-thenoic acid. The acids were then recrystallized. The 2-thienylacetic acid was recrystallized three times from 6 ml of heptane, dried *in vacuo*, and sublimed. It assayed at 1.93 mc/mole. The aliquot weighed 33.25 mg and was diluted with 299.5 mg of pure 2-thienylacetic acid. The calculation is

$$(299.5 + x)1.93 = 30.11x \ ,$$

$$x = \frac{299.5 \times 1.93}{28.18} = 20.50 \text{ mg} \ .$$

Therefore

$$\frac{20.50 \times 100}{33.25} = 61.7\% \text{ of 2-thienylacetic acid present in the crude acids.}$$

The 2-methyl-3-thenoic and 5-methyl-2-thenoic acids were dissolved in base, stirred vigorously to homogenize the samples, acidified with 10% sulfuric acid, and centrifuged. The samples were then recrystallized twice from 10% acetic acid and once from water, dried *in vacuo*, and sublimed. After assay and calculation as above, it was shown that there were present 30.15% of 2-methyl-3-thenoic acid and 3.73% of 5-methyl-2-thenoic acid, which account for 95.6% of the total starting product. In all three of the above recrystallizations, a small amount of brown oil was seen to adhere to the walls of the centrifuge tube. This substance was base-soluble but could not be recrystallized. A sample was transferred in ether to a watch glass, evaporated to dryness, and placed under a laboratory monitor. It was found to be quite radioactive. Therefore, a small amount of resinous carboxylated product is formed also.

In view of the small amount of 5-methyl-2-thenoic acid obtained and because of the importance of this finding, that is, a *para*-product in reaction with CO_2, it was necessary to prove beyond doubt that this activity was really due to the formation of 5-methyl-2-thenoic acid in the reaction and not to the carrying along of some 2-methyl-3-thenoic acid, which was recrystallizable from the same

solvent. Therefore, 13.7 mg of the 2-methyl-3-thenoic acid (30.11 mc/mole), which had been isolated to determine the molar activity of the preparation, was mixed with 197 mg of pure 5-methyl-2-thenoic acid; the sample was recrystallized as before, that is, twice from 10% acetic acid and once from water. The molar activity of the isolated material was 0.14, in contrast with 0.24 for that isolated from the crude carboxylation mixture. Since the radioactive 2-methyl-3-thenoic acid may have contained some 5-methyl-2-thenoic acid, the experiment is inconclusive.

In order to clarify this situation and to confirm the previous experiments, a second sample of 2-thenylmagnesium chloride was carboxylated with $C^{14}O_2$. The crude acids were separated (56% yield), and a fraction was recrystallized and assayed as before. The molar activity of the preparation was found to be 26.0. Aliquot samples were then diluted with the three pure acids and recrystallized as before, with the exception that the 5-methyl-2-thenoic acid fraction was recrystallized twice from 10% acetic acid, once from water, three more times from 10% acetic acid, and then washed with water. At the same time, the model 5-methyl-2-thenoic acid system (13.7 mg of 2-methyl-3-thenoic acid-$C^{14}OOH$ plus 197 mg of 5-methyl-2-thenoic acid) was recrystallized three more times from 10% acetic acid and washed with water. It is hoped that assay of these samples will show whether more activity is washed out by these further recrystallizations. From these results, an estimate of the significance of the value 3.73%, for 5-methyl-2-thenoic acid, may be made.

Conclusions

In the reaction of benzylmagnesium bromide with carbon dioxide, no *o*- or *p*-toluic acid is formed. In the carboxylation of 2-thenylmagnesium chloride, 61.7% of 2-thienylacetic acid and 30.1% of 2-methyl-3-thenoic acid (the *ortho*-product) are formed. 5-Methyl-2-thenoic acid (the *para*-product) is apparently formed to the extent of 3.7%. However, the reality of this value must be confirmed.

CHEMICAL PHYSICS

RADIO-FREQUENCY SPECTROSCOPY

H. Zeldes R. Livingston

Quadrupole Spectroscopy

Pure quadrupole resonance frequencies can be shifted in value by applying pressure to the sample being studied. This effect has never been explored in a detailed manner. A series of measurements has been started in which the pressure effects in several types of substances will be measured and compared. The only modification made in the quadrupole spectrometer has been to enclose the sample coil in a pressure cell. The samples are then subjected to nitrogen pressures up to 9000 psi. The pressures are achieved by condensing liquid nitrogen in a vessel on a high-pressure manifold and then allowing the liquid nitrogen to warm up and create the high pressure. Table 15 gives the measured values on the three substances, all chlorates, for which measurements have been completed.

As might be expected, the frequency shifts become smaller at the lower temperatures, where the crystalline materials are less readily deformed. The frequencies always increase with increasing pressure. They also increase with decreasing temperature, which suggests a comparison of the two effects, with the volume change used as a parameter. The comparison for $NaClO_3$, which is cubic, shows the order of magnitude of the two effects to be the same. Measurements are continuing on a larger variety of materials.

Paramagnetic Resonance

The microwave spectrometer used in the 9000-Mc region has been rebuilt with a number of refinements. The spectrometer does not have the basic sensitivity of 23,000 Mc which equipment used in much of the earlier work had. Very much larger sample sizes can be used, however, so that the lower sensitivity with respect to number of unpaired electrons is not of serious concern in those cases where an adequate sample size is available. A microwave frequency standard has been put into operation, and now g-factor values can be measured by directly determining the microwave frequency and magnetic field. Previous g-factor measurements were made by comparing the unknown substance with a paramagnetic species whose g factor was measured elsewhere. A number of observations have been made and are summarized below.

α,α-Diphenyl-β-picrylhydrazyl (Hydrazyl). – The free radical, hydrazyl, has been studied by a number of investigators, since it is chemically stable, gives a sharp resonance absorption line, and is useful as a g-factor standard. In order to

TABLE 15. PRESSURE EFFECTS ON THE QUADRUPOLE RESONANCE FREQUENCIES FOR Cl^{35} IN THREE CHLORATES

Substance	Temperature (°C)	Atmospheric-Pressure Frequency (Mc)	Frequency-Shift (kc) Increase for 1000 psi
$NaClO_3$	45.85	29.8249	2.19 ± 0.05
	0	30.0326	1.84 ± 0.05
	–78	30.3240	1.43 ± 0.05
	–196	30.6320	1.11 ± 0.05
$KClO_3$	27.4	28.0751	2.08 ± 0.05
	0	28.2132	1.75 ± 0.05
	–78	28.5599	1.11 ± 0.05
	–196	28.9534	0.45 ± 0.05
$Ba(ClO_3)_2 \cdot H_2O$	27.4	29.3279	0.74 ± 0.05
	0	29.4177	0.76 ± 0.05
	–78	29.6513	0.66 ± 0.05
	–196	29.9222	0.53 ± 0.05

test the measuring equipment mentioned above, an absolute g-factor measurement was made on powdered hydrazyl. The measured value was 2.00363, as compared with the Holden *et al.*[1] value of 2.0036 ± 0.0002 and with the Hutchison and Pastor[2] value of 2.0037 ± 0.0001.

Singer and Kikuchi[3] recently reported on the small g-factor anisotropy in single crystals of hydrazyl at various temperatures. They reported that the line width was constant within their experimental uncertainty of ±20%. This is in contrast with recent findings[4] here, where a pronounced anisotropy in line width was found. Further measurements on the line-width anisotropy have been made.[5]

Electric-Discharge Products. – A study on the condensed products of electric discharges through water vapor and related substances[4] in collaboration with J. Ghormley has been summarized in a publication to appear soon.[6]

Calcium Hydroxide. – Single crystals of $Ca(OH)_2$ have been irradiated and examined at 77°K. Three absorption lines are present. Two of them are very weak and correspond to a very small yield of atomic hydrogen. There is no anisotropy in the g value of the hydrogen lines, since the atom is in an S state. There is a pronounced anisotropy in the width of the hydrogen lines, however, which demonstrates that the hydrogen is associated with the crystal structure and is not randomly distributed in the lattice. This width anisotropy presumably is a consequence of magnetic dipole-dipole interactions, and its detailed study could conceivably lead to information on the location of the hydrogen atoms. The remaining third line is sharp and shows a pronounced g-factor anisotropy which has very clearly been shown to be axially symmetric, with the symmetry axis along the c axis of the hexagonal crystal. The measured g values are $g_{\parallel} = 2.0018$ and $g_{\perp} = 2.07425$. This line shows a pronounced width anisotropy. At 77°K the full widths at half height are 5.2 gauss for the $g_{\perp}$ orientation, about 4.6 gauss for the $g_{\parallel}$ orientation, and 8.0 gauss at maximum broadness which appears at an inclination of roughly 45 deg on one side of the $g_{\perp}$ orientation. The line, moreover, shows weak satellite lines due to a weak interaction with near-neighbor protons.[7] At 77°K the satellites are only partly resolved at 9000 Mc but are clearly resolved at 23,000 Mc. The width of the line changes greatly with temperature. At a somewhat lower temperature, achieved by pumping on liquid nitrogen, the line sharpens sufficiently that the satellites can be clearly resolved at 9000 Mc. In some orientations the line itself starts to split into a doublet. This line has tentatively been assigned to the OH radical. Additional measurements including lower temperature studies are under way.

Ice. – Large samples of polycrystalline gamma-irradiated H_2O and D_2O ice at 77°K have been examined in the 9000-Mc spectrometer. The absorption in the H_2O ice is a crude doublet. The two components are of unequal strength, and there is some indication that additional lines are present in the over-all doublet structure. The doublet spacing is roughly 40 gauss, or 115 Mc. The damage giving rise to the doublet anneals slowly at –175°C. The intensity in one typical sample dropped to about half in 15 min. The D_2O ice shows an irregularly shaped line having unresolved components. The line structure thus appears to show hyperfine effects. These lines may very well be the same lines reported by Matheson and Smaller[8] in a spectrometer operating at very much lower frequencies.

Irradiated single crystals of H_2O ice examined at 77°K showed a number of lines with pronounced anisotropy in the g values. The lines are not clearly resolved, but a minimum of five is present; they are shown in Fig. 28. The crude doublet structure in polycrystalline ice, hence, is the envelope of these lines averaged over random orientations. The single-crystal data have not been interpreted, and the possibility of trapped charges such as an F center as well as free radicals must be included.

[1] A. N. Holden *et al.*, *Phys. Rev.* **77**, 147 (1950).

[2] C. A. Hutchison, Jr., and R. C. Pastor, *Phys. Rev.* **81**, 282 (1951).

[3] L. S. Singer and C. Kikuchi, *J. Chem. Phys.* **23**, 1738 (1955).

[4] R. Livingston and H. Zeldes, *Chem. Semiann. Prog. Rep. June 20, 1955*, ORNL-1940, p 44.

[5] R. Livingston and H. Zeldes, *J. Chem. Phys.* **24**, 170 (1956).

[6] R. Livingston and H. Zeldes, *J. Chem. Phys.* (to be published).

[7] H. Zeldes and R. Livingston, *Phys. Rev.* **96**, 1702 (1954).

[8] M. S. Matheson and B. Smaller, *J. Chem. Phys.* **23**, 521 (1955).

Fig. 28. Absorption Lines of Gamma-irradiated Ice Crystal at 77°K. Rotation from top to bottom was 16.5 deg.

NEUTRON DIFFRACTION STUDY OF $Ca(OH)_2$ AT −140°C

W. R. Busing H. A. Levy

The results of a single-crystal neutron diffraction study of $Ca(OH)_2$ at room temperature have recently been reported.[9] This work has now been repeated at −140°C, and the position parameters and temperature-factor coefficients obtained from the intensities of 53 reflections by means of a complete least-squares treatment are listed below:

z (O)	0.2346 ± 0.0002
z (H)	0.4280 ± 0.0004
B (Ca, ⊥ to c axis)	0.30 ± 0.04 Å^2
B (Ca, ∥ to c axis)	0.63 ± 0.05 Å^2
B (O, ⊥)	0.40 ± 0.03 Å^2
B (O, ∥)	0.52 ± 0.03 Å^2
B (H, ⊥)	3.30 ± 0.08 Å^2
B (H, ∥)	0.83 ± 0.06 Å^2
$c(z_H - z_O)$	0.942 ± 0.002 Å
"True" OH distance	0.980 ± 0.002 Å

The conventional discrepancy factor

$$\frac{\Sigma\left||F_{obs}| - |F_{calc}|\right|}{\Sigma|F_{obs}|}$$

is 3.3%, all reflections included.

In the course of this work, it was found that the previously reported results are somewhat in error because of incorrect weighting of the observations. The correct room-temperature results will be reported when the recalculation is complete. At present, it appears that the changes in the position parameters will be negligible but that those of the temperature-factor coefficients will be appreciable. For this reason a quantitative comparison of these coefficients at the two temperatures cannot be made now.

It was suggested in the previous report that the apparent O-H distance, $c(z_H - z_O)$, of 0.934 ± 0.002 Å was shorter than the true O-H distance because thermal motion of the hydrogen atom gives the OH bond an appreciable average inclination to the c axis. This supposition is supported by the present work, which shows that the apparent O-H distance increases to 0.942 ± 0.002 Å at −140°C, presumably because the thermal motion of the hydrogen atom is decreased. An estimate of the true O-H distance should then be the hypotenuse of a right triangle, one side of which is the apparent distance and the other side of which is the mean thermal displacement of hydrogen atom relative to the oxygen atom in the direction perpendicular to the c axis. This "true" distance is then

$$\sqrt{c^2(z_H - z_O)^2 + 2[B(H,\perp) - B(O,\perp)]/8\pi^2} = 0.980 \pm 0.002 \text{ Å} .$$

Preliminary indications are that the recalculated room-temperature results will give a true O-H distance in agreement with the above. Instead of being unusually short, the interatomic distance in OH^- ion is probably longer than the O-H distance of 0.958 Å found in water.[10]

[9] W. R. Busing and H. A. Levy, *Chem. Semiann. Prog. Rep. June 20, 1955*, ORNL-1940, p 43.

[10] D. M. Dennison, *Revs. Mod. Phys.* **12**, 175 (1940).

PARTIAL VAPOR PRESSURES OVER MIXTURES OF SALTS

S. Datz R. E. Minturn[11]

The observations reported previously[12] on differential detection of alkali metals and their halides by a surface ionization gage are about to be applied to the measurement by the effusion technique of the partial vapor pressures of such components over salt mixtures. The vacuum chamber and the detector have been completed, and the effusion cells (or ovens) have been revised to minimize thermal gradients and are now satisfactory. The ovens have been operated up to about 850°C with no more than a 25°C gradient between the effusion hole and the salt well, with the latter the coolest part of the oven. Both these temperatures need to be known, that of the salt well being the condensed-phase temperature to which the measurement applies and that of the effusion hole being required to convert the measured flux to the desired vapor concentration.

Effusion plates have been prepared with holes down to 2×10^{-4} in. in diameter, making effusive flow obtainable up to total vapor pressures of about 10 mm Hg. This may not be the upper limit of pressure, since molecular flow may prove not to be necessary. The lower limit of pressure will be no greater than 10^{-6} mm.

[11] On loan from U.S. Air Force.

[12] S. Datz and E. H. Taylor, *Chem. Semiann. Prog. Rep. June 20, 1955*, ORNL-1940, p 44.

CHEMISTRY OF SEPARATION PROCESSES

FUNDAMENTAL STUDIES ON ION EXCHANGE RESINS

G. E. Myers S. Lindenbaum
G. E. Boyd

Thermodynamic Calculation of Cation Exchange Selectivities

In a paper to appear in the March 1956 issue of the *Journal of Physical Chemistry*, it has been demonstrated that a complete and thermodynamically rigorous computation of the selectivity coefficients, D, shown by variously cross-linked sulfonated polystyrene cation exchangers may be carried out for the exchange of hydrogen, lithium, potassium, and cesium ions with sodium ion. Exact evaluations of the osmotic free energy and activity coefficient ratio terms appearing in the Gibbs-Donnan equation for D were performed by using cross-differentiation relationships. Agreement within the errors involved was found on comparing the computed with the experimentally determined selectivity coefficient values, except for the most highly cross-linked exchangers, where significant discrepancies occurred. It was concluded that cation exchangers prepared by the sulfonation of polystyrene-divinyl-benzene copolymers are not truly monofunctional and that the differing thermodynamic properties of the variously substituted sulfonic acid groups they contain are probably the cause of the observed unexpected variation of D with "loading."

Zinc-Sodium Ion Exchange Equilibrium in Sulfonated Polystyrene Resins

An effort is being made to extend the above thermodynamic computation of selectivities to exchanges between ions of unequal charge. Measurements have been performed upon variously cross-linked sulfonated polystyrene resins for the exchange of sodium with zinc ions. Shown in Fig. 29 are plots of the equilibrium quotients for the reaction

$$Zn_w^{++} + 2Na_r^+ \rightleftharpoons Zn_r^{++} + 2Na_w^+$$

$$k = \frac{n_{Zn}^r}{n_{Zn}^w} \cdot \left(\frac{n_{Na}^w}{n_{Na}^r}\right)^2 ,$$

where n represents equivalents, and w and r represent the external aqueous phase and the resin phase, respectively. As may be seen, zinc ion is very strongly preferred over sodium ion by resins of all cross-linking. The general pattern of the data is in qualitative agreement with unpublished measurements[1] upon the zinc-hydrogen and the copper-hydrogen exchanges with similar resins. If, instead of the equilibrium quotient, the selectivity coefficient

$$D = \frac{(m_{Zn}/m_{Na})_r}{(m_{Zn}/m_{Na})_w}$$

is plotted, the strong dependence of the equilibrium distribution upon resin loading becomes even more apparent; sharp minima in the D occur at X_{Zn} equal to about 0.8 for all but the ½% and the 2% DVB resins. It appears likely, then, that quite specific interactions must take place in this system, particularly with the more highly cross-linked resins. It is hoped that some insight into the nature of these interactions will be gained by comparing the observed selectivities with those to be calculated thermodynamically and by further comparing the latter with activity coefficients now being measured in the aqueous zinc nitrate–sodium nitrate system.

Osmotic Coefficients of 0.5% DVB Polymethacrylate Resin Salts

Osmotic coefficients of a number of salts of a very weakly cross-linked (0.5% DVB) polymethacrylate resin have been obtained in the continuation of a general program of isopiestic studies with ion exchange resins of varying structures. Such a resin contains weakly acid carboxyl groups and shows a relatively large exchange capacity. Figures 30 and 31 present, respectively, osmotic coefficients for several univalent and divalent salts of this exchanger. Since these data are as yet somewhat tentative and since it is expected in the future to compare them with analogous results for variously cross-linked polyacrylate resins, the present discussion will remain qualitative in nature.

The most pronounced effect observed here is the reversal in the order of osmotic coefficients of alkali salts from that existing in a weakly

[1] O. D. Bonner, private communication, April 1955.

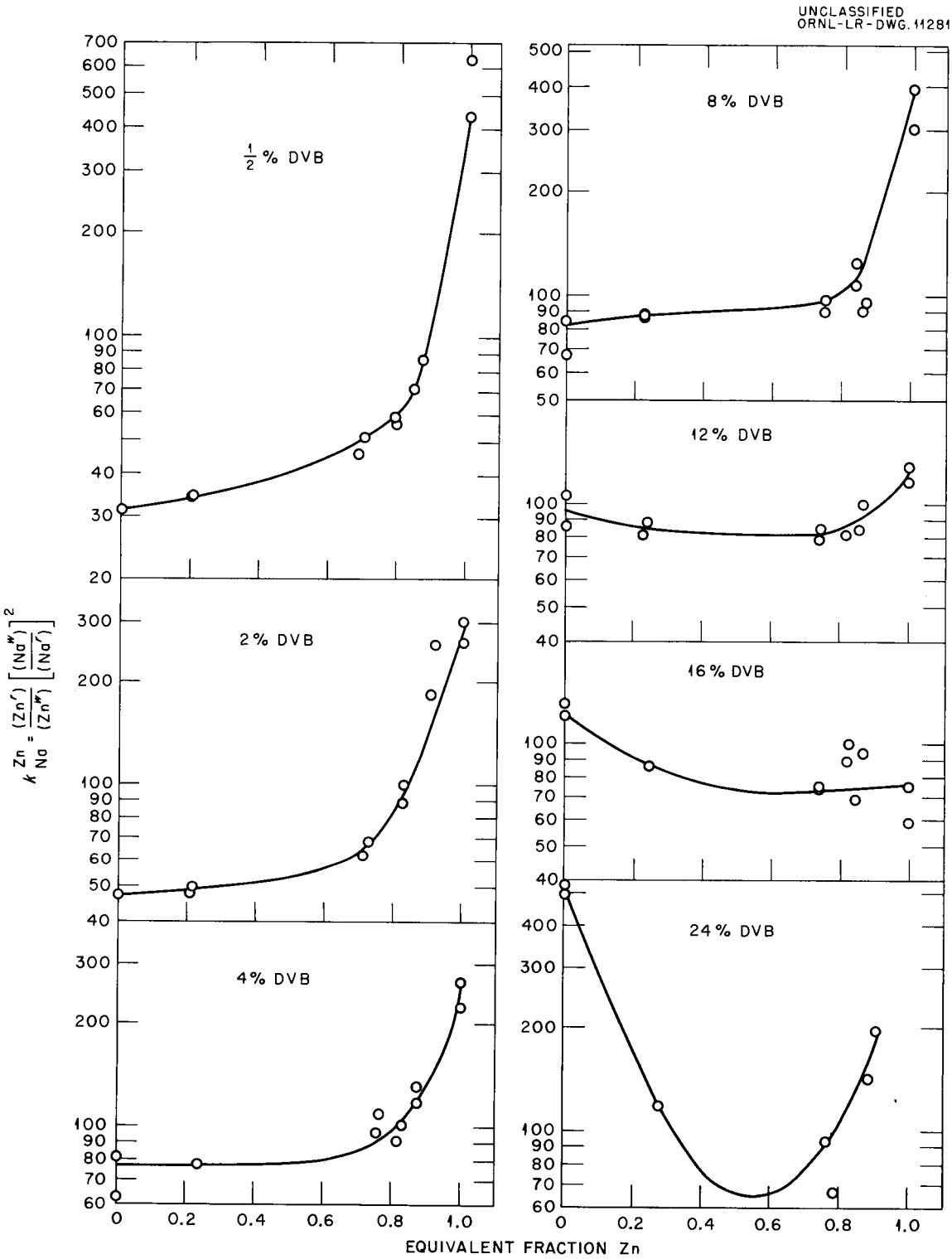

Fig. 29. Equilibrium Quotients for the Zn-Na Exchange Reaction on Variously Cross-linked Sulfonated Polystyrene Resins.

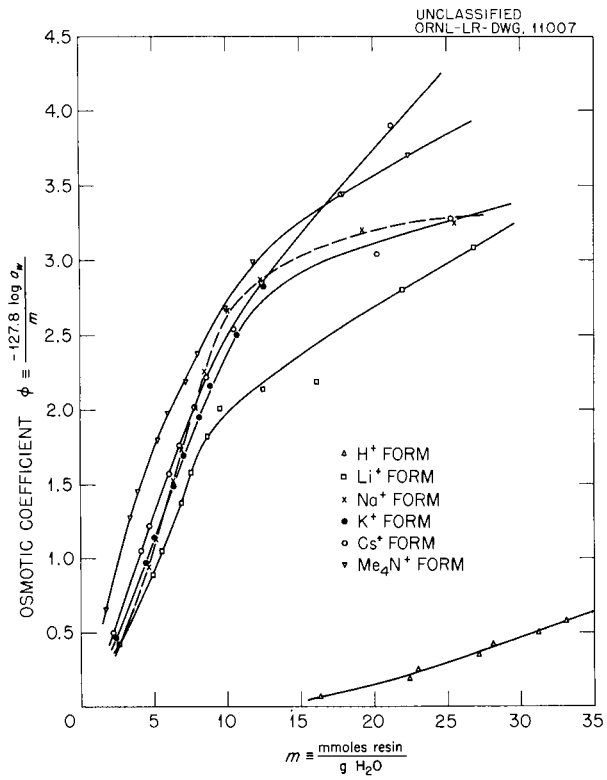

Fig. 30. Osmotic Coefficients of Monovalent Cation Salts of 0.5% DVB Polymethacrylate Resin.

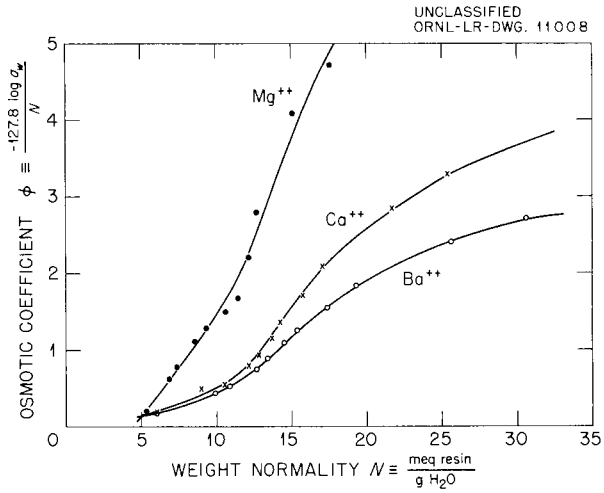

Fig. 31. Osmotic Coefficients of Alkaline-Earth Salt Forms of 0.5% DVB Polymethacrylate Resin.

cross-linked sulfonate resin,[2–4] while the order for the alkaline-earth cation salts[5] is the same for both types of resin.

It may be predicted, then, that highly cross-linked methacrylate resins should prefer lithium to cesium ions, just the reverse of the known pattern for highly cross-linked sulfonate resins. It is also noteworthy that the orders of osmotic coefficients for the series of the alkali and of the alkaline-earth cation salts of the methacrylate resin are the same as those observed in aqueous solutions of the same salts of acetic acid.[6] The fact that the curves for the barium and calcium salts (Fig. 31) appear to be crossing above the curve for magnesium at lower concentrations further parallels the behavior of acetates.[7]

Harned has proposed that the sequence of osmotic coefficients in the alkali acetates arises from a "localized hydrolysis," resulting from the interaction of a proton of the hydration water of the cation with the acetate ion; thus the more highly hydrated ions will possess the smaller osmotic coefficients. For the alkaline-earth salts the effect of localized hydrolysis probably is overcome by their tendency to form ion pairs as the concentration increases, this tendency being greatest for the barium ion. Presumably, these same factors are responsible for the sequence observed in the methacrylate resin.

In the case of the weakly cross-linked resin, however, these factors are complicated by the resin network and by the relatively great density of charges along the chains. The fact that the charge density along the methacrylate chains is approximately twice that in the polystyrene sulfonate resins makes it somewhat surprising that the methacrylate osmotic coefficients are in general as large as those in the sulfonate resin, or larger. It may well be, however, that the increased charge density causes greater swelling of the methacrylate resin and consequently greater water uptake. This same effect

[2] G. E. Boyd and B. A. Soldano, *Z. Elektrochem.* 57, 162 (1953).

[3] E. Glueckauf, *Proc. Roy. Soc. (London)* A214, 207 (1952).

[4] B. A. Soldano and Q. V. Larson, *J. Am. Chem. Soc.* 77, 1331 (1955).

[5] G. E. Myers and G. E. Boyd, *Chem. Semiann. Prog. Rep. June 20, 1955*, ORNL-1940, p 47.

[6] H. S. Harned and B. B. Owen, *The Physical Chemistry of Electrolyte Solutions*, 2d ed. (rev.), Reinhold, New York, 1950.

[7] R. H. Stokes, *J. Am. Chem. Soc.* 75, 3856 (1953).

may explain the relatively large osmotic coefficients of the $(CH_3)_4N^+$ form of the methacrylate resin; that ion, being so large in size, cannot closely approach the carboxyl groups on the resin chains and therefore permits considerable repulsion between the carboxyl groups, with resultant swelling. This consideration also holds for the $(CH_3)_4N^+$ form of the sulfonate resins.

Water Sorption Studies with the Tetraalkyl Ammonium Salts of Polystyrene Sulfonic Acid Resins

Earlier studies[2,3] have shown that a linear relationship exists between swelling pressure and resin volume for univalent salt forms of cross-linked Dowex 50 and Dowex 1 ion exchangers. Within the salt forms investigated the relationships were independent of salt form but were dependent upon cross-linking. It was deemed of interest to determine whether identical relationships were valid for the tetraalkyl ammonium ions. These might be expected to complicate the elastic properties, first, because of the possibility that their relatively large size might hinder complete contraction of the resin network and, second, because of the possibility that energetic effects might be introduced as a result of interaction between the relatively nonpolar groups and the organic portions of the resin chains. Accordingly, water sorption isotherms were obtained for the tetramethyl, tetraethyl, tetra-*n*-propyl, and tetra-*n*-butyl ammonium forms of 8% DVB sulfonated polystyrene resins. The data for the tetraalkyl ammonium, hydrogen, and ammonium salt forms of the 8% DVB resin are shown in Fig. 32. Since the desired volume data are not yet available, only a qualitative discussion of the water sorption curves will be attempted for the present.

The total influence of the various ions involved here upon the water sorption of a particular resin may be divided into four primary, though not entirely independent, factors: (1) degree of hydration, which increases water sorption in the order $NH_4^+ > Me_4N^+ > Et_4N^+ > Pr_4N^+ > Bu_4N^+$, (2) ion size and its expansion of the resin network, causing increased pressure and thus excluding water in the order $Bu_4N^+ > Pr_4N^+ > Et_4N^+ > Me_4N^+ > NH_4^+$, (3) interaction of the nonpolar groups with themselves and/or with the nonpolar chain backbone, which decreases water sorption in the same order as the second effect, and (4)

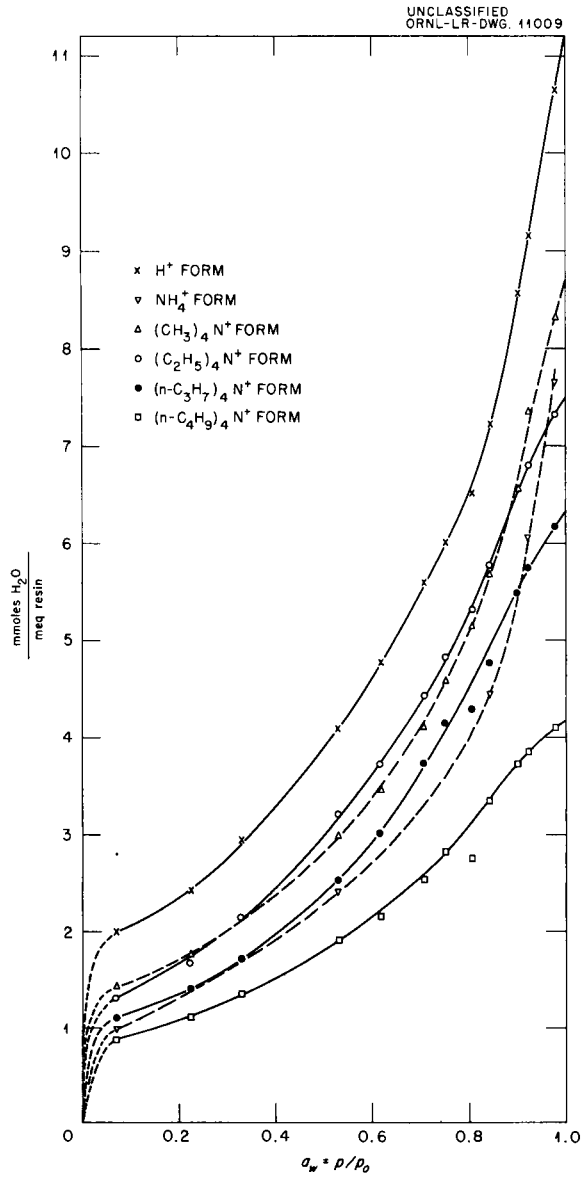

Fig. 32. Water Sorption of Tetraalkyl Ammonium Salts of Nominal 8% DVB Sulfonated Polystyrene Resin.

interaction with the sulfonate group (i.e., ion-pair formation), which should *decrease* water sorption in the order $NH_4^+ > Me_4N^+ > Et_4N^+ > Pr_4N^+ > Bu_4N^+$ at low water content, although the NH_4^+ may well change position in the scale at higher water contents.

At very low water contents the curves of Fig. 32 indicate that the second and third factors above

are those which predominate among the substituted ammonium ions, whereas the relatively low water content of the ammonium salt must be the consequence of a considerable degree of ion-pair formation between that relatively small ion and the sulfonate ions. In view of the several conflicting factors, no clear-cut explanation for the crossing of the Me_4N^+ curve under the Et_4N^+ in the middle range appears possible. However, at the highest water content the same effects of ion size expanding the network and of nonpolar interactions again seem to predominate among the substituted ammonium salt forms, resulting in a repression of water sorption relative to the H^+ and NH_4^+ salts. This repressing action is even more strikingly evident when it is considered that water sorption data for a very weakly cross-linked sulfonate resin demonstrate that the unsubstituted ammonium ion is less osmotically active than are the Me_4N^+, Et_4N^+, and Pr_4N^+ ions in this concentration range. The greater osmotic activity of these last three ions over ammonium ion indicates further that the nonpolar interactions discussed above may be a minor consideration in the repression of water sorption and that therefore it is the large size of the tetraalkyl ammonium ions which is primarily responsible for that repression.

EXTRACTION OF MONOVALENT ELECTROLYTES BY TRIBUTYL PHOSPHATE

B. A. Soldano W. H. Baldwin

The general problem of synthesizing and evaluating new organic solvents for their extraction ability tends to highlight the need of a general quantitative method for representing these systems.

In any attempt to characterize the distribution of salts between water and neutral organic systems, two basic problems become self-evident:

1. the determination of the actual hydrated species that is distributed between the two phases,
2. evaluation of the radical changes that occur when the concentrations of the aqueous solutions are increased from the dilute to the concentrated range.

This report will be concerned with the findings based upon the investigation of 11 salt systems from the dilute to the concentrated region.

An earlier attempt[8] to extend the Flory, Huggins, Hildebrand equation to the hydrated salt–organic solvent systems revealed the following difficulties when enough systems had been studied:

1. The entropy term in the equation proved to be of little importance and thus did not warrant the added complication.
2. The rapid change of the hydrated salt–organic solvent interaction term with change in the salt concentration made the assumptions of the equation inadequate to handle concentrated salt effects.

After an extensive evaluation of existing equations in the literature, the following equation was found to be the most effective in representing the experimental findings:

$$(1)\quad 2 \log (m\gamma\pm) + n \log a_w = \log K + \log m_r + b_r m_r \ ,$$

where

m = molality of the electrolyte in the aqueous phase,

$\gamma\pm$ = the mean ionic activity coefficient of the aqueous electrolyte solution,

n = the number of moles of water per mole of species distributed,

a_w = the activity of the water in the electrolyte solution,

$-RT \ln K = \Delta F$ = the change in free energy associated with varying the environment from aqueous electrolyte to electrolyte in the organic solvent,

m_r = molality of salt in the organic solvent,

b_r = empirical constant characteristic of each system.

The above equation is based on the assumptions that (1) an equilibrium can be written

$$K = \frac{[\text{Electrolyte}]^2 a_w^n}{[\text{Electrolyte}\cdot\text{organic}]} \ ,$$

when

[Electrolyte] = mean ionic activity of the electrolyte in water,

[Electrolyte·organic] = activity of the hydrated electrolyte in the organic solvent;

(2) the logarithm of the activity coefficient, γ_r, of the associated salt in the organic phase can be represented by a term linear in molality:

$$\frac{\partial \log \gamma_r}{\partial m_r} = b_r \quad ;$$

[8] W. H. Baldwin and B. A. Soldano, *Chem. Semiann. Prog. Rep. June 20, 1955*, ORNL-1940, p 52.

(3) the hydrated salt in the organic phase is highly associated.

The use of Eq. 1, with the constants shown in Table 16, permits an accurate reproduction, within 2%, of the salt distribution between the aqueous and tributyl phosphate phases from aqueous electrolyte concentrations of approximately 0.1 m to as high as 9 m.

TABLE 16. CONSTANTS FOR THE EXTRACTION OF ELECTROLYTES BY TRIBUTYL PHOSPHATE

Electrolyte	n	log K	b_r
HI	3.8	−0.9	1.2
LiI	3	−0.5	0.77
NaI	1.5	1.32	0.0
KI	0.6	1.64	0.0
HBr	3.8	0.5	1.00
LiBr	3	1.98	0.42
HCl	3.8	1.15	0.24
LiCl	3	2.95	0.0
CsCl	0	3.64	0.0
HNO_3	2	−0.8	0.30
HNO_3*	2	−0.03	0.30

*Diluted with n-hexane.

It is pertinent to examine the nature of the constants needed in Eq. 1. Since the activity of the assumed extracted component varies with a_w^n, it is obvious that the resulting treatment of the data by use of Eq. 1 will be strongly influenced by the values of n. This problem becomes extremely important in concentrated solutions, where the activity of water differs greatly from unity, while at high dilution, where a_w is approximately unity, the product $n \log a_w \cong 0$.

For years investigators have, on the basis of extraction experiments in the dilute range, arrived at extremely high values of n; for example, $n = 10$ for NaCl. Such answers resulted from the fact that, at low salt concentrations, water held by the organic solvent because of its own affinity for water cannot be distinguished from water held by the ions.

A better value for the number of moles of water in the extracted hydrated component can be obtained, however, in the concentrated region. As was expected, the experimentally measured amount of water per equivalent of salt in the organic phase decreases with the molality m_r of the salt in the organic phase but approaches a limiting value for each salt at high concentrations (Fig. 33). The salt concentration at which leveling occurs must be indicative of strong salt-water interaction, and it seems reasonable to suppose that the true average hydration is reflected by these numbers. The amount of water retained per equivalent of halogen acid is independent of the anion type as n approaches a value of 3.8. The lithium halides show different moisture retention at low concentrations, but, again, all the salts retain the same amount of water at high concentrations in the organic phase ($n = 3$).

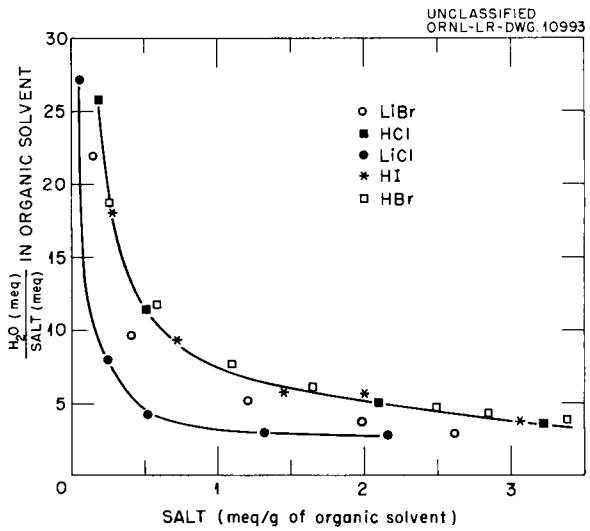

Fig. 33. Moisture Characteristics of TBP.

The values of hydration numbers so measured agree fairly well with those proposed by Glueckauf and Kitt[9] on the basis of the study of cation exchange behavior.

A calculation of the free-energy term represented by $RT \ln K$ gives values ranging from 0 to 5000 cal. This is the range encountered in the formation of hydrogen bonds and suggests that for the systems investigated, where there is little evidence of specific anion effects, extraction is

[9]E. Glueckauf and G. P. Kitt, *Proc. Roy. Soc. (London)* **A228**, 322 (1955).

essentially due to the formation of such bonds between the tributyl phosphate and the hydrated electrolyte. This theory will be discussed in detail in a paper now being prepared for publication.

PYROLYSIS OF BUTYL PHOSPHATE ESTERS

C. E. Higgins W. H. Baldwin

It has been shown previously[10] that the reaction between unlabeled tributyl phosphate and P^{32}-labeled H_3PO_4 can be used to prepare the labeled butyl esters. It has now been shown that the esters themselves undergo pyrolytic reactions.

Labeled esters were heated for the times and temperatures indicated in Table 17. At the end of this time the reaction mixture was neutralized with sodium hydroxide. The neutral tributyl phosphate was extracted into CCl_4. Aliquots of the CCl_4 solution were counted to obtain the P^{32} activity. Aliquots removed from the aqueous solution were placed on an anion exchange resin column and selectively eluted for estimation of the individual component acids.

The over-all reaction can be summarized as one involving a redistribution of the butyl ester groups accompanied by the loss of some of the butyl groups. It can be readily seen (Table 17) that stability decreases with an increase in the number of acidic hydrogens. Similar behavior has been noted in mixtures of tributyl phosphate and phosphoric acid, the more acidic mixtures being less stable to heat. This pyrolytic behavior explains some of the difficulties encountered during the attempted distillation of these esters.

[10] C. E. Higgins and W. H. Baldwin, *Ester Interchange Between Tributyl Phosphate and Phosphoric Acid*, Paper 62 presented before the Division of Organic Chemistry, 128th Annual Meeting of the American Chemical Society, Minneapolis, Minn., September 1955.

PREPARATION OF DIPHOSPHINE DIOXIDES

W. H. Baldwin

Since trialkyl phosphine oxides are useful compounds for the extraction of uranium, it was desirable to test compounds that contain two phosphine oxide groups in the molecule. A series of such compounds may be represented by the general formula $Bu_2P(O)(CH_2)_xP(O)Bu_2$. After several unsuccessful attempts to prepare the compound where $x = 2$, attention was shifted to the compound where $x = 5$. The double-ended Grignard reagent was prepared from pentamethylene bromide, thus:

$$Br(CH_2)_5Br + 2Mg \longrightarrow BrMg(CH_2)_5MgBr$$

To this Grignard reagent was added dibutyl phosphinyl chloride according to the reaction:

$$BrMg(CH_2)_5MgBr + 2Bu_2P(O)Cl \longrightarrow Bu_2P(O)(CH_2)_5P(O)Bu_2 + 2MgBrCl$$

P,P,P′,P′-Tetrabutyl pentamethylenediphosphine dioxide is a white solid that melts between 105 and 106°C when crystallized from hexane. It is soluble in water, ethanol, carbon tetrachloride, and benzene but only slightly soluble in ether

TABLE 17. DISTRIBUTION OF P^{32} AFTER PYROLYSIS OF ESTERS

Ester Pyrolyzed[a]	P^{32} (%) in Products of Pyrolysis				
	H_3PO_4	Monobutyl Dihydrogen Phosphate	Dibutyl Hydrogen Phosphate	Tributyl Phosphate	Unidentified Acids[b]
Tributyl phosphate-P^{32}	0.05	0.27	2.79	95.7	0.08
Dibutyl hydrogen phosphate-P^{32}	2.0	20.6	58.5	19.2	
Monobutyl[c] dihydrogen phosphate-P^{32}	32.3	33.2	14.2	0.8	20.4

[a] The first ester listed was pyrolyzed for 1 hr at 206°C, the second one for 3 hr at 177°C, and the third one for ½ hr at 177°C.

[b] Polyphosphoric acids and esters.

[c] 95% pure, contaminated with small amounts of $H_3P^{32}O_4$ and dibutyl hydrogen phosphate-P^{32}.

and in petroleum ether. The amount of phosphorus found in two determinations was 15.70 and 15.60%; the amount calculated for $C_{21}H_{46}P_2O_2$ is 15.78%.

Despite its solubility in water, this compound seems to be worth testing for its merits in solvent extraction.

COMPLEXING OF CATIONS WITH ORGANOPHOSPHORUS ACIDS

B. E. Bryant[11] W. H. Baldwin

The ability of organophosphorus acids to extract uranium from aqueous solutions prompted an attempt to obtain quantitative measures of the solution stabilities of these complexes. The first method attempted was that of Bjerrum as modified by Calvin and Wilson[12] for acidic chelating agents. As representative acids, diethyl phosphinic, di-*n*-butyl phosphinic, and di-*n*-hexyl phosphinic were chosen. The slight water solubilities of the two heavier acids necessitated the use of 50% dioxane as a solvent. All titrations were conducted in a constant-temperature bath set for 25°C in a manner described previously.[13]

The acid dissociation constants of each of the acids were determined in this solvent by potentiometric titration with a standardized aqueous solution of tetramethylammonium hydroxide. The following values were determined, in the form of pK_D, and, for comparison, the values in water as determined by Crofts and Kosolapoff[14] for two of the acids are shown:

	pK_D	
	50% Dioxane	Water
Diethyl phosphinic acid	4.78	3.29
Di-*n*-butyl phosphinic acid	5.00	3.41
Di-*n*-hexyl phosphinic acid	5.18	

It is seen that the apparent dissociation of the acids is less in 50% dioxane, as would be expected from the lower dielectric constant of the mixture. Similarly, the dissociation of any metal complexes should be less in the mixed solvent than in pure water. However, it was found that many of the common divalent metal ions combine with the acids to form compounds which are insoluble even in 50% dioxane. For example, UO_2^{++}, Zn^{++}, and Cu^{++} almost invariably form insoluble powders upon addition of their compounds to a dilute solution of these acids. Cobalt and nickel, with one exception, were sufficiently soluble in the presence of the acids to permit titration in the normal fashion.

The behavior of these metals in the presence of the phosphinic acids was rather unusual. Bjerrum has defined the symbol $\bar{n}$ as equal to the ratio of bound ligand to metal ion in the solution. Since the phosphinic acids have a single ionizable proton and form a monovalent anion, it would be anticipated that the divalent metals would form neutral complexes of the general formula $M(R_2PO_2)_2$. From the definition of $\bar{n}$, it obviously should approach a value of 2. However, in no case did the value of $\bar{n}$ exceed, or even reach, a value of unity. In several cases, even with nickel and cobalt, it was found that a precipitate formed as the value of $\bar{n}$ approached 1. This might be a logical consequence of Bjerrum's theory of stepwise equilibrium, which predicts that the concentration of $M(R_2PO_2)^+$ must be large before an appreciable concentration of $M(R_2PO_2)_2$ can be formed. If the species $M(R_2PO_2)^+$ is soluble and if $M(R_2PO_2)_2$ is relatively insoluble, precipitation would occur when $\bar{n} \sim 1$.

Calculations of the formation constant K_1 were made by the method of Block and McIntyre,[15] with several determinations for each complex (Table 18); K_1 is defined as

$$K_1 = \frac{[M(R_2PO_2)^+]}{[M^{++}][R_2PO_2^-]} .$$

It can be seen that differences between individual calculations for the nickel complexes are of the same order as the differences between the complexes with different acids. This poor precision and the failure to detect the formation of the species $M(R_2PO_2)_2$ led to an attempt to utilize a method developed by Schubert[16] for

[11] Research participant, University of Oklahoma; present address, University of Utah.

[12] M. Calvin and K. W. Wilson, *J. Am. Chem. Soc.* 67, 2003 (1945).

[13] B. E. Bryant, W. C. Fernelius, and B. E. Douglas, *J. Am. Chem. Soc.* 75, 3784 (1953).

[14] P. C. Crofts and G. M. Kosolapoff, *J. Am. Chem. Soc.* 75, 3379 (1953).

[15] B. P. Block and G. H. McIntyre, Jr., *J. Am. Chem. Soc.* 75, 5667 (1953).

[16] J. Schubert, *J. Phys. & Colloid Chem.* 52, 340 (1948).

TABLE 18. FORMATION CONSTANTS FOR SOME PHOSPHINATE SALTS

Phosphinic Acid	Log K_1		
	Ni	Co	Cu
Diethyl	2.29	2.42	
	2.29	2.63	
Di-*n*-butyl	2.56	2.16	3.21
	2.57	2.33	3.13
	2.42		3.15
Di-*n*-hexyl	2.48	Form immediately	
	2.39	precipitates	
	2.19		

determining formation constants. This method depends upon the formation of a complex entity which is not absorbed by an ion exchange resin.

By the use of a $Co^{60}Cl_2$ solution, it is possible to work at low concentrations of cobalt and still be able to determine the distribution of cobalt between solution and resin. The resin used was the ammonium form of Amberlite IR-120, prepared by washing with dilute HCl, then with distilled water, followed by several washes with concentrated NH_4NO_3 and copious quantities of distilled water. The resin used was 60 to 80 mesh and had been air-dried.

In the absence of a "loading" electrolyte, all the Co^{60} was absorbed from solution. All solutions used were 0.79 *M* in ammonium ion and were adjusted to a pH of 7.7. Because of the extremely limited solubility of di-*n*-butyl and di-*n*-hexyl phosphonic acids, it was impossible to prepare stock solutions of these acids at an appreciably lower pH. Ammonium nitrate was used as the loading electrolyte to minimize unwanted anion effects. All solutions contained an excess of ammonium hydroxide, and the pH was adjusted by the dropwise addition of concentrated nitric acid.

Solutions for equilibration were prepared by adding 500 μl of a stock $Co^{60}Cl_2$ solution to 50 ml of a buffered solution of the phosphinic acid. After mixing, a 1-ml sample was drawn for determination of the initial concentration of cobalt in the solution. To the solution was then added 0.50 g of the resin, and the mixture was tumbled for at least 12 hr at 25 ± 1°C. The solution was then centrifuged and another 1-ml sample was drawn for counting. Calculations were performed as indicated by Schubert. True formation constants can be obtained by this method only if

1. the formula of the complex is known,
2. the complex formed is not absorbed by the resin,
3. the complexing agent is unaffected by the resin.

Stock solutions containing different concentrations of the phosphinic acids were prepared. The following values for log K_f were calculated for the cobalt complexes, assuming that the species formed was $Co(R_2PO_2)_2$:

	Solution A	Solution B
Di-*n*-butyl phosphinic acid	3.99	3.76
	4.00	3.93
Di-*n*-hexyl phosphinic acid	4.31	3.71
	4.32	3.77

The differences between the values calculated at different concentrations (solutions A and B) indicate that at least one of the conditions mentioned above is not fulfilled. With diethyl phosphinic acid and di-*n*-butyl phosphate it was found that more cobalt was absorbed by the resin in the presence of these materials than in their absence. This suggests that either the complex formed is a cationic species such as $M(R_2PO_2)^+$ or that the acids themselves are strongly absorbed and, in turn, tend to bind the cobalt to the resin. Another possibility is that the acids themselves are associated in solution and that the complexes formed are entirely different in nature from what had been assumed in the calculations.

It appears that in the 50% dioxane solutions, where the acid-to-metal ratio is approximately 4, the predominant species formed contains only one molecule of acid per metal ion. It is possible that there is an appreciable concentration of a neutral species in solutions containing di-*n*-butyl or di-*n*-hexyl phosphinic acids where the acid-to-metal ratio is approximately 10^6. Since the precision in the determination of constant K_f at one concentration was not greater than the variation of K_f with concentration, it is not possible to decide on the basis of the present data whether the species existing in solution are or are not more complex than was assumed.

NEPTUNIUM RECOVERY FROM PUREX PROCESS PLUTONIUM WASTES

G. W. Parker P. M. Lantz
W. J. Martin G. E. Creek

Earlier discussions[17,18] refer to several attempts to establish the extraction behavior of Np^{237} in the current ORNL Metal Recovery Purex Process. The failure of laboratory batch-type demonstrations to correlate with results of actual plant continuous operation has been pointed out, and several explanations based on inherent differences in contact-time, temperature, and local concentration effects have been proposed.

Recent changes in the Metal Recovery Plant flowsheet made for the purpose of increasing acid recovery in the plant have resulted in re-use of the low-activity streams, the second uranium (IDW) and second plutonium (IIAW) wastes, as dissolver acid. Thus small amounts of sodium nitrite, sulfate, sulfamate, ferrous sulfate, etc., as well as any residual fissionable material in such wastes, are being recycled to the feed. Coincident with this change and with steadily improved analytical service, it was observed that neptunium seemed to follow only the plutonium stream and that certain wastes from the ion-exchange concentration process appeared to contain nearly pure neptunium.

Partitioning of Neptunium in the Plutonium Stream

By collecting daily samples over an extended period and combining equal portions to provide a single composite, generally more satisfactory material balances have been obtained. Table 19 indicates results obtained on different dates corresponding to somewhat different irradiation levels. As shown, it is found that about 90% of the neptunium is now being extracted and that 10% is being lost to IAW waste. After being extracted, the neptunium partitions in the IB column and follows plutonium almost quantitatively to the second cycle. It is believed that the neptunium is present essentially as Np(IV) at this point. In the extraction column in the presence of uranium, it is probably in the hexavalent state. In the second plutonium cycle, the addition of some nitrite ion and a high nitric acid concentration combine to effect a division of the neptunium, with one-third to one-half being lost to the IIAW stream. This, however, is recycled and explains the presence of more neptunium in the feed than was required by the ratio of 0.3% of the plutonium.

TABLE 19. NEPTUNIUM DISTRIBUTION IN ORNL METAL RECOVERY PROCESS

Stream Analyzed	Irradiation Level (counts/min/ml[a])	
	210 g/T Np^{237}	145 g/T Np^{237}
IAF (feed)	235 (188[b])	172 (130[b])
IAW (fission-product waste)	0	14
IBU (U first cycle)	0	0
IBP (Pu first cycle)	231	160
IIBP (Pu second cycle)	122	124
IIAW (Pu waste, recycled[c])	100	40

[a]Corrected for volume relation.
[b]Theoretical, based on 0.3% of Pu.
[c]Portion recycled, variable.

Adsorption and Elution of Np(IV)

The remaining one-half to two-thirds of the neptunium is carried in the IIBP stream to the ion-exchange plutonium concentration column. During this step Np(IV) is adsorbed strongly by the resin. Only small amounts of neptunium have been detected in the column effluent. After the column is loaded with one-third to one-half its capacity of plutonium, it is normally treated with a small amount of 0.25 *M* H_2SO_4 containing 0.05 *M* $(NH_2OH)_2 \cdot H_2SO_4$ to remove uranium from the product. At this point neptunium was observed to be eluted with the uranium, at times in rather high purity. Figure 34 shows typical concentration curves of Np(IV), U(VI), and Pu(IV) in the eluate during a uranium stripping step. It is apparent that not all the neptunium is removed and that some is probably contained in the usual 5.8 *M* nitric acid elution of the plutonium. Figure 35 gives a satisfactory explanation for this condition. With the normal 0.30 *M* sulfate [0.25 *M* H_2SO_4 and

[17]G. W. Parker *et al.*, *Chem. Semiann. Prog. Rep. June 20, 1955*, ORNL-1940, p 57.

[18]G. W. Parker and P. M. Lantz, *Notes on Conference at Savannah River Concerning Neptunium-237*, ORNL CF-55-12-62 (Dec. 13, 1955).

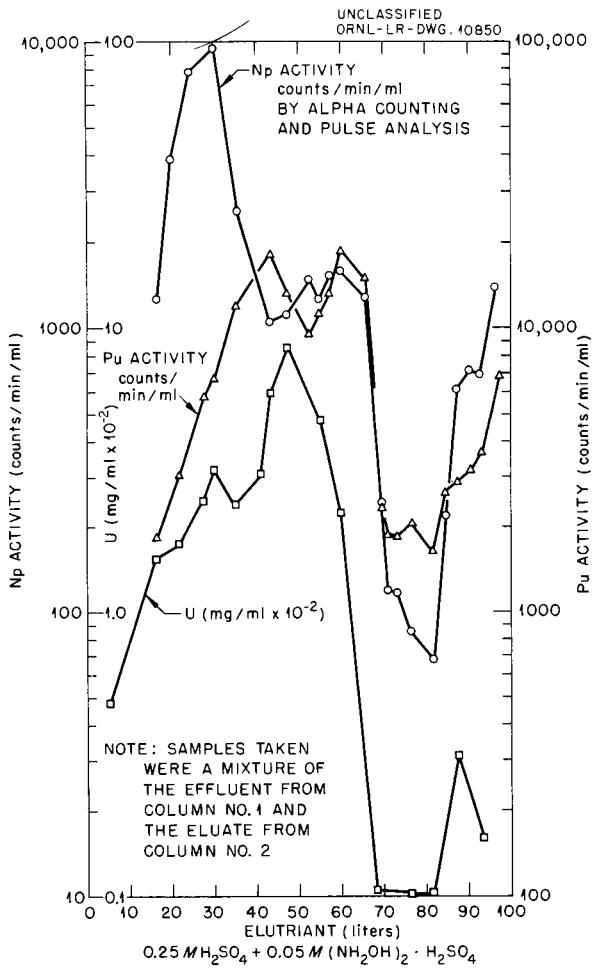

Fig. 34. Typical Elution Curves for Np(IV), U(VI), and Pu(IV).

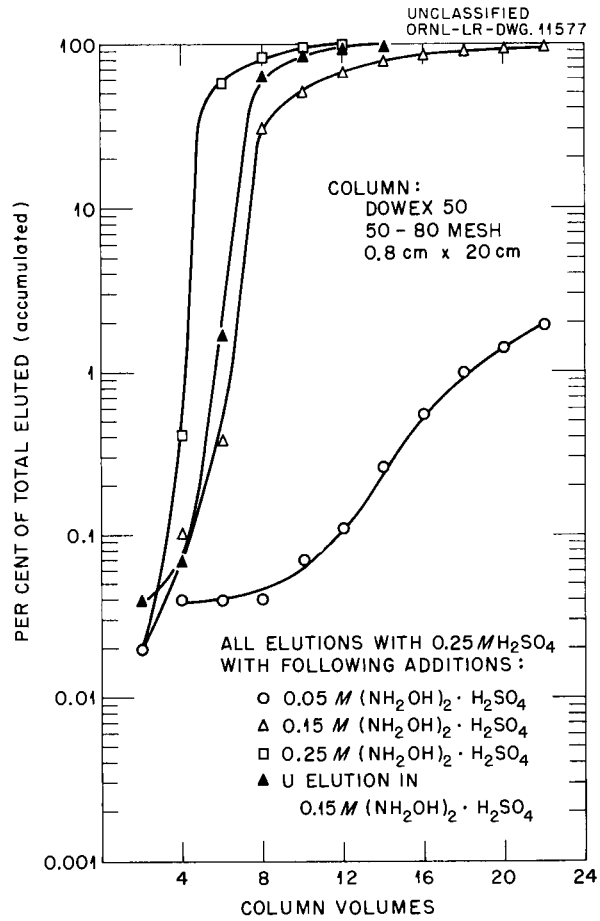

Fig. 35. Effect of SO_4^{--} Concentration on Rate of Elution of Np(IV).

0.05 *M* $(NH_2OH)_2 \cdot H_2SO_4$], the elution of neptunium is very slow. An increase to even 0.4 *M* sulfate is shown to effect a very rapid and complete elution. The strength of the neptunium(IV) sulfate complex signified by the suppression of its extraction into TTA is also shown in Fig. 36.

Yield of Neptunium from the Plutonium Ion Exchange Waste

The theoretical yield of neptunium in irradiated normal uranium is in the ratio of 2.5 to 3.0 g for each kilogram of plutonium. During the current metal recovery operation involving 5 kg of plutonium, 2 g of neptunium has been isolated, and an additional 2 g, or more, is in the process of being recovered. It is felt that this quantity might have been substantially higher if a mechanical defect in one ion exchange column had not essentially prevented the application of the full uranium stripping step. The analysis of the plutonium products for neptunium essentially supports this observation, since up to 0.5 g of neptunium was found in 500 g of plutonium from this column.

Isolation of Np^{237} by Ion Exchange and TTA Extraction

In practice, the uranium strip and the column effluent waste are combined in a catch tank at the plant, and at intervals this material is delivered by pipeline to the Chemistry Division Hot Laboratory. It is then fed, entirely unaltered, to another ion exchange column. Neptunium(IV) is adsorbed, together with uranium and plutonium.

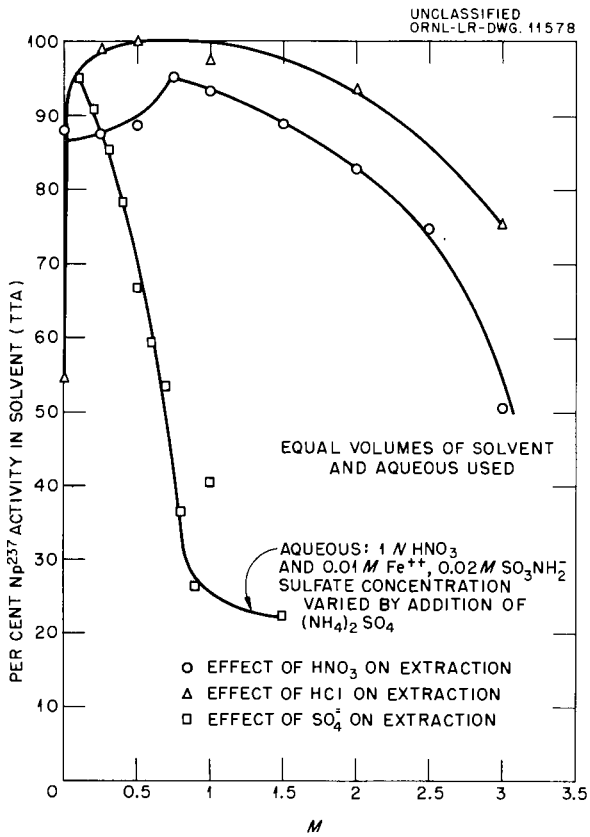

Fig. 36. Effect of SO_4^{--}, HNO_3, and HCl on the TTA Extraction of Np^{237}.

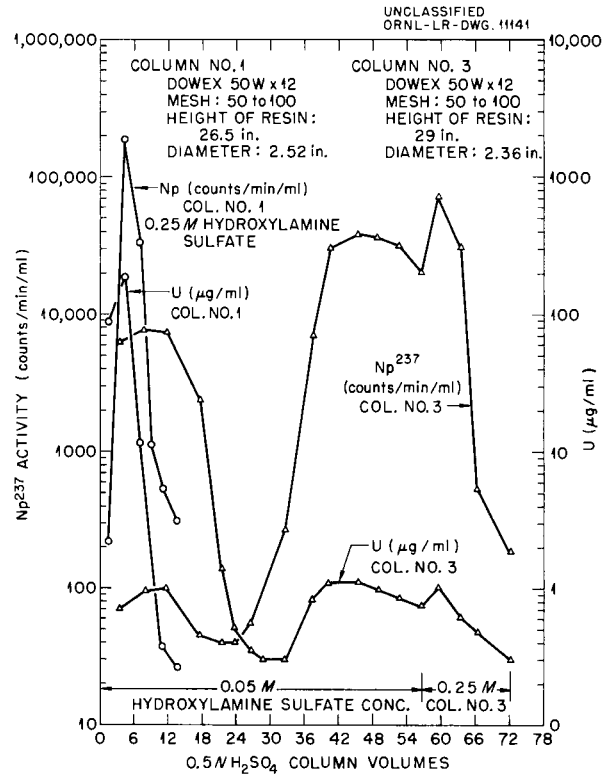

Fig. 37. Effect of SO_4^{--} Concentration on Elution of Uranium and Neptunium.

In the absence of large quantities of plutonium, these columns can be used for extremely long periods without break-through.

When elution is desired, a solution 0.25 *M* in H_2SO_4 and 0.25 *M* in $(NH_2OH)_2 \cdot H_2SO_4$ is passed through the column, resulting in the removal of uranium and neptunium just ahead of the plutonium. The advantage in the use of 0.5 *M* total sulfate over 0.3 *M* is shown further in Fig. 37. Identical columns required only ten column volumes for elution at the higher molarity, compared with more than 70 column volumes at the lower molarity which is normally used for uranium stripping. Final purification is accomplished by a TTA extraction of the sulfate solution following extensive dilution to reach a satisfactory distribution coefficient referred to in Fig. 36.

Possibilities of Neptunium Recovery from Production Plant Purex Wastes

In order to evaluate the possibility of establishing a production type of source for the eventual large-scale isolation of neptunium, some additional survey is planned for the Savannah River Purex Plant and perhaps for the future Hanford Plant. It was recognized, however, that the current flowsheet at ORNL is unique and that the favorable distribution of neptunium will perhaps not be duplicated elsewhere. It is reported that on one occasion following dissolution of several green slugs at Savannah River a highly gamma-active uranium product resulted, which was attributed to the presence of large amounts of Np^{239}. According to estimates made at the time, about 10 to 20% of the total neptunium activity had remained in the uranium. No decontamination was observed in the second uranium cycle.

While samples were being requested particularly for the ion exchange column waste and uranium strip, it was convenient to obtain samples of the calcined UO_3 from Savannah River at the K-25 plant. Analysis of these samples show a surprisingly large neptunium content, about 70% of theoretical (Table 20). That this is not a transient condition is shown by the results from the composite sample, which was collected over several months. Although the bulk of the neptunium is obviously not presently available in a separated condition, the plutonium wastes will be examined for the smaller portion because of the simplicity of treatment.

TABLE 20. NEPTUNIUM CONTENT OF SAVANNAH RIVER CALCINED UO_3

Sample	Np^{237} Found (counts/min per g of UO_3)	U in UO_3 (%)	Np^{237} (counts/min per g of U)	Theoretical Yield* of Np^{237} (g per ton of U)	Np^{237} Present (mg per ton of U)	Np^{237} in Savannah River Product UO_3 (% of theoretical)
K-25, lot 168						
Composite No. 1	498	81.35	612	1.0–1.2	694	57.8–69.4
Composite No. 2	490	81.35	602	1.0–1.2	682	56.8–68.2
K-25, lot 1196						
Trailer load No. 1	526	79.79	659	1.0–1.2	747	62.2–74.7
Trailer load No. 2	535	79.79	671	1.0–1.2	769	64.0–76.9

*Basis of yield:
400 g/T irradiation level
0.25–0.30% of the plutonium

RADIATION CHEMISTRY

EFFECT OF IONIZING RADIATION ON HETEROGENEOUS CATALYSTS

H. W. Kohn E. H. Taylor

Damage to solids by ionizing radiation is of potential use in the study of heterogeneous catalysis, and previous work[1,2] has shown that catalytic activity is indeed affected by both electromagnetic and heavy-particle irradiation of certain catalysts. In order to observe the effects of more labile damage, experiments have now been started, with the exchange reaction between H_2 and D_2 used as the indicator of catalytic activity. This reaction proceeds at a measurable rate on ZnO at –78°C, which makes it possible to observe the effect of trapped electrons or holes that would be released at higher temperatures. Previous work employed reactions studied at 0°C or above.

Preliminary results indicate that overnight irradiation with gamma rays at –78°C increases the activity of ZnO for H_2-D_2 exchange and that this increase is annealed out by warming the catalyst to –22°C. The results are being checked on separate samples of ZnO and are being extended to other catalysts.

GAS-PHASE IRRADIATION

S. C. Lind P. S. Rudolph

Alpha-Ray Irradiation of a Mixture of Acetylene and Benzene

Since data were available for the alpha-ray radiolysis of acetylene[3] and benzene,[4] it was decided to irradiate a mixture of these gases with alpha rays to see what effect acetylene or benzene in their mixture would have on their individual reaction yields. Since the ionization potentials of acetylene and benzene are 11.4 and 9.4 ev, respectively, it is conceivable that acetylene ions could transfer their energy to benzene, decreasing the yield for acetylene and increasing the yield for the benzene.

A mixture of 515.6 mm of acetylene and 169.0 mm of benzene at 100°C was irradiated in a reaction sphere of 7.86 cc with 157.4 mc of radon. This ratio of acetylene to benzene (3:1) was used because it gives both gases the same relative stopping powers and specific ionizations.

The velocity constants for this mixture corrected to a 2-cm sphere are: for total pressure, 131.9; for acetylene pressure, 154.8; and for benzene pressure, 41.2. The comparable velocity constants are 194.7 for pure acetylene[3] and 11.8 for pure benzene.[4]

The data for pure acetylene[3] and pure benzene[4] fit a log P vs $e^{-\lambda t}$ plot for a considerable pressure drop. In the case of the mixture the same plot held only when P represented the acetylene pressure. When P represented the total pressure or benzene pressure, the plot had a definite curvature. This is understandable since 21% of the acetylene which disappears appears as benzene.[5] Hence new kinetic equations were derived from the following information:

$$C_2H_2 \longrightarrow \text{polymer}$$
$$C_2H_2 \longrightarrow \text{benzene}$$
$$C_6H_6 \longrightarrow \text{polymer}$$

The differential forms of the derived equations are

$$(1) \qquad \frac{-dP_A}{dt} = -k_A S_A P_A \frac{dE}{dt} ,$$

$$(2) \qquad \frac{-dP_B}{dt} = -k_B S_B P_B \frac{dE}{dt} + \beta k_A S_A P_A \frac{dE}{dt} ,$$

where subscripts A and B refer to acetylene and benzene, respectively, and

P = pressure of gas at any time t,
k = the velocity constant,
S = the stopping power,
E = amount of radon,
β = the per cent of acetylene which disappears and appears as benzene,[5] which value is 0.21/3.

[1] E. H. Taylor and J. A. Wethington, Jr., *J. Am. Chem. Soc.* **76**, 971 (1954).

[2] P. B. Weisz and E. W. Swegler, *J. Chem. Phys.* **23**, 1567 (1955).

[3] S. C. Lind, D. C. Bardwell, and J. H. Perry, *J. Am. Chem. Soc.* **48**, 1556, 1575 (1926); W. Mund and W. Koch, *J. Phys. Chem.* **30**, 289 (1926).

[4] S. C. Lind, A. C. Stewart, and P. S. Rudolph, *Chem. Semiann. Prog. Rep. June 20, 1955*, ORNL-1940, p 68.

[5] W. Mund and C. Rosenblum, *J. Phys. Chem.* **41**, 469 (1937); C. Rosenblum, *J. Phys. & Colloid Chem.* **52**, 474 (1948); L. M. Dorfman and F. J. Shipko, *J. Am. Chem. Soc.* **77**, 4723 (1955).

These equations were integrated and analyzed by J. Z. Hearon.[6] The integrated forms are

$$(3) \qquad P_A = P_A^0 e^{-K_A E_0 (1-e^{-\lambda t})} ,$$

$$(4) \quad P_B = \frac{\beta K_A P_A^0}{K_A - K_B} \left[e^{-K_B E_0 (1-e^{-\lambda t})} - e^{-K_A E_0 (1-e^{-\lambda t})} \right] + P_B^0 e^{-K_B E_0 (1-e^{-\lambda t})} ,$$

where the symbols defined above apply, and where

P^0 = initial pressure,

E_0 = initial amount of radon,

$e^{-\lambda t}$ = fraction of radon remaining at any time t,

K = proportionality constant = kS.

The proportionality constants corrected to these experimental conditions are: K_A for pure acetylene, 143.5 and K_B for pure benzene, 25.8. Use of this value of K_A in Eq. 3 did not give good agreement between observed and calculated pressures (Table 21). Equation 3 was then solved for K_A, using the experimental data for the first reading, to give a value of 110. Employing this value in Eq. 3 and solving for P_A gave good agreement, as indicated in Table 21.

The discrepancy noted when K_A = 143.5 is used is explicable if acetylene transfers energy to benzene. If this is true, then K_B should be greater than 25.8. Using K_A = 110 and K_B = 25.8 did not give good agreement between observed and calculated values for P_B; this value of K_B is too low, as shown by Table 22. An attempt was made to ascertain the correct value of K_B by using a straight proportion of K for the pure gases and mixtures:

$$K_{B_m} = \frac{K_{A_p}}{K_{A_m}} \times K_{B_p} ,$$

$$= 33.7 ,$$

where p is the pure gas and m is the mixture. This value was better and in the right direction but still not correct. A better value will be determined by trial and error.

[6]Formerly of the Mathematics Panel, ORNL.

TABLE 21. COMPARISON OF OBSERVED AND CALCULATED PRESSURES FOR ACETYLENE

P_A* Observed	P_A Calculated with K_A = 143.5	P_A Calculated with K_A = 110
374.5	338.7	374.3
304.7	261.4	306.8
239.8	195.4	245.9
180.4	131.0	180.5
130.9	82.0	125.8
92.3	45.9	80.9

*These pressures include an undetermined amount of H_2, the pressure of which increases with time.

TABLE 22. COMPARISON OF OBSERVED AND CALCULATED PRESSURES FOR BENZENE

P_B Observed	P_B Calculated with K_A = 110, K_B = 25.8	P_B Calculated with K_A = 110, K_B = 33.7
166.2	165.3	162.1
154.1	163.7	157.4
147.0	159.8	150.7
131.5	151.7	142.3
116.6	143.2	131.0
99.7	133.2	116.7

When the correct value of K_B is determined, quantitative data will be available for the extent of energy transfer from the acetylene to the benzene. Additional runs will be made on this system to further test the validity of the derived kinetic equations.

RADIATION-INDUCED CHEMICAL REACTIONS

T. J. Sworski

Ceric Ion–Thallous Ion Reaction

In the decomposition of water by ionizing radiation, the 100-ev yields of the intermediate H, OH, H_2, and H_2O_2 may be denoted by G_H, G_{OH}, G_{H_2}, and $G_{H_2O_2}$. Cobalt-60 gamma radiation induces[7] reduction of ceric ion by thallous ion in 0.8 N sulfuric acid. Thallous ion increases the cerous ion yield from $2G_{H_2O_2} + G_H - G_{OH}$ to an initial yield of $2G_{H_2O_2} + G_H + G_{OH}$ according to the

[7]T. J. Sworski, *J. Am. Chem. Soc.* **77**, 4689 (1955).

following sequence of reactions:

(1) $Tl^{+} + OH \longrightarrow Tl^{2+} + OH^{-}$

(2) $Ce^{4+} + Tl^{2+} \longrightarrow Ce^{3+} + Tl^{3+}$

Although the initial cerous ion yield is independent of thallous ion concentration (10^5 to 10^{-2} M), the thallic ion yield increases with increasing thallous ion concentration, as shown in Fig. 38. This is attributed to the previously reported[8] decrease of $G_{H_2O_2}$ (with concomitant increase of G_{OH}) by thallous ion through reaction 1 in regions of high ionization density before OH radicals combine to form H_2O_2.

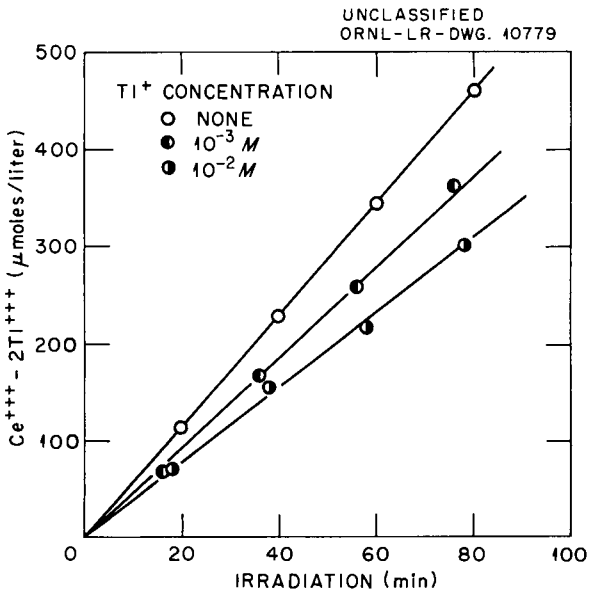

Fig. 38. Effect of Thallous Ion Concentration on the Yield of Thallic Ion. Dosimeter: 38.6 μmoles of Fe^{++} oxidized per liter per minute.

Cerous ion reacts with OH radical according to the following reaction:

(3) $Ce^{3+} + OH \longrightarrow Ce^{4+} + OH^{-}$

Reaction 3 has been experimentally confirmed[9] by a demonstration of concomitant oxidation of radioactive cerous ion during the course of ceric ion reduction. The cerous ion yield decreases with increasing initially added cerous ion, as shown in Fig. 39. This is also attributed to a decrease in $G_{H_2O_2}$ by cerous ion through reaction 3 in regions of high ionization density. The effect of thallous and cerous ions further confirms the mechanism previously proposed for the decrease of $G_{H_2O_2}$ by bromide[10] and chloride[11] ions through their reaction with OH radical.

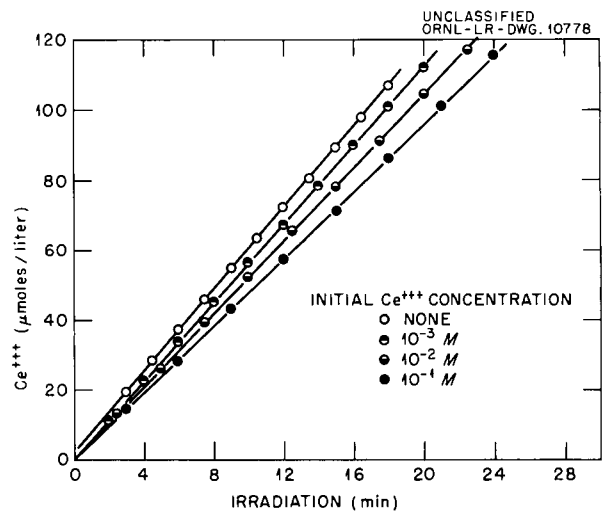

Fig. 39. Effect of Initially Added Cerous Ion on the Reduction of Ceric Ion. Dosimeter: 37.8 μmoles of Fe^{++} oxidized per liter per minute.

The reduction of ceric ion in solutions containing initially a mixture of both cerous and thallous ions was investigated, as shown in Fig. 40. The initial yield of cerous ion in these mixtures is given by the following kinetic expression:

$$2G_{H_2O_2} + G_H - G_{OH} + \frac{2G_{OH}}{1 + \dfrac{k_3[Ce^{3+}]}{k_1[Tl^{+}]}} .$$

From the measured initial yields of cerous ion in these mixtures, a value of 38 was calculated for k_1/k_3.

[8] T. J. Sworski, *Chem. Semiann. Prog. Rep. June 20, 1955*, ORNL-1940, p 64.

[9] G. E. Challenger and B. J. Masters, *J. Am. Chem. Soc.* 77, 1063 (1955).

[10] T. J. Sworski, *J. Am. Chem. Soc.* 76, 4687 (1954).

[11] T. J. Sworski, *Radiation Research* 2, 26 (1955).

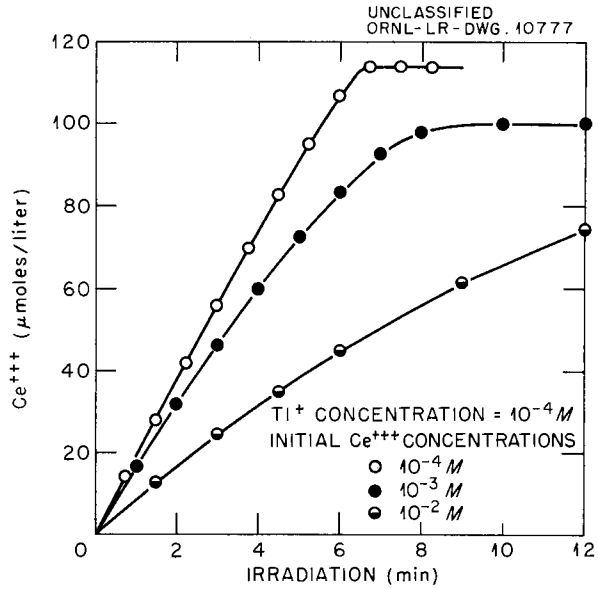

Fig. 40. Effect of Ce^{+++}/Tl^{+} Ratio on the Reduction of Ceric Ion. Dosimeter: 37.9 μmoles of Fe^{++} oxidized per liter per minute.

$K_2Cr_2O_7$–Thallous Ion Reaction

Cobalt-60 gamma radiation induces reduction of $K_2Cr_2O_7$ by thallous ion in 0.8 *N* sulfuric acid. Thallous ion increases the chromic ion yield from $\frac{1}{3}(2G_{H_2O_2} + G_H - G_{OH})$ to an initial yield of $\frac{1}{3}(2G_{H_2O_2} + G_H + G_{OH})$. The factor of $\frac{1}{3}$ is present, since chromium is reduced from the Cr(VI) ion to the Cr(III) ion. This system merits further study, since preliminary experiments have shown that this mixture, unlike the mixture of ceric ion and thallous ion, can be studied in sulfuric acid solutions at a pH of 2 or more.

$K_2Cr_2O_7$–Bromide Ion Reaction

Cobalt-60 gamma radiation induces reduction of $K_2Cr_2O_7$ by bromide ion in 0.8 *N* sulfuric acid. At constant bromide ion concentration, the yield of chromic ion increases with increasing $K_2Cr_2O_7$ concentration, as shown in Fig. 41. At constant $K_2Cr_2O_7$ concentration, the yield of chromic ion decreases with increasing bromide ion concentration, as shown in Fig. 42. In both cases, illustrated by Figs. 41 and 42, the yield of chromic ion increases with increasing $K_2Cr_2O_7/Br^-$ ratio. If

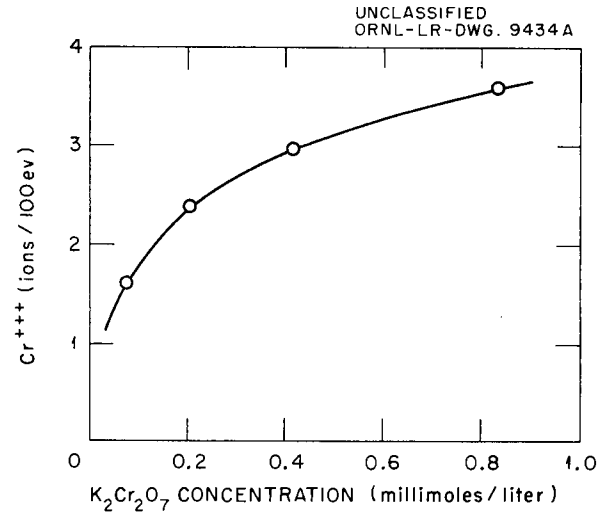

Fig. 41. Radiation-induced Reduction of $K_2Cr_2O_7$ by Bromide Ion. Bromide-ion concentration constant at 2×10^{-3} *M*.

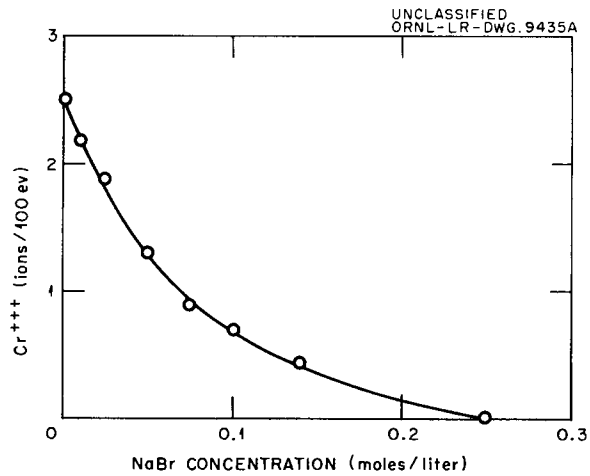

Fig. 42. Radiation-induced Reduction of $K_2Cr_2O_7$ by Bromide Ion. $K_2Cr_2O_7$ concentration constant at 2×10^{-4} *M*.

it is assumed that every OH radical oxidizes bromide ion, the maximum yield of chromic ion could only be 1.75 or $\frac{1}{3}(2G_{H_2O_2} + G_H)$. The higher yields shown in Figs. 41 and 42 may indicate that intermediate chromium ions formed in the reduction of $K_2Cr_2O_7$ are capable of oxidizing bromide ion.

RADIATION STUDIES ON NITRATE SOLUTIONS

J. W. Boyle H. A. Mahlman

Yields of hydrogen, oxygen, and nitrogen have been determined[12,13] for thorium nitrate solutions irradiated in the ORNL Graphite Reactor. In the thorium nitrate blanket of a breeder reactor the formation of hydrogen probably does not present any great problem because there are a number of ways in which hydrogen can be combined with oxygen, and therefore no great partial pressure of hydrogen need build up. Because the use of low-cross-section N^{15} is necessary, the formation of nitrogen by decomposition of the nitrate necessitates developing an economical method for recombining to nitrate. The method has to be efficient, as N^{15} is expensive to produce and must be conserved.

If a radiation-induced back reaction resulting in the fixation of N_2 occurs, then possibly a moderate partial pressure of N_2 will prevent any net formation of N_2. Although there are some indications that a back reaction does occur, the yields presented previously[12,13] give no indication of the magnitude of the back reaction.

Experiments are under way to determine the extent of the back reaction of N_2. These experiments consist in irradiating solutions of thorium nitrate for extended periods of time in the reactor to see whether a steady-state pressure of N_2 does occur. The total pressure will be followed continuously until a steady state is obtained or until high gas pressures necessitate the removal of the experiment from the reactor for safety reasons. Before such an in-pile test can be run, several preliminary measurements must be made; they are discussed below.

Recombination Studies

In a long-term experiment, designed to evaluate the extent or existence of a steady-state molecular nitrogen pressure, it is imperative that recombination of hydrogen and oxygen be effected in order to limit the pressure of radiolytic gas. It is also necessary to determine to what extent N_2 reacts with H_2 or O_2 at elevated temperatures and pressures in the absence of radiation.

A platinum-lined stainless steel bomb has been fabricated which can be used for out-of-pile as well as in-pile studies. The platinum liner will eliminate problems associated with corrosion and will also act as a recombination catalyst for hydrogen and oxygen. The liner has a volume of 8.0 cm^3 and a calculated surface area of 27.5 cm^2.

Recombination studies were made by adding 5 cm^3 of water to the bomb and then admitting predetermined volumes of the gases so that the desired stoichiometry existed in the bomb. The surface area above the liquid which was available to act as a catalyzing surface was 10.4 cm^2 at 23.5°C. Combination of the gas was detected by changes in pressure. A Baldwin strain gage monitored the pressure, while the temperature was measured with an iron-constantan thermocouple. The pressure and temperature were recorded on a modified Brown recorder, the accuracy of which was found to be ±3 psi from 0 to 2500 psi and within ±2°C over the range of 25 to 300°C.

At room temperature it was found that H_2 and O_2 present in the ratio 2:1 combined on the platinum surface at a rate such that the pressure was reduced to half its original value in 31 min. At 84.5°C the observed $T_{1/2}$ was 8 min.

No combination of N_2 with either H_2, O_2, or an H_2-O_2 mixture was detected in 16 hr, although the temperature was raised to 290°C and the total pressure to over 2000 psi. Out-of-pile studies will be extended to include thorium nitrate solutions preliminary to the investigation of an in-pile molecular nitrogen steady state.

Thermal Expansion of Thorium Nitrate Solutions

In order to evaluate gas yields in a bomb experiment from the measurement of the total pressure, it is necessary to know accurately the gas and liquid volumes at all temperatures. As thermal expansion data are not available in the literature for the solutions to be used, known amounts of the solutions were sealed in calibrated pyrex tubes, and their expansion was observed as the temperature was raised. The tubes, about 150 mm in length and 3 to 4 mm OD, were heated in a constant-temperature air bath.[14] The expansion of the liquid phase was measured with a cathetometer by observing the position of the meniscus relative to the top of the tube as the temperature was raised.

Thorium nitrate solutions without excess nitric

[12] J. W. Boyle and H. A. Mahlman, *Chem. Semiann. Prog. Rep. Dec. 20, 1954*, ORNL-1832, p 69.

[13] J. W. Boyle and H. A. Mahlman, *Chem. Semiann. Prog. Rep. June 20, 1955*, ORNL-1940, p 61.

[14] We gratefully acknowledge the assistance of D. W. Sherwood and G. Hebert, who supplied the equipment and helped set it up.

acid precipitate at elevated temperatures,[15] therefore nitric acid was added to the thorium nitrate solutions to give a NO_3^-/Th ratio of 6/1. The densities plotted in Fig. 43 are isomolal lines, the values having been corrected for the water in the vapor phase. From the data available it was impossible to correct for the NO_2 present in the vapor phase. Perhaps this is the reason that the 7.18 and 7.21 *m* thorium lines do not conform to the generalities of the other lines, namely, linearity and near constant slope over a temperature range of about 200°C.

General observations during the experiments indicated that the extent of thermal decomposition to NO_2 was dependent upon the NO_3^- concentration. After cooling, the 3.23 *m* solution was colorless, whereas the 7.21 *m* solution was a straw-yellow color, probably due to dissolved NO_2.

RADIOLYSIS OF TRI-*n*-BUTYL PHOSPHATE

J. G. Burr, Jr.

The radiolysis of tri-*n*-butyl phosphate has been investigated for two reasons: (1) radiation damage to this material is of technical interest, since it is the active ingredient of certain solvent-extraction processes; (2) it represents a substituted hydrocarbon of low volatility convenient for the study of radiation effects in hydrocarbons.

The radiolysis products which have been studied are as follows:

1. the production rate and composition of the gases produced by the effect of radiation,
2. the production rate of mono- and di-*n*-butyl phosphates,
3. the production rate of polymeric material,
4. the amount of TBP which disappears by all processes, that is, the value of G_{-M}.

Procedure and Equipment

The radiation cell is shown in Fig. 44. Twenty-five milliliters of vacuum-distilled tributyl phosphate was pipetted into arm B of the apparatus, which was then connected to a Toepler pump by joint D. Cooling water was passed through the

[15] M. H. Lietzke and W. L. Marshall, *Present Status of the Investigation of Aqueous Solutions Suitable for Use in a Thorium Breeder Blanket*, ORNL-1711 (May 19, 1954), p 2.

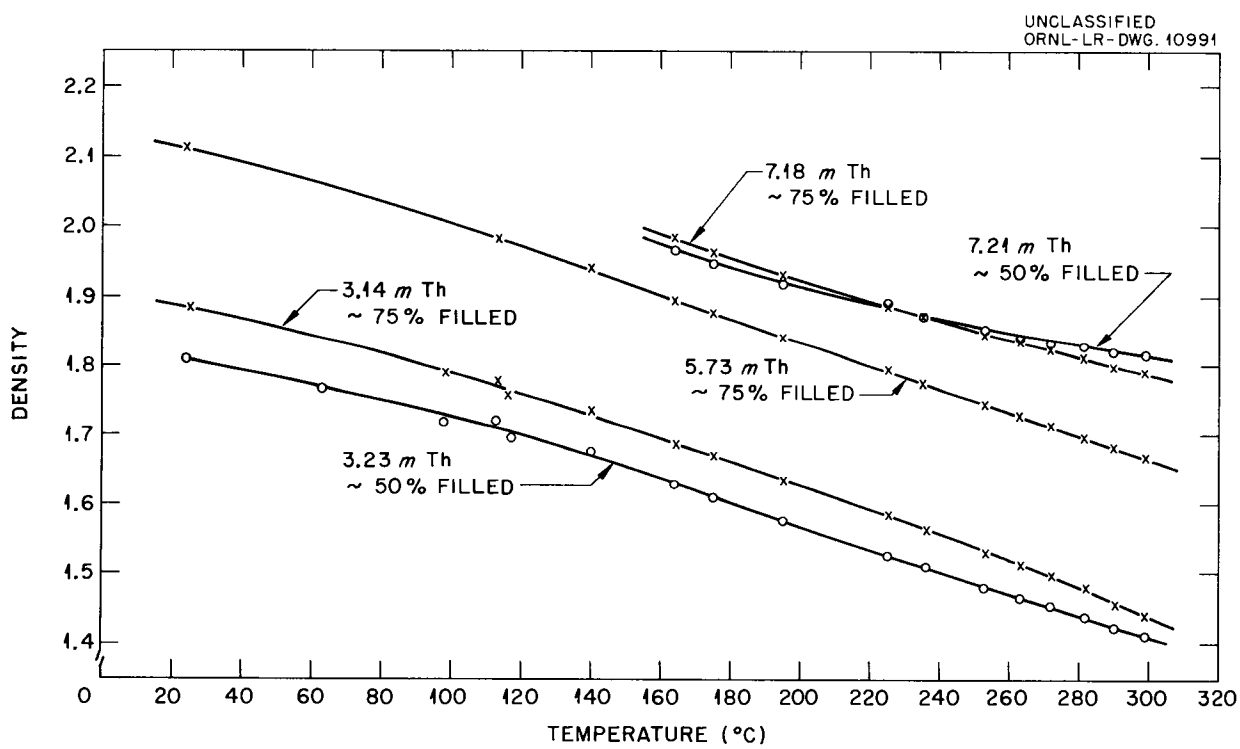

Fig. 43. Density of $Th(NO_3)_4 \cdot 2HNO_3$ Solutions as a Function of Temperature.

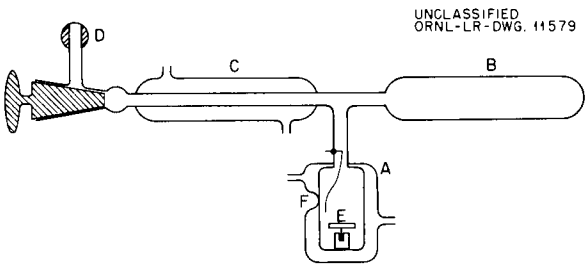

Fig. 44. Radiation Cell.

condenser C. Gases were evacuated from the apparatus through the Toepler pump, with periodic refluxing of the TBP in arm B. This operation was continued until no more gas could be obtained. Mass spectrographic analysis of the gas so obtained showed that slight decomposition of the TBP occurred during this degassing procedure, but it was not considered extensive enough to affect the experiment. After degassing the TBP in B, the stopcock was closed, the apparatus removed from the vacuum line, and the ester carefully decanted into the cell A. This cell was fitted with a thin glass window, F; a glass-sealed iron bar, E, suspended upon a platinum pivot for magnetic stirring; a platinum grounding lead; and a water-cooled jacket.

The source of radiation was a Van de Graaff generator. The electron beam was used at a potential of 1.66 Mev and at a current of 5 μa for periods of 15 or 30 min. Window and other corrections for the cell (shown in Fig. 44) were obtained by calibration with a ceric sulfate dosimeter solution. In this way it was determined that 74.0 ± 1.4% of the incident radiation (as determined from measurements of voltage and current through the cell) was absorbed in the solution. This correction factor was used to estimate the energy absorption in the TBP. The temperature of the cooling water in the cell jacket was 18 to 19°C for all irradiations.

After completion of the irradiation the material was transferred to arm B, the cell was again attached to the Toepler pump system, and the gaseous products of the radiation were pumped off, with periodic refluxing of the irradiated TBP to ensure complete degassing. The product gases were pumped into a gas buret, and their volume was observed. Samples of the gas were taken for mass spectrometer analysis and were also examined on a Perkin-Elmer model 21 infrared spectrometer.

The gaseous products were analyzed mass spectrometrically. It was hoped that the precision of this method would be sufficient to allow study of the variation in gas composition with dosage, thus providing some information about primary and secondary processes in the radiation; however, as is evident from Table 23, the precision is insufficient, under the conditions employed. Of the four gas samples whose analyses are reported in Table 23, samples 1 and 2 were analyzed by Consolidated Engineering Corporation, Pasadena, California, and samples 3 and 4 were analyzed by the ORNL Mass Spectrometer Group. Samples 2, 3, and 4 were gases from TBP radiations made as nearly identical as possible. Analyses of a known hydrocarbon mixture produced results of a similar accuracy.

In addition to the substances discussed above (gases at room temperature), there was evidence during the degassing operation of the presence of less volatile products. Since the mass spectrograph found only traces of hydrocarbons heavier than butanes in the gaseous products, these less volatile materials must have been octanes and heavier molecules. On mechanistic grounds the formation of octanes would be expected.

The infrared spectra of the gases were examined, but the mixture has too many components for any sort of analysis by this means. Prior separation of components by distillation would be required, and this is not practical for such small quantities of the gas mixture. However, the spectra did indicate the presence in the gas mixture of large amounts of unsaturates.

The irradiated TBP was decanted from the cell, and the following operations were carried out upon small portions of the material.

1. Potentiometric titration was performed to measure the acidity. The curves obtained indicated the amount of dialkyl and monoalkyl phosphate esters present in the irradiated material, which are reported as the amounts of di-*n*-butyl phosphate and mono-*n*-butyl phosphate. No indication of the presence of pyrophosphates was observed during the titrations.

2. Isotope-dilution experiments were carried out to determine the disappearance of TBP by all processes. To weighed samples of the irradiated TBP were added weighed amounts of C^{14}-labeled

TABLE 23. COMPOSITION OF GASEOUS PRODUCTS FROM TBP RADIOLYSIS

Gaseous Product*	Composition (mole %)				Average of Samples 2, 3, and 4
	Source of Analysis and Sample No.				
	Consolidated Engineering		ORNL		
	1	2	3	4	
Methane**	8.5	13.2	6.9	4.2	8.1 ± 3.4
Ethane	5.8	8.1	7.6	6.2	7.3 ± 0.8
Ethylene	15.9	15.2	11.0	11.5	12.6 ± 1.8
Propane	9.3	10.0	12.0	12.3	11.4 ± 1.0
Propylene	3.1	3.6	2.5	2.1	2.7 ± 0.6
n-Butane	22.1	22.8	25.0	28.2	25.3 ± 1.9
i-Butane	0	0	4.4	6.1	3.5 ± 2.3
1-Butene	0	0	2.9	0	1.0 ± 1.3
2-Butene	13.6	23.3	27.0	35.2	28.3 ± 4.3
i-Butene	16.3	0	0.5	0.9	0.5 ± 0.2
Total butanes	22.1	22.8	29.4	34.3	28.8 ± 4.0
Total butenes	29.9	23.3	30.4	36.1	30.0 ± 4.3
Hydrogen	72.8	78.9	56.9	55.0	63.6 ± 6.9
Total hydrocarbons	24.6	19.4	38.7	39.6	32.8 ± 8.7

*Irradiation time: sample 1, 15 min; sample 2, 3, and 4, 30 min.

**The hydrocarbon compositions are reported on a hydrogen-free basis. The last two entries show the relative hydrogen-hydrocarbon ratios.

TBP (prepared by the reaction of butanol-1-C^{14} with phosphorus oxychloride in the presence of pyridine). This mixture was vacuum-distilled twice to eliminate high- and low-boiling radiation products. One-gram quantities of the purified mixture were converted to butyl-1-C^{14} *p*-nitrobenzoate by heating for 1 hr at 200°C with vacuum-dried sodium *p*-nitrobenzoate. The ester was obtained by alcohol extraction of the reaction mass and was crystallized four times from dilute ethanol; the melting point was 65°C. Samples of this ester were converted to carbon dioxide by wet combustion,[16] and the carbon dioxide was analyzed for C^{14} in an ionization chamber with a vibrating-reed electrometer.

Although a total of five such dilutions was made and from three to four C^{14} determinations were carried out upon the butyl nitrobenzoate from each dilution, it is apparent, from Table 24, that the precision obtained by this procedure is not high. The isotope-dilution procedure described here determines the amount of unchanged TBP remaining in the irradiated sample, with a precision of 1 to 2%. The quantity desired, however, is the amount of TBP which has been changed, and this is obtained, of course, by difference, whereupon the precision becomes worse by a factor of 20 (for a sample irradiated to 5% decomposition). Therefore to determine the amount of TBP changed with a precision of 2%, the isotope-dilution analysis must be carried out with an over-all precision of 0.1%. This is not practical with present equipment. However, the determination of G_{-M} values for organic materials by any other method is completely impractical, save for a few simple substances, and the isotope-dilution procedure remains the only feasible means for obtaining such measurements.

[16] J. G. Burr, Jr., *Anal. Chem.* 26, 1395 (1954).

TABLE 24. YIELD OF GASEOUS RADIOLYSIS PRODUCTS

Gas	G (molecules per 100 ev absorbed)
Hydrogen	1.73
Methane	0.072
Ethane	0.065
Ethylene	0.112
Propane	0.102
Propylene	0.027
Butanes	0.257
Butenes	0.268

3. The amount of polymeric material obtained was determined by high-vacuum evaporation at 140°C of weighed samples of the irradiated TBP. The material nonvolatile under these conditions was assumed to be a mixture of polymer, dibutyl phosphate, and monobutyl phosphate. The amount of phosphate esters (obtained in part 1 above) was subtracted from the residue, and the difference is called "polymer." It was a pale-yellow viscous material and was not further examined.

4. The infrared spectra of the irradiated TBP were compared with the spectrum of pure TBP and found to be nearly identical. The principal conclusion which can be drawn from this is that no unsaturation is introduced by irradiation into TBP or into any of its nonvolatile radiolysis products.

Results and Discussion

The results obtained by the above procedures are shown in Tables 24 and 25. It is apparent that the principal radiolysis products are hydrogen, di-*n*-butyl phosphate, and polymer. The formation of these and of the minor products can be described in terms of two primary processes and a number of secondary processes. The secondary processes have been drawn from those which the photochemistry and thermochemistry of butane and substituted butanes have shown to be probable reactions for butyl radicals.

[17]E. W. R. Steacie, *Atomic and Free Radical Reactions*, 2d ed., p 97, Reinhold, New York, 1954.

[18]*Ibid.*, p 511–521.

TABLE 25. YIELD* OF TBP RADIOLYSIS PRODUCTS

Radiation time, min	15	30
Energy absorbed, ev	3.47×10^{22}	6.94×10^{22}
Yield of gas	3.10	2.72
Yield of dibutyl phosphate	2.78	2.44
Yield of monobutyl phosphate	0.065	0.14
Yield of polymer	1.50	2.47
G_{-M}	5.5 ± 0.9	5.5 ± 1.0
Average	5.7 ± 1.0	

*Molecules per 100 ev absorbed.

Primary Processes. – The two reactions given below have been chosen rather arbitrarily but are entirely probable processes:

$$(1)\quad C_4H_9OPO_2Bu_2 \rightsquigarrow C_4H_8OPO_2Bu_2 + H$$

$$(2)\quad C_4H_9OPO_2Bu_2 \rightsquigarrow C_4H_9 + OPO_2Bu_2$$

Since the amount of polymer, dibutyl phosphate, and hydrogen formed are roughly equivalent, the two reactions must be assumed to occur with about equal probabilities. This is in agreement with similarity in bond dissociation energies[17] for C-H bonds (94 kcal in butane) and C-O bonds (91–93 kcal).

Formation of Hydrogen, Dibutyl Phosphate, and Polymer. – The formation of these products is in accord with reactions 3, 4, and 5:

$$(3)\quad H + C_4H_9OPO_2Bu_2 \longrightarrow H_2 + C_4H_8OPO_2Bu_2$$

$$(4)\quad OPO_2Bu_2 + e \longrightarrow {}^-OPO_2Bu_2$$

or

$$OPO_2Bu_2 + RH \longrightarrow HOPO_2Bu_2 + R$$

$$(5)\quad 2C_4H_8OPO_2Bu_2 \longrightarrow \text{Polymer}$$

Reaction 3 is a typical hydrogen abstraction reaction.[18] Owing to the strong electron affinity of oxygen, formation of dibutyl phosphate ion (reaction 4) seems more probable by reaction of the phosphate radical with thermal electrons than by hydrogen abstraction. Reaction 5 is a typical dimerization process. It is suggested that the other products of the reaction result mostly from reactions of the butyl radical.

Ethane and Ethylene. – The ethylene-ethane ratio found experimentally (~3) is what would be expected from reactions 6 and 7, so that they are sufficient to explain these two products:

$$(6) \qquad C_4H_9 \longrightarrow C_2H_4 + C_2H_5$$

$$(7) \qquad 2C_2H_5 \longrightarrow C_2H_4 + C_2H_6$$

Butanes and Butenes. – The disproportionation reaction (8) predicts the formation of equal amounts of butanes and butenes, which is what is experimentally observed:

$$(8) \qquad 2C_4H_9 \longrightarrow C_4H_8 + C_4H_{10}$$

Reactions 6, 7, and 8 have been adduced to explain the products formed in the photolysis of di-*n*-butyl mercury[19] and are mentioned[20] frequently in discussions of the photochemical and thermal reactions of butane and substituted butanes. Occurrence of reaction 9 is, however, excluded by such evidence (the activation energy for this process is apparently about 40 kcal), and the formation of butene by reaction 10 seems unlikely also owing to the similarity in bond strengths of C-H and C-O, and also by the fact that the combination of reactions 9 and 10 would predict the formation of greater amounts of butenes than butanes, contrary to the experimental data:

$$(9) \qquad C_4H_9 \longrightarrow C_4H_8 + H$$

$$(10) \qquad C_4H_8OPO_2Bu_2 \longrightarrow C_4H_8 + OPO_2Bu_2$$

One further reaction which undoubtedly occurs to a large extent but which would not have been measured in the experiments here would be dimerization of the butyl radical:

$$(11) \qquad 2C_4H_9 \longrightarrow C_8H_{18}$$

This would account for the presence of the octane-like products that were observed qualitatively among the radiolysis products of TBP.

Methane, Propane, and Propylene. – Many reaction sequences can be written to explain the formation of these products, and the experimental data do not permit the choice among them to be anything but arbitrary. The sequence 12 through 16 is suggested as at least typical:

$$(12) \qquad H + C_4H_9OPO_2Bu_2 \longrightarrow C_3H_7 + CH_3OPO_2Bu_2$$

$$(13) \qquad H + C_4H_9OPO_2Bu_2 \longrightarrow CH_3 + C_3H_7OPO_2Bu_2$$

$$(14) \qquad CH_3 + RH \longrightarrow CH_4 + R_1$$

$$(15) \qquad C_3H_7 + RH \longrightarrow C_3H_8 + R_1$$

$$(16) \qquad 2C_3H_7 \longrightarrow C_3H_6 + C_3H_8$$

Reactions 12 and 13 are typical of the cracking produced by the reaction of hydrogen atoms with hydrocarbons. Reactions 15 and 16 serve to explain the high propane/propylene ratio observed in the radiolysis products.

The reaction sequences suggested above are a convenient means of rationalizing and correlating the data rather than representations of the actual reactions, which are undoubtedly far more complex, and they are not proposed as anything more than this.

WARMING CURVES FOR THE CONDENSED PRODUCT OF DISSOCIATED WATER VAPOR AND FOR HYDROGEN PEROXIDE GLASS

J. A. Ghormley

The product obtained when water vapor is dissociated by an electric discharge and is then condensed at low temperature and the similar product obtained by the reaction of hydrogen atoms with molecular oxygen have been studied by a number of investigators.[21] In connection with a study of paramagnetic resonance absorption due to free radicals in the condensed product,[22] some observations have been made on the behavior of the product when it is warmed.

The product condensed at –196°C is a yellow, transparent solid. On warming, the paramagnetic resonance and the yellow color disappear at about –135°C.[22] Previous investigators observed that, at about –115 to –110°C, oxygen is evolved and

[19] F. E. Frey and H. J. Hepp, *J. Am. Chem. Soc.* 55, 3357 (1933).

[20] E. W. R. Steacie, *Atomic and Free Radical Reactions*, chaps. IV and V, 2d ed., Reinhold, New York, 1954.

[21] For references to previous work see, for example, J. D. McKinley, Jr., and D. Garven, *J. Am. Chem. Soc.* 77, 5802 (1955).

[22] R. Livingston and H. Zeldes, *Chem. Semiann. Prog. Rep. June 20, 1955*, ORNL-1940, p 44–46; and R. Livingston, H. Zeldes, and J. Ghormley; "Paramagnetic Resonance Observations on the Condensed Products of Electric Discharges Through Water Vapor and Related Substances" (submitted to *J. Chem. Phys.*).

the material crystallizes to a white solid. In the paramagnetic resonance work the material was condensed on the outside of a capillary tube of about 1 mm in diameter, such that the over-all diameter of the product on the tube was only about 2 mm. When this tube was removed from liquid nitrogen and held in air at room temperature, in a short time the yellow color disappeared; then the material bubbled slightly and became sufficiently fluid to flow to the tip of the capillary. A few seconds later the drop of liquid bubbled violently for about ½ sec, but no further change was observed. The resulting solution contained about 50% H_2O_2. This behavior indicated that the product which normally crystallized at about –110°C did not crystallize when warmed rapidly and suggested that hydrogen peroxide solution might form a glass if cooled rapidly.

When a 3-mm-dia thin-walled glass tube containing 60% H_2O_2 solution was immersed in liquid nitrogen, the solution froze to a clear glass. Figure 45 (curve A) shows a typical warming curve for such a glass. At about –115°C, just before the material crystallized, the thermocouple junction used to indicate the temperature could easily be moved up and down in the viscous liquid. Crystallization, as indicated by a change in appearance, started at the top and very rapidly progressed through the entire sample.

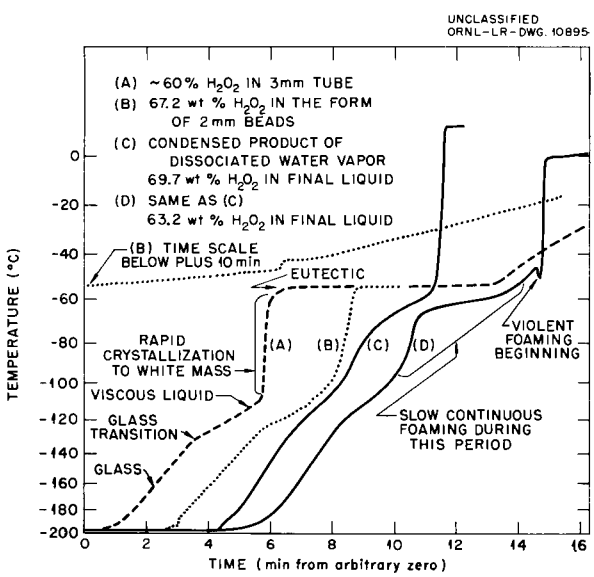

Fig. 45. Warming Curves.

In order to compare ordinary hydrogen peroxide glass with the condensed product of dissociated water vapor, warming curves were determined for the two materials under conditions as nearly the same as possible. Water vapor was passed through an electric discharge for 5 hr while the products were condensed on the inside of a 1-cm glass tube cooled with liquid nitrogen. This tube was then removed from the discharge apparatus, and some of the product was scraped off the tube (in liquid nitrogen) into a special unsilvered Dewar vessel, which had a diameter of about 5 mm in the lower 2-cm-long thin-walled section. (This Dewar vessel is the one used by Livingston and Zeldes for low-temperature paramagnetic resonance absorptions at 9000 Mc.) A copper-constantan thermocouple junction pushed into the product collected in the bottom of the vessel was connected with a Brown 10-mv recorder. The curves shown in Fig. 45 were traced directly from recorder charts.

For comparison, hydrogen peroxide glass was prepared by shaking small drops of solution from the tip of a micropipet into liquid nitrogen. Warming curves were determined for the resulting 2-mm-dia hydrogen peroxide glass beads in the same manner as for the discharge product.

As seen in Fig. 45, the warming curve for hydrogen peroxide solutions frozen in a tube (curve A) shows a fairly sharp break at about –135°C, where the heat capacity increases sharply, indicating a glass transition. This portion of the curve could be reproduced repeatedly when the tube was cooled with liquid nitrogen before crystallization began. When the tube was cooled after crystallization had occurred, the warming curve showed no breaks from liquid-nitrogen temperature to the eutectic temperature.

The difference between curves A and B is attributed to poor thermal contact and lack of homogeneity in B. Both curves show the glass transition and, after crystallization begins, the rapid temperature rise which terminates abruptly at about –55°C, the the eutectic temperature.[23]

Warming curves (C and D) for the condensed product of dissociated water vapor are very similar to the curve for hydrogen peroxide (B) from –196 up to about –80°C. At about –110°C, crystallization appeared to start, accompanied by foaming

[23] W. C. Schumb, C. N. Satterfield, and R. L. Wentworth, *Hydrogen Peroxide*, p 211, Reinhold, New York, 1955.

which continued to the second rapid temperature rise. This continuous foaming indicated the presence of liquid at all times. The coexistence of liquid and solid in the system at a temperature somewhat below that of the lowest eutectic temperature for the H_2O-H_2O_2 system is interpreted as indicating the presence of appreciable quantities of at least one additional component.

The violent evolution of gas, accompanied by a rapid temperature rise beginning at about –60°C, is further indication of the existence of a third chemical species below –60°C in the discharge product. The actual amount of heat evolved estimated from the temperature rise for curve C is about 1400 cal per mole of solution. On the basis of the product ratios given by Jones and Winkler,[24] this is equivalent to about 21 kcal per mole of O_2 evolved.

[24] R. A. Jones and C. A. Winkler, *Can. J. Chem.* **29**, 1010 (1951).

REACTOR CHEMISTRY

EFFECT OF BATCH VS CONTINUOUS PROCESSING ON FLUIDIZED REACTORS

R. W. Stoughton J. Halperin

An investigation has been carried out on the effect of batch and continuous processing on both the production of transmutation products and the neutron losses that would be suffered due to their production in fluidized reactors. In general, neutron losses due to any transmutation product N_n formed in the reactor are lower when batch-processed, and the disparity between these two processing methods increases as n increases (where n refers to the nth product in a sequence of nuclear transformations). In the short time limit the advantage factor for batch processing approaches $(n + 1)!$. Similarly, the buildup of transmutation products is such that, in the short time limit, batch processing yields a lower content of the higher-order transmutation products, approaching an advantage factor of $n!$. Several special cases, including the U^{232} buildup in U^{233} produced in a thorium blanket, were examined. It was concluded that in a representative two-region power reactor a sixfold reduction in the U^{232} content of the U^{233} could be realized by batch rather than continuous processing. This relative advantage would have been much greater but for the fast-neutron leakage from the core. A report of this work is being prepared for publication.

ALKALI OXIDE–URANIUM TRIOXIDE–CARBON DIOXIDE AQUEOUS SYSTEMS AT HIGH TEMPERATURE

W. L. Marshall F. J. Loprest

The investigation of the lithium oxide–uranium trioxide–carbon dioxide aqueous systems has continued. New experimental data on the solubility of lithium carbonate as a function of temperature, CO_2 pressure, and uranium concentration are given in Tables 26 and 27. Experimental methods have been described previously,[1,2] with the exception of a new analytical technique for lithium, in which Dowex A-1 ion exchange resin in the hydroxide form is being used for quantitative removal of uranium and carbonate and subsequent acid-base titration of the pure $LiOH-H_2O$ eluent. This method is found to be precise and accurate to ±0.4%, as compared with ±1 to 2% for the flame spectrophotometric method.

The tests in Table 26 represent attempts to further define the system at 250°C. Experiments II-79, II-85, and II-90 were attempts to prepare and study an unsaturated solution of interest for operation of a homogeneous reactor. The data indicate that an unsaturated solution was obtained at 250°C and probably at 260°C for II-85 and II-90, as evidenced by the negligible to small increase in uranium and lithium concentrations after equilibration. Before being opened, the bomb was rapidly cooled, and in II-90 there was no solid, while in II-85 only a trace of yellow solid was evident. An appreciable amount of yellow solid found in run II-79 indicated a saturated solution. Experiments II-67 and II-82 present valid solubility data for the solid, Li_2CO_3, in $UO_3-CO_2-H_2O$ solution at 250°C. Analysis of the air-dried solid from II-67 gave: Li_2O, 40.50%; CO_2, 59.20%; CO_2/Li_2O mole ratio, 0.993. The liquid-phase compositions at 1500 psi total pressure ($P_{H_2O} + P_{CO_2}$) may be read from the plotted data, and in the case of II-82 the composition is: UO_3, 2.09%; Li_2O, 0.82%. A +2% correction may be applied for residual CO_2 to give a point on the Jänecke projection of: UO_3, 2.13%; Li_2O, 0.84%. If these data are compared on the Jänecke projection at 1500 psi total pressure at 250°C for $Li_2O-UO_3-H_2O$, given in the previous report[1] and shown in Fig. 46, it is clearly indicated that the solubility surfaces of lithium carbonate and the lithium uranyl carbonates postulated as the saturating phases of the liquid are very close to each other, especially at the higher uranium concentrations. Therefore, in actual practice it would be difficult to maintain an unsaturated solution containing a maximum amount of uranium at 250°C (at 1500 psi total pressure, CO_2 plus H_2O, point A of Fig. 46).

After a careful evaluation of the data at 250°C and of the literature data[3,4] for the solubility of

[1] F. J. Loprest, W. L. Marshall, and C. H. Secoy, *Chem. Semiann. Prog. Rep. June 20, 1955*, ORNL-1940, p 70–79.

[2] F. J. Loprest and W. L. Marshall, *HRP Quar. Prog. Rep. July 31, 1955*, ORNL-1943, p 227–235.

[3] A. Seidell, *Solubilities of Inorganic and Metal Organic Compounds*, p 909, 3d ed., Van Nostrand, New York, 1940.

[4] O. Haehnel, *J. prakt. Chem.* 148, 295–309 (1937).

TABLE 26. THE SYSTEM Li_2O-UO_3-CO_2-H_2O AT 250°C

Run No.	Total Mixture[a] (wt %)		Liquid Phase[b]				Density[c] of Liquid	Total Pressure[d] of CO_2 (psi)	Agitation Time[e] (hr)
			Weight %		Molality				
	UO_3	Li_2O	UO_3	Li_2O	UO_2CO_3	$LiHCO_3$			
II-67	0.980	5.033	1.074	0.602	0.0391	0.420		515	2
			0.982	0.622	0.0357	0.433		575	2
			1.071	0.621	0.0390	0.433		675	3
			1.071	0.636	0.0390	0.444		765	2
			1.082	0.641	0.0395	0.448		755	1
			1.066	0.668	0.0389	0.467	1.019	825	2
			1.093	0.681	0.0399	0.477	1.006	935	4
			1.094	0.693	0.0400	0.485	1.021	935	1
			1.131	0.719	0.0414	0.504	1.035	1115	1
			1.110	0.750	0.0407	0.527	1.017	1175	1
II-72	3.723	5.695	2.300	0.724				495	5
			3.022	0.894			1.048	655	1
			3.551	1.039			1.056	895	1
			3.527	1.006			1.055	1115	4
II-76	3.273	2.944	1.782	0.785	0.0660	0.557		595	3
			2.059	0.933	0.0771	0.669	1.034	775	4
			3.292	1.070	0.126	0.784	1.052	975	2
			3.462	1.039	0.133	0.762	1.053	1195	3
II-79	1.943	0.584	1.268	0.577	0.0462	0.403	1.020	775	2
			1.237	0.561	0.0450	0.391	1.018	1045	2
			1.265	0.568	0.0461	0.396	1.023	1135	2
			1.343	0.593	0.0490	0.414	1.021	1155	2
II-82	2.038	4.888	2.061	0.750	0.0765	0.533	1.034	435	2
			2.081				1.035	585	3
			2.093	0.824	0.0780	0.588	1.036	825	2
			2.087	0.820	0.0777	0.585	1.041	1035	2
			2.006	0.842	0.0747	0.601	1.032	1245	2
II-85	1.002[f]	0.550	1.076	0.608	0.0402	0.424	1.021	625	1
			1.101	0.616	0.0401	0.430	1.021	1105	2
			1.084	0.616	0.0395	0.430	1.021	1375	2
			0.937[g]	0.518	0.0339	0.359	1.017	419	1
			1.104[g]	0.597	0.0402	0.416	1.021	829	2
			1.095[g]	0.609	0.0399	0.425	1.021	1249	2
II-90	1.038	0.547	1.053	0.563	0.0382	0.392	1.018	525	3
			1.039	0.584	0.0378	0.407	1.018	1125	2
			1.064	0.558	0.0387	0.388	1.021	1195	2
			g	0.563				529	3
			1.086[g]	0.569	0.0395	0.396		829	3
			1.056[g]	0.563	0.0383	0.392	1.021	1069	3

[a]Points on Jänecke projection on Li_2O-UO_3-H_2O face.

[b]Not corrected for residual CO_2 and are not points on the projection.

[c]Density measured at room temperature with 1- or 2-ml volumetric pipet.

[d]Total psi − psi H_2O at t°C − 50 psi O_2 introduced at 100°C.

[e]Not cumulative.

[f]In doubt because of loss of some water vapor through a leak.

[g]Equilibria at 260°C.

TABLE 27. SOLUBILITY DATA* FOR Li_2CO_3 IN WATER AND IN UO_2CO_3-H_2O SOLUTION

CO_2 (psi)	Li_2O (wt %)	$LiHCO_3$ (m)	$K_6 \times 10^2$
At 40°C (in H_2O)			
73		1.40	5.26
147		1.40	2.61
294		1.92	4.62
441		2.06	4.08
500		2.06	3.60
			Av K_6 = 4.03
			$K_6 \times 10^4$
At 200°C (in H_2O)			
0	0.123	0.0824	
0	0.124	0.0829	
615	0.824	0.556	1.55
1040	0.940	0.635	1.56
1065	0.947	0.640	1.57
1125	0.954	0.645	1.54
1500	1.039	0.703	1.63
1855	1.099	0.744	1.65
2245	1.147	0.776	1.62
2775	1.201	0.814	1.58
			Av K_6 = 1.59
			UO_2CO_3 (m)
At 200°C (in UO_2CO_3-H_2O Solution)			
200	1.076	0.771	0.0663
250	1.086	0.781	0.0661
805	1.192	0.861	0.0654
870	1.182	0.854	0.0673
1145	1.259	0.913	0.0660
1425	1.331	0.969	0.0656
1525	1.343	0.978	0.0650
1825	1.388	1.013	0.0653
2370	1.437	1.051	0.0655
2575	1.442	1.055	0.0645
			$K_6 \times 10^5$
At 250°C (in H_2O)			
0	0.0	0.0639	
0		0.0655	

TABLE 27 (continued)

CO_2 (psi)	Li_2O (wt %)	$LiHCO_3$ (m)	$K_6 \times 10^5$
At 250°C (in H_2O)			
335		0.265	1.47
425		0.283	1.51
565		0.299	1.41
600		0.296	1.28
785		0.316	1.27
905		0.336	1.41
975		0.347	1.49
			Av K_6 = 1.41
			$K_6 \times 10^7$
At 290°C (in H_2O)			
370	0.1716	0.1151	4.74**
545	0.2198	0.1475	8.68
725	0.2377	0.1596	8.95
925	0.2476	0.1661	8.23
1130	0.2629	0.1764	8.57
1350	0.2724	0.1828	8.27
1510	0.2828	0.1898	8.59
1695	0.2848	0.1912	7.88
1920	0.2922	0.1962	7.72
			Av K_6 = 8.36

*The K's were calculated from data of Haehnel (see ref. 4).

**Hydrolysis according to Eq. 2 becomes predominant, therefore this value is not included in the average.

Li_2CO_3 as a function of temperature and CO_2 pressure at low temperature and on considering the uncertainty involved in completely establishing the composition of solid phases containing uranium, it was decided, first, to concentrate on the equilibria of Li_2CO_3 in water alone as a function of CO_2 pressure and temperature and, second, to investigate similar solubilities of Li_2CO_3 (as the stable solid) in UO_3-CO_2-H_2O solutions as a function of CO_2 pressure and temperature. The investigation will then be continued on that portion of the system in which uranium-lithium compounds are the stable solids. The apparatus and techniques are being improved in order to obtain a higher degree of precision and accuracy.

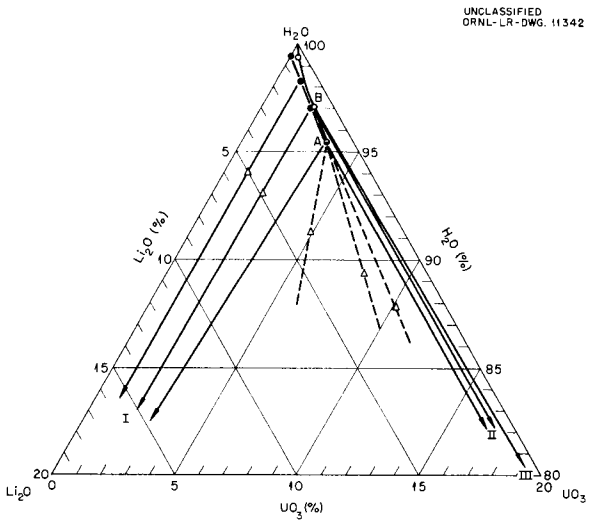

Fig. 46. The System Li_2O-UO_3-CO_2-H_2O at 250°C and at 1500 psi Total Pressure, Where $P_{total} = P_{H_2O} + P_{CO_2}$ (Jänecke Projection). A and B are invariant points; I = Li_2CO_3 solid; II, III = lithium-uranium solids.

It is hoped that a study of the equilibria will provide the means of developing a practical equation defining the limits of the unsaturated region. Following is a list of the various equilibria which may be operative in the Li_2O-CO_2-H_2O system where Li_2CO_3 is the saturating solid phase. All species are in aqueous solution except when noted by the subscripts s and g.

$$(1) \quad Li_2CO_{3(s)} \overset{K_1}{\rightleftharpoons} 2Li^+ + CO_3^{--}$$

$$(2) \quad CO_3^{--} + H_2O \overset{K_2}{\rightleftharpoons} 2OH^- + CO_2$$

$$(3) \quad CO_3^{--} + CO_2 + H_2O \overset{K_3}{\rightleftharpoons} 2HCO_3^-$$

$$(4) \quad CO_{2(g)} + \text{water} \overset{K_4}{\rightleftharpoons} CO_2$$

$$(5) \quad \begin{cases} CO_2 + H_2O \overset{K_5}{\rightleftharpoons} H_2CO_3 \\ CO_2 + H_2O \overset{Ka_1}{\rightleftharpoons} H^+ + HCO_3^- \\ HCO_3^- \overset{Ka_2}{\rightleftharpoons} H^+ + CO_3^{--} \end{cases}$$

The solubility data for Li_2CO_3 in water thus far obtained are listed in Table 27 and plotted in Fig. 47. Only the concentration of lithium was experimentally determined; and if it is expressed as molality of $LiHCO_3$, m, the quotient m^4/P_{CO_2} turns out to be a constant, within experimental error, above a certain minimum pressure of CO_2 below which it is believed that hydrolysis according to Eq. 2 is the predominating process. This constant will be designated K_6. It is seen that K_6 is equal to the product $K_1K_3K_4$, assuming that $[Li^+] = [HCO_3^-]$, K_1 being the solubility product constant of Li_2CO_3 and K_4 the Henry's law constant of CO_2. From the knowledge of K_6 as a function of temperature (Fig. 48) it is possible to determine the concentration of lithium in water over a wide range of pressure and temperature.

It has been shown previously[1,2] that the solubility of UO_2CO_3 in H_2O is of the order of 10 to 25 ppm up to 1200 psi CO_2 and 290°C. Therefore

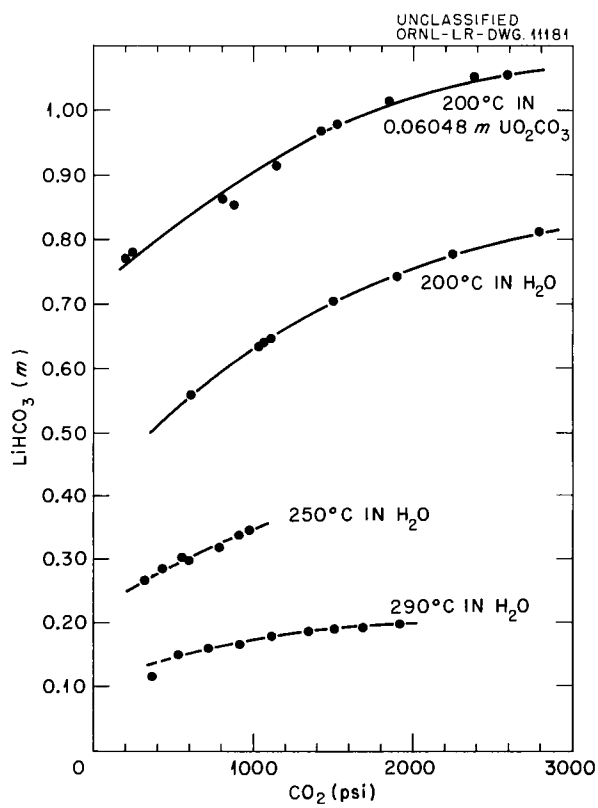

Fig. 47. Solubility of Li_2CO_3 (Expressed as Molality of $LiHCO_3$) as a Function of CO_2 Pressure.

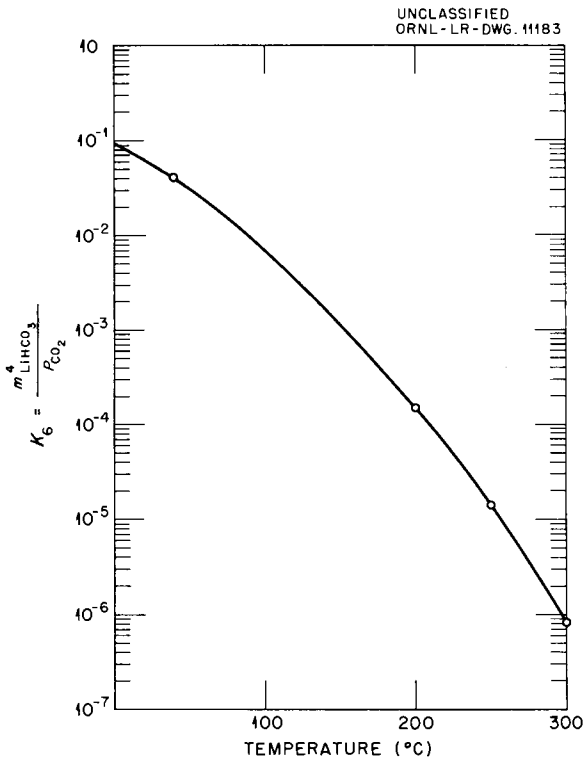

Fig. 48. Variation of K_6 with Temperature.

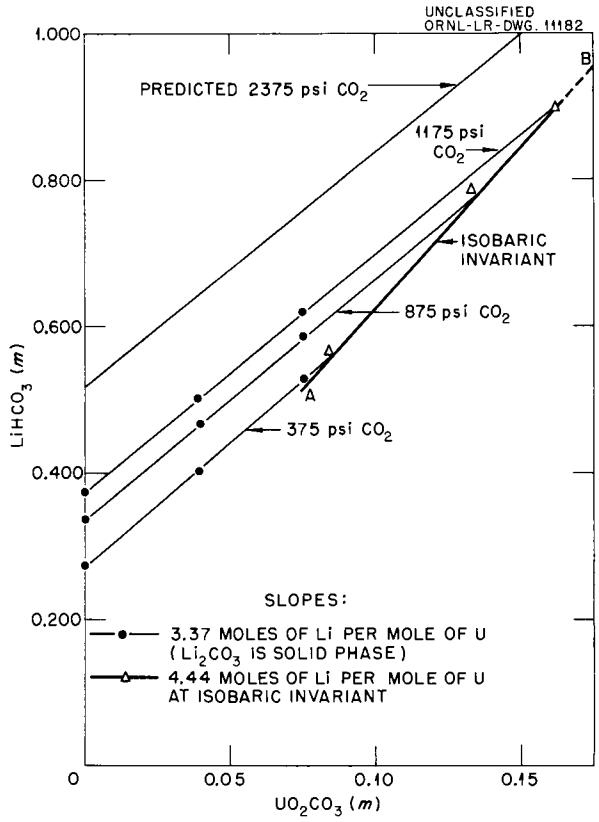

Fig. 49. Variation of Li_2CO_3 Solubility (Expressed as Molality of $LiHCO_3$) with UO_2CO_3 Concentration at Constant CO_2 Pressure (250°C).

the stabilization and very much increased solubility of uranyl ion in lithium carbonate solutions must be due to the formation of complex ions containing uranyl and carbonate or bicarbonate ions. At moderately high CO_2 pressure the bicarbonate ion would be expected to play a more significant part in the equilibria. Figure 49 represents an interpretation of the solubility data at 250°C and shows the increase in lithium concentration at saturation as a function of the concentration of uranium in the solution at constant pressures. The solid phase is Li_2CO_3 up to concentrations shown at the isobaric invariant, AB, at which point there are two solids, Li_2CO_3 and a basic lithium uranyl carbonate. The slopes, $\Delta[Li]/\Delta[U]$, are equal to 3.37 for all curves in the pressure and concentration ranges at 250°C in which lithium carbonate is the stable solid phase.

The following types of equilibria in saturated solution can be postulated at 250°C:

$$3HCO_3^- + UO_2(OH)_2 \xrightleftharpoons{K_a\,(\text{very large})} UO_2(HCO_3)(CO_3)_2^{3-} + 2H_2O$$

$$HCO_3^- + UO_2(HCO_3)(CO_3)_2^{3-} \xrightleftharpoons{K_b} UO_2(HCO_3)_2(CO_3)_2^{4-}$$

If these equilibria, the constancy of $[HCO_3^-]$ at fixed CO_2 pressure and at saturation, and $K_a = \infty$ are assumed, then

$$K_b' = \frac{[UO_2(HCO_3)_2(CO_3)_2^{4-}]}{[UO_2(HCO_3)(CO_3)_2^{3-}]} = 0.59 \ .$$

In other words, at 250°C it appears that uranium is maintained in solution as the complex ions, $UO_2(HCO_3)(CO_3)_2^{3-}$ and $UO_2(HCO_3)_2(CO_3)_2^{4-}$.

Next, the behavior of the various constituents in solution will be compared as a function of CO_2 pressure. Since the plots of concentration of lithium against CO_2 pressure at a constant temperature for various uranium concentrations are

[redacted]

essentially parallel, it is possible to obtain a constant value of the derivative $(\partial X/\partial p)_t$ at a given pressure. For 900 psi this value is listed in Table 28 along with values of $(\partial X/\partial p)_t$ for both lithium and uranium at the isobaric invariant (two solid phases present). The ratios of these derivatives $(\partial X/\partial p)_t$ are listed in the third column of Table 28 (reduced to the nearest simple whole numbers).

If the relative changes in lithium concentration per unit change of pressure are compared in the region in which Li_2CO_3 is the solid, the values are equal to 1 whether or not uranium is present in the solution. At the isobaric invariant the relative change is 4 for lithium and 1 for uranium; therefore three of the four units of $(\partial X/\partial p)_t$ for lithium must be attributed to the solubilization of the lithium-uranium compound, which is probably of the type $Li_3UO_2(OH)(CO_3)_2$, a basic lithium uranyl carbonate. If this reasoning from the available data is correct, then the stable solids at invariant A on Fig. 46 are Li_2CO_3 and $Li_3UO_2(OH)(CO_3)_2$. The uranium lithium compound follows the previously mentioned concepts concerning the nature of the species in solution. The hydroxyl radical is replaced by bicarbonate, and solubilization of $Li_3UO_2(OH)(CO_3)_2$ occurs by virtue of the formation of $UO_2(HCO_3)(CO_3)_2^{3-}$ ion.

The values of K_6 calculated at different temperatures are given in Table 27, and a plot of average values of K_6 vs temperature is shown in Fig. 48. These values of K_6 show agreement within 3% over a range of 300 to 2500 psi CO_2 at least at 200 and 290°C. Therefore, it is seen that lithium carbonate solubility in water at any temperature and at any pressure of CO_2 at least up to 2500 psi should be approximately equal to $(K_6 P_{CO_2})^{1/4}$. In this deduction a relatively small value of K_1 is assumed. Also, at least at 250°C and to a good approximation at 200°C the increase in solubility due to the formation of the uranium carbonate complexes in solution should be equal to 3.4 × molality of uranium in solution (Fig. 49). Of course, the uranium concentration may not exceed the value at the isobaric invariant. The following equation should express the solubility of Li_2CO_3 at near 250°C from approximately 200 to 2500 psi CO_2:

$$S_{LiHCO_3} = (K_6 P_{CO_2})^{1/4} + 3.4 m_U ,$$

where

$P_{CO_2} = (P_{total} - P_{H_2O})$ = psi CO_2 ,

m_U = molality of uranium in solution,

K_6 = constant at temperature t,

S_{LiHCO_3} = saturation molality of $LiHCO_3$ (solid phase is Li_2CO_3).

Low-temperature solubility data indicated that systems involving UO_3-CO_2-H_2O and either rubidium oxide, thallous oxide, magnesium oxide, or ammonia may have liquid phases with high uranium content at high temperature. These systems have been given an initial exploration at 250°C. The results show a negligible amount of uranium in the thallous, magnesium, and ammonium systems at 250°C. In these cases the solid phases appear to be uranates rather than carbonates. In the rubidium system, however, solutions containing between 2 and 2.5% of UO_3 at an Rb/U ratio of about 15 have been obtained at total pressures (CO_2 plus H_2O) between 1200 and 1900 psi, and this system appears worthy of further investigation.

TABLE 28. INCREASE IN SOLUBILITY OF Li_2O-UO_3-CO_2-H_2O COMPONENTS PER UNIT CHANGE OF PRESSURE AT 250°C AND 900 psi CO_2

X	Molal Change per psi Unit $(\partial X/\partial p)$ at 250°C	Nearest Simple Whole Number Ratio of $(\partial X/\partial p)$ at 250°C
Lithium (in H_2O)	11.0×10^{-5}	1
Lithium (in UO_2CO_3) solutions	11.0×10^{-5}	1
Lithium (at isobaric invariant)	44.8×10^{-5}	4
Uranium (at isobaric invariant)	9.80×10^{-5}	1

[redacted]